Angefertigt am

Fachbereich 08 - Biologie und Chemie

in Zusammenarbeit mit dem Institut für Medizinische Virologie

am Fachbereich 11 - Medizin

der Justus-Liebig-Universität Gießen

Identification and characterization of specific amino acid residues in the NS1 protein that facilitated viral replication of avian influenza viruses in mammalian host

Inauguraldissertation

zur Erlangung des akademischen Grades

d o c t o r r e r u m n a t u r a l i u m

(Dr. rer. nat.)

des Fachbereichs 08 - Biologie und Chemie

der Justus-Liebig-Universität Gießen

vorgelegt von

Pumaree Kanrai

Master of Science

Gießen 2015

Erklärung

„Ich erkläre: Ich habe die vorgelegte Dissertation selbständig und ohne unerlaubte fremde Hilfe und nur mit der Hilfe angefertigt, die ich in der Dissertation angegeben habe. Alle Textstellen, die wörtlich oder sinngemäß aus veröffentlichten oder nicht veröffentlichten Schriften entnommen sind, und alle Angaben, die auf mündlichen Auskünften beruhen, sind als solche kenntlich gemacht. Bei den von mir durchgeführten und in der Dissertation erwähnten Untersuchungen habe ich die Gründsätze guter wissenschaftlicher Praxis, wie sie in der „Satzung der Justus-Liebig-Universität Gießen zur Sicherung guter wissenschaftlicher Praxis" niedergelegt sind, eingehalten."

Pumaree Kanrai

Contents

List of Figures

List of Tables

Abbreviations

aa	amino acid
Amp	ampicillin
APS	ammonium persulfate
AI	avian influenza
AIV	avian influenza virus
bp	base pairs
BSA	bovine serum albumin
°C	grade celcius
cm	centimetre
DAG	diacylglycerol
ddH2O	deionized distilled water
DMEM	Dulbecco's Modified Eagle's medium
DMSO	dimethylsulfoxide
DNA	deoxyribonucleic acid
dNTP	deoxynucleoside triphosphate
DTT	dithiothreitol
EDTA	ethylenediamine tetraacetic acid
ECL	enhanced chemoluminiscence
eIF2	eukaryotic translation initiation factor 2
ERK	extracellular signal regulated kinase
et al.	et alii (and others)
FCS	fetal calf serum
FFU	foci forming unit(s)
FPV	fowl plague virus
g	gram
h	hour(s)
HA	haemagglutinin
HEPES	N-2-hydroxyethylpiperazine
HPAIV	highly pathogenic avian influenza virus
IFA	indirect immunofluoresces assay
IFN	interferon
IRF3	IFN regulatory factor 3

kb	kilobase pairs
LPAIV	low pathogenic avian influenza virus
M	molar
M1	matrixprotein
M2	ion channel protein
MAPK	mitogen-activated protein kinase
MAPKK	MAPK kinase
MAPKKK	MAPKK kinase
MEK	MAPK/ERK activated kinase
MEKK	MAPK/ERK activated kinase kinase
MCD	methyl-ß-cyclodextrin
mg	milligram
min	minute(s)
ml	milliliter
mM	millimolar
m.o.i.	multiplicity of infection
mRNA	messenger RNA
NA	neuraminidase
NCR	noncoding region(s)
NEP/NS2	nuclear export factor
NES	nuclear export signal
NLS	nuclear localization signal
NP	nucleocapsid protein
NPC	nuclear pore complex
NS1	nonstructural protein
ng	nanogram
nt	nucleotide(s)
OD	optical density
PA	polymerase acidic
PAGE	polyacrylamide gel eletrophoresis
PB1	polymerase basic 1
PB2	polymerase basic 2
PBS	phosphate buffered saline
PCR	polymerase chain reaction

PFU	plaque forming unit(s)
p.i.	post infection
PKR	dsRNA activated protein kinase
pmol	picomolar
PolyA	polyadenylic acid
Pol I	RNA polymerase I
p.t.	post transfection
RDRP	RNA-dependent RNA-polymerase
RNA	ribonucleic acid
RNPs	ribonucleoproteins
rpm	rounds per minute
RSK	ribosomal S6 kinase
RTK	receptor tyrosine kinase
s	second(s)
SDS	sodium dodecyl sulfate
TEMED	N,N,N',N'-tetramethylethylenediamine
TPA	12-O-Tetradecanoylphorbol-13-acetate
Tris	tris-hydroxymethylaminomethane
Tween 20	polyoxyethylenesorbiten monolaurate
V	volt
vRNA	viral RNA
v/v	volume percentage
w/v	weight percentage
µg	microgram
µl	microliter
µM	micromolar

Summary

Recently, it was shown that the NS-segment of the avian influenza virus strain A/Goose/Guangdong/1/1996 (GD, H5N1) promotes replication and increases pathogenicity of the strictly avian strain A/FPV/Rostock/34 (FPV, H7N1) in mammalian cells and mice, whereas the NS-segment of A/Mallard/NL/12/2000 (MA, H7N3) impaired FPV replication in mammalian cells. The NS1 proteins of GD and Ma differ only by eight amino acids. Nevertheless, the critical genetic differences were not yet identified. In this report, I demonstrate that the specific amino acid changes D74N and/or P3S+R41K+D74N in the NS1-MA protein are sufficient to allow mammalian adaption of avian influenza viruses. They lead to enhanced virus propagation in mammalian cells and increased plaque size, suggesting shorter replication cycles. On a molecular level, I show the importance of these specific residues for strongly enhanced mRNA production as well as viral protein production in mammalian cells. At the same time this adaptive changes are not disadvantageous in avian cells. My study suggests that the D74N and/or P3S+R41K+D74N substitutions are involved in the temperature adaptation of the polymerase of avian influenza virus from birds to mammals. They also confer the ability to the otherwise strictly avian influenza virus to replicate in mice and cause disease. Global gene expression of mammalian A549 cells upon infection with FPV harboring NS-MA (FPV-NS^{MA}) or with FPV harboring NS-MA mutants (FPV-NS$^{MA\_D74N}$ and FPV-NS$^{MA\_P3S+R41K+D74N}$) viruses are qualitatively similar in the activation of biological host inflammatory response including type I interferon (IFN) and chemokine signaling, However, in comparison to FPV-NS^{MA} virus infected cells, the mutants NS1-MA^{D74N} and/or NS1-MA$^{P3S+R41K+D74N}$ elicit a quantitatively weaker host inflammatory response of type I interferon (IFN) and pro-inflammatory cytokine/chemokine response. This points to a reduced innate immune response, which is correlated with increased viral replication competence. Together, these adaptive mutations in the NS1 protein seem to allow to establish successful infections in mammalian cells.

Zusammenfassung

Vor kurzem konnten wir zeigen, dass das NS-Segment des Influenza-Virus A/Goose/Guangdong/1/1996 (GD, H5N1) sowohl die Replikation von A/FPV/Rostock/34 (FPV, H7N3) in Säugerzellen und Mäusen begünstigt wie auch dessen Pathogenität in eben diesen erhöht. Im Gegensatz dazu beeinflusst das NS-Segment von A/Mallard/NL/12/2000 (MA, H7N3) die FPV Replikation in Säugerzellen negativ. Die NS1-Proteine von GD und MA unterscheiden sich in nur acht Aminosäuren. Jedoch wurden bisher die verantwortlichen Aminosäuren für diesen funktionellen Unterschied nicht identifiziert. In dieser Arbeit zeige ich, dass die spezifischen Aminosäure-Änderungen D74N und/oder P3S+R41K+D74N im NS1-MA Protein ausreichen, um eine Adaption des Virus an Säugerzellen zu ermöglichen. So führen sie zu einer gesteigerten Virus-Replikation und größeren Plaques in Säugerzellen, was einen kürzeren Replikationszyklus nahe legt. Auf molekularer Ebene zeige ich, dass diese Aminosäure-Änderungen zu einer stark vermehrten mRNA Produktion wie auch zu einer gesteigerten Protein-Synthese in Säugerzellen führen, während diese Adaptionen jedoch keine Replikations-Nachteile in Vogelzellen zeigen. Meine Studie zeigt auch, dass die Mutationen D74N und/oder P3S+R41K+D74N eine Rolle in der Temperatur-Adaption der Polymerasen von Vogelgrippe-Viren an Säuger spielen. Außerdem ermöglichen sie originär strikt aviären Vogelgrippe-Viren, sich in Mäusen zu vermehren und sie erkranken zu lassen. Die Gesamtgenexpression in infizierten Säugerzellen ist zwischen Wildtyp und mutiertem Virus qualitativ ähnlich, insbesondere im Hinblick auf die fast identischen Immunantworten durch Typ1 Interferon (IFN) und Cytokine/Chemokine. Eine Infektion von FPV, welches das NS1-MA mit den Mutationen D74N und/oder P3S+R41K+D74N besitzt, löst aber im Vergleich zum NS1-MA Wildtyp eine quantitativ schwächere Immunantwort insbesondere bezogen auf Typ1 Interferon (IFN) und pro-entzündliche Cytokine/Chemokine aus. Dies ist ein Hinweis auf eine wahrscheinlich weniger starke humorale Immunantwort, die mit einer verbesserten Virus-Replikation einhergeht. Zusammengefasst erlauben o.g. adaptive Mutationen des NS1-Proteins es, aviären Influenza-Viren eine erfolgreiche Infektion in Säugerzellen zu etablieren.

List of Publications

1. **Kanrai P**, Mostafa A, Madhugiri R, Lechner M, Wilk E, Schughart K, Ziebuhr J, and Pleschka S. Novel residues in avian influenza virus NS1 protein enhance polymerase activity and virulence in mammalian host. (Submited)

2. **Kanrai P**, Madhugiri R, Mostafa A, Lechner M, Wilhelm J, Ziebuhr J, and Pleschka S. Cellular transcription profile response to infection of different NS gene reassortant of avian influenza viruses in mammalian host. (Manuscript preparation)

3. Mostafa A, **Kanrai P**, Ziebuhr J and Pleschka P. The PB1 Segment of 2009 pandemic influenza virus confers efficient replication of different influenza vaccine strains in cell cultures and embryonated eggs. (Manuscript preparation)

4. Mostafa A, **Kanrai P**, Petersen H, Ibrahim S, Rautenschlein S, Pleschka S. Efficient Generation of Recombinant Influenza A Viruses Employing a New Approach to Overcome the Genetic Instability of HA Segments. PLoS One. 2015 Jan 23;10(1).

5. Krumbholz A, Lange J, Sauerbrei A, Groth M, Platzer M, **Kanrai P**, Pleschka S, Scholtissek C, Büttner M, Dürrwald R, Zell R. (2014). Origin of the European avian-like swine influenza viruses. J Gen Virol. 2014 Nov; 95 (Pt 11):2372-6.

6. Groth M, Lange J, **Kanrai P**, Pleschka S, Scholtissek C, Krumbholz A, Platzer M, Sauerbrei A, Zell R. 2014. The genome of an influenza virus from a pilot whale: relation to influenza viruses of gulls and marine mammals. Infect Genet Evol. 2014 Jun; 24:183-6.

7. Lange J, Groth M, **Kanrai P**, Pleschka S, Scholtissek C, Dürrwald R, Platzer M, Sauerbrei A, Zell R.2014. Circulation of classical swine influenza virus in Europe between the wars. Arch Virol. 2014 Jun; 159 (6):1467-73.

8. Mostafa A, **Kanrai P**, Ziebuhr J, Pleschka S. 2013. Improved dual promotor-driven reverse genetics system for influenza viruses. J Virol Methods. 2013 Nov193 (2):603-10.

Chapter 1

Introduction

1.1 Influenza A viruses

Influenza is considered to be one of the life-threatening infectious diseases. In many countries seasonal influenza affects annually up to 40% of the population and 500000 people die from it worldwide every year. Occasionally, influenza affects 20-40% of the world's population in a single year. Such unpredictable influenza "pandemics" (global increases in incidence) occurred three times in the 20th century: 1918-1919, 1957-1958, and 1968. The 1918 ("Spanish flu") pandemic was the most severe, and is estimated to have clinically affected ~500 million people and caused >40 million deaths [1]. The pandemics of 1957 ("Asian flu") and 1968 ("Hong Kong flu") had much lower, but still significant mortality rates [2]. New highly-virulent influenza strains can arise unexpectedly to cause world-wide pandemics with markedly increased morbidity and mortality, such as the "avian flu" in 1997 and "swine flu" in 2009 [3].

Influenza viruses were first isolated as the causative agent of influenza in 1933 by Wilson Smith. They belong to the Orthomyxoviridae family and are divided into three genera, namely influenza A, B and C viruses. The genera can be distinguished by their Haemagglutinin (HA) and neuraminidase (NA) protein antigens [4]. Influenza A and B viruses can cause major outbreaks and severe disease, whereas influenza C viruses are mostly responsible for sporadic upper respiratory tract illness in children. It is believed that most mammalian influenza A viruses are derived from an avian, which circulates in wild aquatic birds [5]. The influenza B and C viruses diverged from the influenza A virus lineage several centuries ago and adapted to infect humans only. In contrast, influenza A viruses can infect a wide range of species (Fig. 1.1), including non-human primates, pigs, horses, cats, seals, whales and minks.

Influenza A viruses are divided into subtypes, based on the nature of their surface glycoproteins, HA and NA [6]. There are 16 different HAs and nine NAs which are distinguishable serologically, i.e. antibodies to one virus subtype do not react with another. All virus subtypes appear to circulate in aquatic birds [7]. Only some of

these subtypes have been identified in humans, specifically the H1N1, H2N2 and H3N2 viruses, corresponding to the three major pandemics of the last century. During recent outbreaks of highly pathogenic avian influenza (HPAI), there have been occasional transmissions of H5N1, H7N7 and H9N2 viruses to humans [8, 9]. There are no influenza B virus subtypes. The B virus primarily infects humans, although it has also been isolated from seals [5].
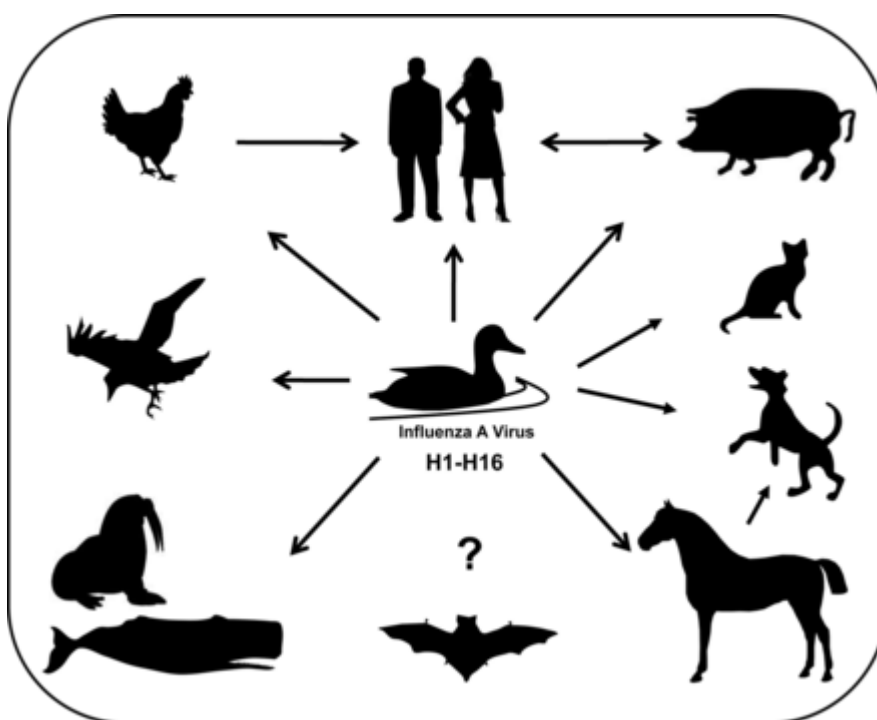
Fig. 1.1 Host range of influenza A viruses. Wild water birds represent the natural reservoir of influenza A viruses, from which they can be transmitted to a wide variety of other hosts, including horses, cats, dogs, whales, seals, wild flying birds, chicken, pigs, and humans. Only recently, influenza A virus has also been detected in bats, although the origin is unclear. (Adapted from Manz *et al* [10])

1.1.1 Morphology and genome structure of influenza A virus

Influenza A virus virion consists of a lipid envelope that is derived from the host cellular membrane during the budding process. They are generally spherical or elliptical in shape, ranging from approximately 80–120 nm in diameter and are occasionally filamentous, reaching more than 20 μm in length. However, they take on an irregular shape, a characteristic dependent upon the viral strain, as well as the cell type used for propagation [10]. The influenza A virus genome consists of eight RNA

segments, and encodes at least 10 well-described proteins (Fig. 1.2). Furthermore, there are a growing number of newly identified proteins encoded by certain strains of influenza A virus, including PB1-F2 [11], PB1-N4 [12], PA-X [13], N-truncated PAs [14], M42 [15] and NS3 [16], which are generated by various co-transcriptional or co-translational strategies. The 10 common viral proteins are expressed in all influenza A viruses, and are functionally essential for a complete infection cycle in immuno-competent hosts. The HA protein present on the surface of the virion, and recognizes sialic acid on the surface of host cells [17]. After binding, virus particles are endocytosed, and the lowering of the pH, caused by subsequent endosome maturation, triggers a conformational change in HA resulting in fusion of the endosome and virion membranes. The viral M2 protein (matrix 2) functions as an ion channel to further lower the pH of the virus particle, thereby aiding in the dissociation of the M1 protein (matrix 1) virion 'shell' such that the eight vRNPs (NP [nucleoprotein]-coated and polymerase complex (PB1, PA, and PB2)-bound viral RNAs) (Fig. 1.3) are released into the cytosol [18]. The vRNPs are then transported into the cell nucleus where accessory cellular components essential for influenza viral replication and transcription are located. After genome replication, transcription and protein synthesis, NEP (nuclear export protein) and M1 act to transport newly synthesized vRNPs out of the nucleus, into the cytoplasm and to the plasma membrane, where assembly of progeny virions take place. At these area, several viral proteins contribute to budding, including M1 and M2. Finally, NA acts to remove sialic acid from glycoproteins in both the viral and cell membranes, thereby preventing interaction between HA and host cell receptors, and thus, ensuring release of new infectious virus particles [6]. NS1 (nonstructural protein 1) acts within the infected cell to counteract innate host-cell defense systems, including interferon (IFN), that may otherwise limit efficient virus replication [19]. A schematic representation of the influenza A virus particle together with its RNA segments and encoded proteins is shown in Fig. 1.2.
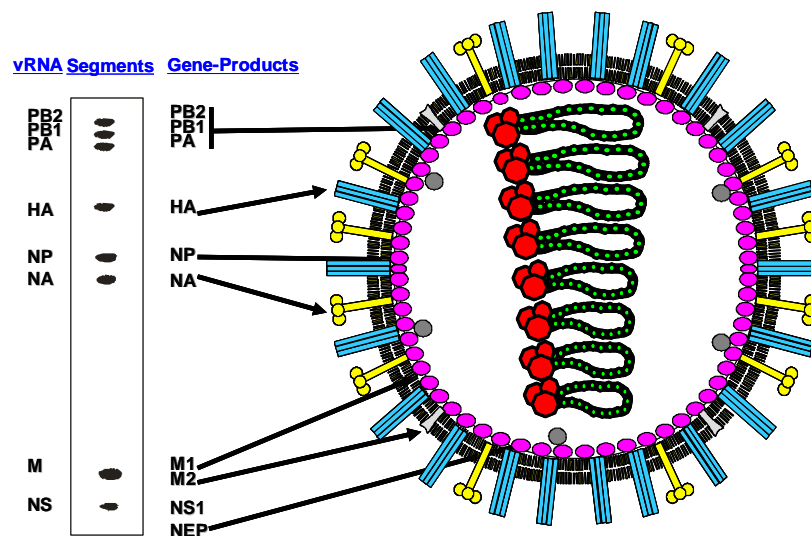
Fig. 1.2 The influenza virus virion. The eight viral RNA segments were separated by electrophoresis (left). The corresponding gene products and their localization within the virus particle are depicted on the right. The non-structural virus protein, the NS1, is only found inside infected cells. (Adapted from Ludwig *et al.* [20])
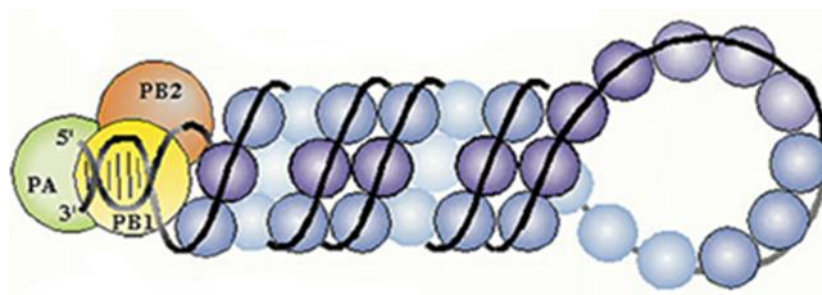
Fig. 1.3 The influenza virus RNP structure. The NP (blue) is associated with (-) sense single-stranded RNA (black line), and the three subunits of RNA-dependent RNA-polymerase (RDRP): PB1 (yellow), PB2 (orange) and PA (green), which bind at a short duplex region of the vRNA. (Adapted from Portela and Digard [21])

1.1.2 Propagation and genome replication of influenza A virus

1.1.2.1 Replication cycle –virus entry

The initial step of the viral entry process is the attachment of influenza A virus (IAV) to the host cell. The primary receptor for IAV is sialic acid and this receptor is recognized and bound by the viral membrane protein HA [23]. Sialic acid is the distal residue in oligosaccharide chains of N- and O-linked glycoproteins and lipids. Often, sialic acid is attached to the underlying galactose by α-2,3 or α-2,6 linkages. This

linkage is the resulting structural consequences influence how well IAV can bind to its receptor.

HA is a multifunctional protein mediating virus attachment and fusion. There are 18 different HA subtypes known, of which 16 circulate in waterfowl and two (H17 and H18) have been isolated from bats [24, 25]. Of note, H17 and H18 do not bind to sialic acid; the receptor for these viruses is not yet known [26, 27]. HA is expressed as a trimer on the virion surface. The stalk region of HA connects HA to the virion envelope by a short hydrophobic sequence [28]. This region is predominate glycosylated on conserved epitopes, which appear to be required for the stability and structure of the molecule [29]. The globular head is also glycosylated, but the glycosylation pattern and its type can be highly variable in different HA subtypes. The receptor-binding pocket (RBP) is located on the distal end of the HA trimer at the globular head (Fig. 1.5a) and is highly conserved among different HA subtypes.
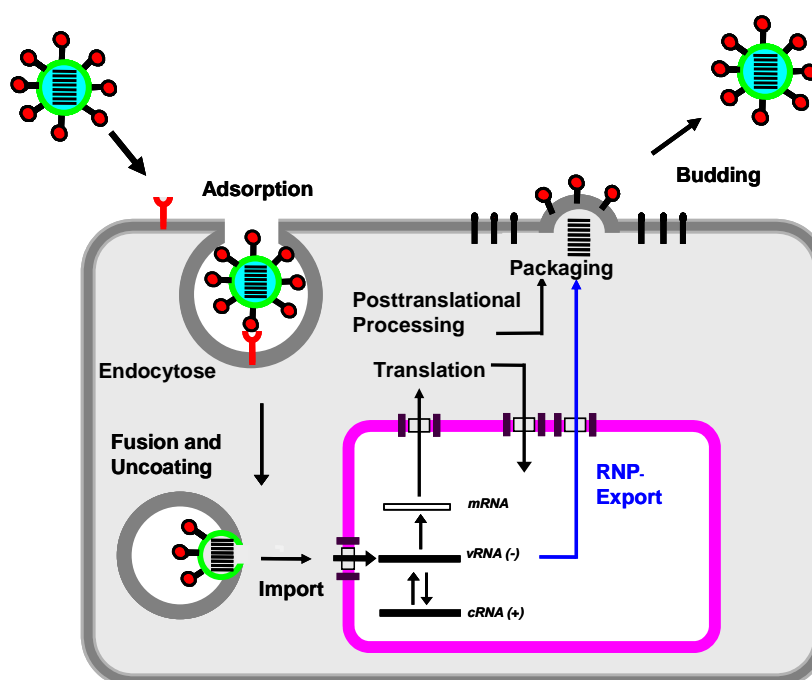
Fig. 1.4 The Replication cycle of influenza virus. It begins with binding of the HA-spike to sialic-acid containing receptors on the cell surface. The virion is then taken up into the cell through endocytosis. The RNPs are released into the cell cytoplasm after fusion between the viral and the endosomal membrane, and then transported into the nucleus, where transcription and replication of the viral RNA takes place. Viral mRNA is exported to the cytoplasm and translated into viral proteins. Some replicative proteins (i.e. NP, PB1, PB2 and PA) are transported back to the nucleus and continue the viral genome replication. Viral surface-glycoproteins (i.e. HA and NA) are transported to the cell surface. Late during virus replication cycle, vRNPs are exported out of the nucleus and packed and progeny virions are then released from the membrane by budding. (Adapted from Pleschka [22])

Mutations in residues of the RBP and those in close proximity can drastically alter the receptor specificity of HA [30, 31]. Sialic acid has been shown to occupy the whole RBP and to be the major point of contact between the virus and the cell [32]. The interaction between sialic acid and HA is believed to be of low affinity. To increase the overall strength of the interaction, multiple HA molecules are used to bind to several glycoproteins, resulting in high-avidity binding to the cell surface [33].
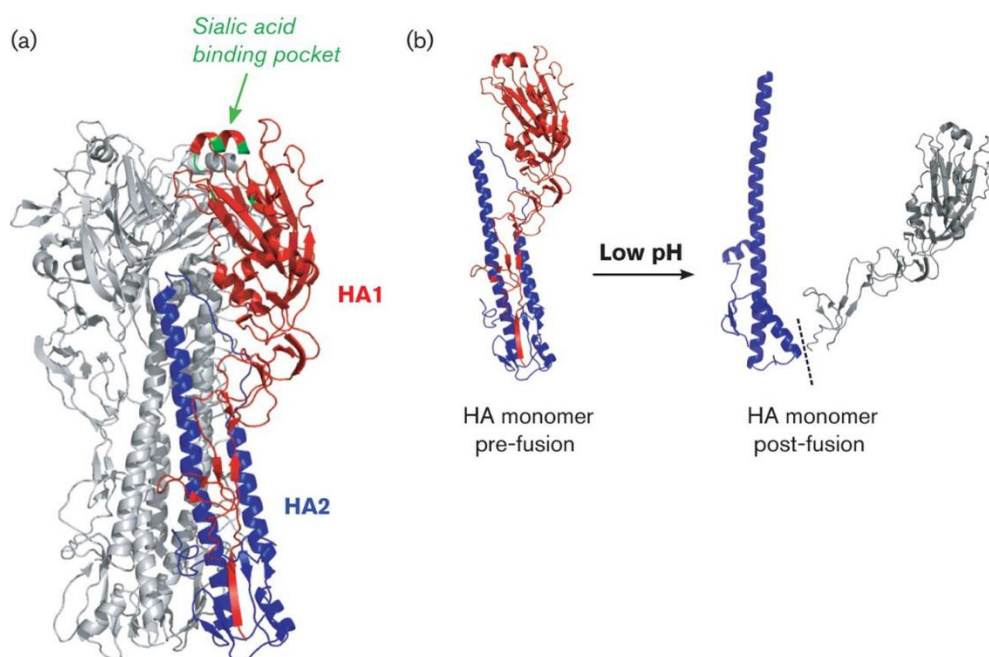
Fig. 1.5 Structure of HA. (A) Structure of the HA of IAV A/SouthCarolina/1918 based on the results of Gamblin *et al.* (2004) [34] [Protein Data Bank (PDB) accession no. 1RUZ]. The trimeric complex of HA is shown with one monomer highlighted in colour. HA1 is depicted in red, HA2 in blue and the RBP in green. **(B)** The pre- and post-fusion conformations of HA are shown (Bullough *et al.* 1994 [35]; PDB accession no. 1HTM). For the post-fusion conformation, only the structure of the part represented in blue could be resolved. HA1 was not included in the structure and is modelled according to Edinger *et al.* [23].

1.1.2.2 Replication cycle – viral mRNA synthesis

After entry into the nucleus, transcription and replication of the influenza virus genome depends on viral polymerase activity, together with cellular co-factors. Influenza A virus RNA synthesis requires four proteins, which together with viral RNA, which make up the functional RNP: NP, PA, PB1 and PB2 [36]. Genomic viral RNA (vRNA) has conserved sequences at the 5' and 3' termini that share some sequence complementarity [37]. A high degree of conservation at the 3' ends as well

as at the 5' ends was observed among the genome segments of each virus and among the segments of the three different virus types. A uridine-rich region was observed from positions 17 through 22 at the 5' end of each segment. Moreover, the conserved 3' and 5'-terminal sequences showed partial and inverted complementarity. This feature results in very similar sequences at the 3' ends of the plus and minus strand RNAs and may also enable single-strand RNAs of influenza virus to form "panhandle" structures. Inverted complementary repeats may play an important role in initiation of viral RNA replication [37, 38]. Each vRNA is encapsidated by NP, and is associated with a single heterotrimeric polymerase complex. The incoming RNP (i.e. from the virion) is all that is required to transcribe mRNA, as long as an appropriate 5' host-derived capped RNA is available [39].

During mRNA synthesis (Fig. 1.6), the polymerase (via PB1) binds to the 5' end of the vRNA segment and thereby stimulates the cap-binding activity of PB2, which allows the polymerase to bind host-cell mRNAs produced as RNA polymerase II transcripts [40]. Subsequent interaction of the 3' end of the vRNA template with the viral polymerase triggers cleavage of the host-cell mRNA by PB1 and PA [41, 42], thus retaining the 5'- methylated host cap structure together with 9-15 cellular mRNA nucleotides. Viral capped mRNAs are protected from cleavage when they interact with the viral polymerase [40]. The cleaved host cap structure acts as a primer for viral transcription initiation by PB1 [43], which is enhanced by the physical interaction of PB2 with the cap structure. Addition of ribonucleotides (elongation) occurs according to the viral template (vRNA), and at some point PB2 dissociates from the cap [21].

Synthesis of viral mRNA terminates at a stretch of uridine (U) residues ~15-22 nucleotides from the 5' end of the vRNA, where steric hindrance of the viral polymerase probably causes it to reiteratively copy the poly(U) tract ("stutter") resulting in the generation of a poly(A) tail [21] (Fig. 1.6). It is unclear what role, if any, is played by the PA polymerase subunit in viral mRNA synthesis, although it may contribute to the nuclear localization of PB1, as well as efficient endonuclease activity and/or elongation [41, 44]. Although pre-mRNAs of most eukaryotic cells are fully spliced (i.e. introns removed) in order to generate functionally mature mRNAs, only two influenza A virus mRNAs require splicing: NS1 and M1. Additionally, unlike

complete cellular mRNA splicing, the splicing of viral NS1 and M1 mRNAs (to produce NEP and M2 mRNAs, respectively) appears to be regulated such that spliced mRNA is only ~10% that of unspliced mRNA [39]. M1 mRNA splicing is controlled by both the viral polymerase and cellular splicing factors, such as the serine/arginine-rich splicing factor SF2/ASF [45]. Splicing of NS1 mRNA to produce NEP mRNA can be regulated by the NS1 protein itself [46]. It is not exactly clear how viral mRNAs (both spliced and un-spliced) can specifically leave the nucleus to be translated into protein, particularly as NS1 has been reported to block the nucleo-cytoplasmic transport of cellular mRNAs [47].

1.1.2.3 Replication cycle – viral genome replication

The replication of genomic virion RNA (vRNA) occurs in two stages: the initial synthesis of "template" RNA that is complementary to full-length vRNA (i.e. a positive-sense strand: cRNA), and the subsequent copying of cRNA into new vRNAs (reviewed in [43] and [21]) (Fig. 1.6). Although viral mRNAs and cRNAs are both positive-sense, mRNA cannot act as a replicative intermediate in the formation of new vRNAs as it has a 5' host-derived cap and is truncated relative to the full-length genomic segments. Thus, the viral polymerase initiates cRNA synthesis in a cap-independent manner, and must "read-through" the polyadenylation signal at the 5' end of vRNA [48]. Additionally, cRNA (but not mRNA) is encapsidated by NP. Unlike mRNA transcription, the incoming viral RNP alone is insufficient to stimulate cRNA synthesis and evidence suggests that an initial round of mRNA and protein synthesis is necessary prior to initiation of cRNA synthesis [42].

It is not clear what viral components constitute the replication polymerase complex. Soluble viral NP appears to be a major factor regulating replication, and its involvement would correlate with the requirement for *de novo* protein synthesis. Soluble NP may simply act in a concentration-dependent manner (i.e. stabilising cRNA transcripts when high enough levels of NP protein are available by modifying the transcription template [40] or by directly modifying polymerase function (i.e. "switching" protein-protein interactions between NP and PB1/PB2 in order to favour a replication polymerase over a transcription polymerase) [49]. Additionally, all three polymerase subunits (PA, PB1, PB2) are required for efficient cRNA synthesis [50], and it is possible that PA acts in a proteolytic manner to clip components of the

transcription polymerase, and thus convert it into a replication polymerase [51]. Possible roles of numerous host-cell proteins (including hCLE, HSP90 and UAP56/BAT1; a DEAD-box ATP-dependent RNA helicase) in viral RNA synthesis have not been fully clarified [52]. Both PA and soluble NP are important for the synthesis of vRNA from cRNA [53]. The binding of NP to nascent viral RNA may be facilitated by UAP56 and Tat-SF1, which proposed to act as chaperones for NP [54, 55]. NS1 protein has also been suggested to be an additional cofactor that directly interacts with the viral replication polymerase complex and affects accumulation of vRNA, but not cRNA [56]. Intriguingly, vRNA only appears to be synthesised at sites of insoluble "nuclear matrix" within the nucleus, whilst both mRNA and cRNA synthesis is detectable in both soluble and insoluble nuclear fractions [57].
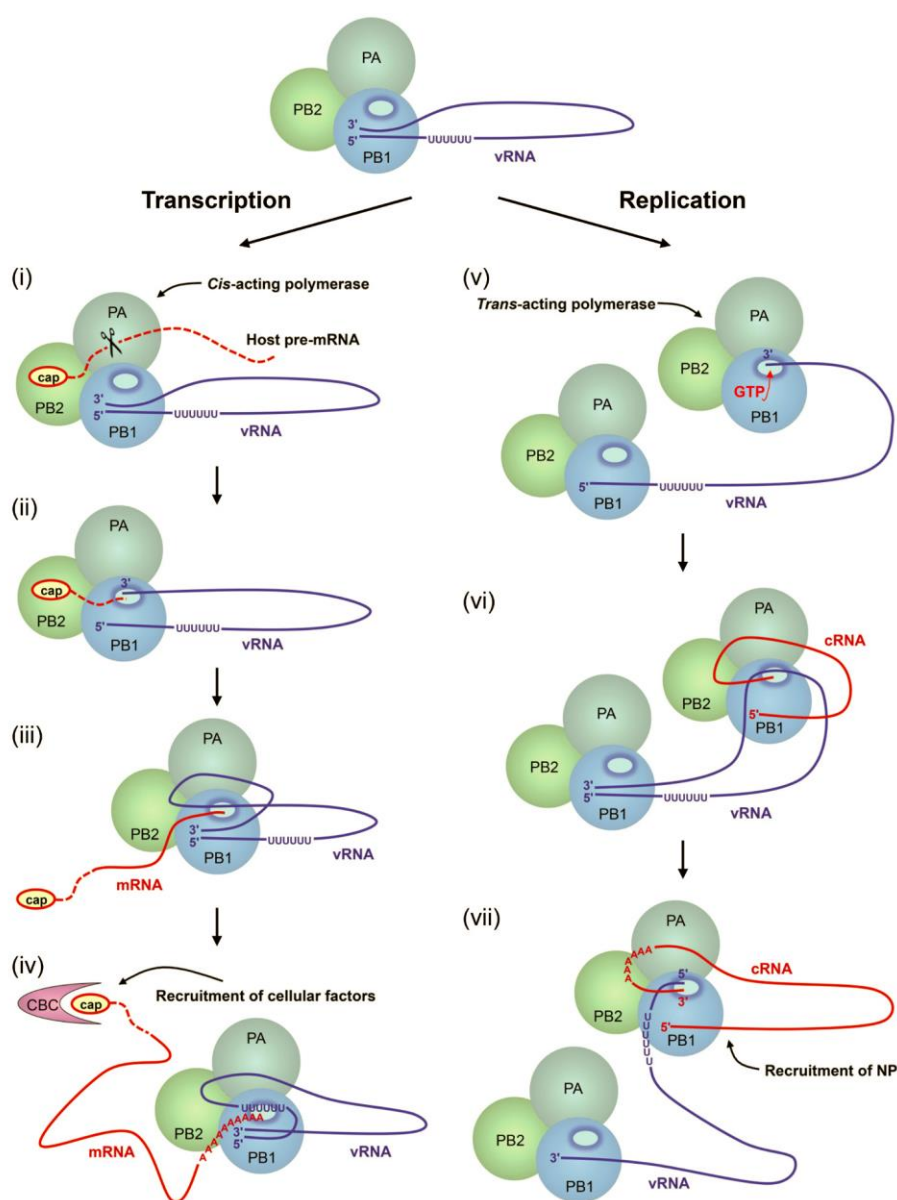
Fig. 1.6 Models for the transcription and replication of the influenza virus vRNP. In a vRNP the viral polymerase, consisting of the PB1, PB2 and PA subunits, is bound to the partially complementary 5' and 3' termini of a vRNA segment. The oligomeric nucleoprotein that associates with the rest of the vRNA is not shown for simplicity. **(i)** Transcription is initiated by PB2 binding to the 5' cap structure of host pre-mRNA followed by endonucleolytic cleavage of the host pre-mRNA by PA. **(ii)** The 3' end of the capped RNA primer is positioned in the active site of PB1, along with the 3' end of the vRNA template, to allow transcription initiation to take place. **(iii)** Once the 3' end of vRNA has been copied it re-binds the polymerase, a process possibly facilitated by base-pairing between the vRNA termini. **(iv)** As elongation proceeds the vRNA template is threaded through the active site of PB1 eventually leading to polyadenylation by repeated copying of the U sequence near the 5' end of the vRNA template, due to steric hindrance caused by the vRNA 5' end remaining bound to the transcribing polymerase. The 5' cap of mRNA is released from PB2 and is bound by the cellular nuclear cap-binding complex (CBC) triggering the recruitment of cellular factors for mRNP assembly. **(v)** Replication of vRNA into cRNA is shown as proposed in the trans-acting polymerase model, but note that alternative models involving a cis-acting polymerase in vRNA→cRNA replication have also been proposed (see text for details). According to the trans-acting polymerase model, the 3' end of the vRNA template is released from the vRNP-associated polymerase by an unknown mechanism that allows it to bind to a trans-acting RNA polymerase. Replication is initiated by the binding of the trans-acting polymerase to GTP, directed by the penultimate residue in the vRNA 3'-terminus, and the generation of pppApG (not shown) to be elongated by the trans-acting polymerase. **(vi)** Once the 3' end of vRNA has been copied it re-binds the vRNP-associated polymerase while the 5' end of the newly synthesized cRNA binds to the trans-acting polymerase. **(vii)** As elongation proceeds the 5' end of vRNA template needs to be released by the vRNA-associated polymerase to allow the trans-acting polymerase to read through the U sequence near the 5' end of vRNA to generate a full-length, run-off copy of vRNA. After the 5´ end of vRNA has been copied it re-binds the vRNP-associated polymerase while the 3' end of the newly synthesized cRNA binds to the trans-acting polymerase, which becomes part of the cRNP complex. Co-replicational encapsidation of cRNA with NP is not shown for simplicity. (Diagrams modified from Fodor [42])

1.1.2.4 Replication cycle – viral genome translation

Influenza virus mRNAs are translated by the host cell translation machinery, including several cellular translation factors such as eIF4A (eukaryotic initiation factor-4A), eIF4E and eIF4G interact with viral mRNAs and/or polymerase complexes [58]. Upon IAV infection, host cell protein synthesis is limited, and IAV mRNAs are preferentially translated [59]. In particular, 'cap-snatching' may deplete newly synthesized, nuclear mRNAs of their cap structures, resulting in their rapid degradation before nuclear export and translation. In addition, the interaction of NS1 with the cellular PABII (poly(A)-binding protein II) [60] and CPSF (cleavage and polyade-nylation specificity factor) proteins [61], and the interaction of the viral polymerase complex with the C-terminal domain of the largest subunit of cellular DNA-dependant RNA polymerase II (Pol II) [62] may contribute to the inhibition of host mRNA synthesis (reviewed in [63]). After their synthesis in the cytoplasm, the

viral polymerase subunit proteins and NP are imported into the nucleus via their nuclear localization signals [64] to catalyse the replication and transcription of vRNA. In addition, the M1 [65], NEP/NS2 [66] and NS1 [19] proteins are imported into the nucleus to execute their roles in vRNP nuclear export (M1 and NEP/NS2) or the processing and export of cellular and viral mRNAs (NS1) (reviewed in [19]).

1.1.2.5 Replication cycle – packaging and budding

There are two models for the packaging of a segmented, monocompartment genome. In a random model, a mechanism exists to distinguish pieces of the viral genome from cellular RNA and non-genomic viral RNAs and incorporate them into virions, but has no way of distinguishing between different segments (Fig. 1.7a). Under this hypothesize, a fully infectious virion would acquire a complete genome purely through chance, which the probability of success being increased by packaging more segments than the minimum required for a complete genome [67]. Infectious bursal disease virus, with a two segment double-stranded (ds)RNA genome, may provide an example of such a strategy, as distinct populations of virions with increasing numbers of segments and specific infectivities can be isolated [68]. Conversely, in a specific packaging model, a mechanism ensures that one copy of each different segment is specifically selected during viral assembly (Fig. 1.7b) [69]. The dsRNA bacteriophage Φ6 is a good example of this strategy as a specific packaging mechanism has been demonstrated for its three segments and the particle. PFU ratio of the virus is close to 1 [70]. These models represent the extreme cases of segment-specificity and absolutely no specificity in the former case and unfailingly rigorous selection in the latter. The extent to which packaging of the influenza A genome is in fact segment-specific has been debated, and evidence for varying degrees of segment-specificity has been presented.
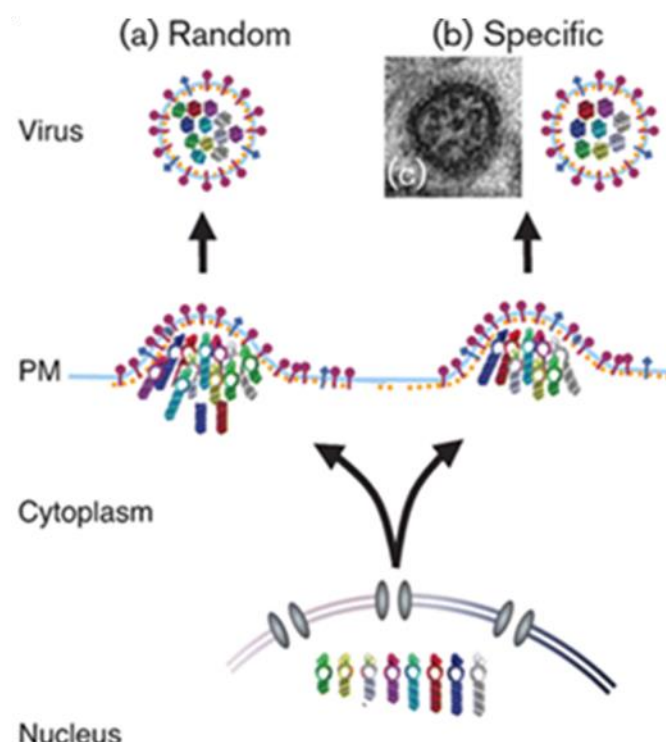
Fig. 1.7 Models of influenza virus particle assembly and genome packaging. The eight individual segments (differentiated by colour) are replicated independently in the nucleus before being exported to the cytoplasm and migrating to the apical plasma membrane. There, they interact with other viral structural proteins and new virus particles formed by budding. (a) The random model for genome packaging proposes that more than eight RNPs are incorporated in a segment non-specific manner such that a reasonable proportion of virions contain at least one copy of each segment. (b) The specific model proposes that unique segment-specific packaging signals operate to form a defined array of eight RNPs containing one copy of each segment. (c) A negatively stained EM section through an A/PuertoRico/8/34 (H1N1) influenza virion showing the distinctive 7+1 array of RNPs (appearing as dots in transverse section). (Diagrams modified from Hutchinson, *et al.* [53])

1.1.3 Host adaptation and transmission of influenza A viruses in mammals

Following the initial and sporadic emergence in humans of highly pathogenic avian H5N1 influenza A viruses in Hong Kong in 1997, I have come to realize the potential for avian influenza A viruses to be transmitted directly from birds to humans. Understanding the basic viral and cellular mechanisms that contribute to infection of mammalian species with avian influenza viruses is essential for developing prevention and control measures against possible future human pandemics. Multiple physical and functional cellular barriers can restrict influenza A virus infection in a new host species, including the cell membrane, the nuclear envelope, the nuclear environment and innate antiviral responses. In this report, I summarize current

knowledge on viral and host factors required for avian H5N1 influenza A viruses to successfully establish infections in mammalian cells.

1.1.3.1 Crossing the Plasma Membrane

The plasma membrane is the first cellular barrier that protects a host cell from virus infection. IAV must recognize specific receptors (sialic acids) in order to begin the infection of a cell [71]. There are two major types of linkages between sialyloligosaccharides (SAs) and galactose (Gal): SA-α2,6-Gal and SA-α2,3-Gal [71]. The HA proteins of human influenza viruses preferentially bind the SA-α2,6-Gal linkage, while the HA proteins of avian influenza virus have a higher affinity for SA-α2,3-Gal [72]. Thus, the tissue distribution of different sialic acid linkages is a major factor in determining the sites of initial virus infection and replication. SA-α2,3-Gal is abundantly expressed on avian intestinal and respiratory epithelial cells, but is only expressed in the lower, and not upper respiratory tracts of humans [73]. SA-α2,6-Gal is mainly distributed on human airway epithelial cells of the upper respiratory tract, but can be detected in the respiratory and intestinal tracts of several avian species [73]. Avian influenza viruses, including H5N1, recognize SA-α2,3-Gal as their receptors and efficiently target and replicate in the intestinal tracts of birds, but not in the upper respiratory tracts of humans. Nevertheless, efficient virus replication in the human upper respiratory tract would be more likely to result in aerosol-mediated human-to-human transmission. In this regard, the avian-origin HA proteins from the 1918, 1957 and 1968 human pandemic strains all recognized the SA-α2,6-Gal receptors [74, 75]. This may suggest that these HA proteins had switched their sialic-acid binding specificity at some point during their adaptation to humans [74]. Thus, it is believed that avian H5N1 viruses would also have to change their receptor binding preference from SA-α2,3-Gal to SA-α2,6-Gal in order to infect humans and transmit efficiently. Current human infections with H5N1 viruses that target SA-α2,3-Gal may lead to virus replication in the lower respiratory tracts of humans, thereby causing severe lung damage and disease. It cannot be excluded that such SA-α2,3-Gal-targeted viruses could also transmit between humans.

In recent years, it has become increasingly apparent that a number of mutations in HA and NA, that would require change their receptor binding preference from SA-α2,3-Gal to SA-α2,6-Gal. (See table 1.1)

Table 1.1 Amino acid mutation involved in receptor binding preference from SA-α2,3-Gal to SA-α2,6-Gal

Protein	Mutation	Adaptive mechanism	Reference
HA	N154S	Increase α2,6 binding	[76]
	A158T	Decrease α2,3 binding	[77]
	N182K	Increase α2,6 binding	[77]
	Q192R	Increase α2,6 binding	[77]
	Q222L	Increase α2,6 binding	[76]
	S223N	Increase α2,6 binding	[76]
	G224S	Increase α2,6 binding	[76]
	Q226L	Increase α2,6 binding	[71, 74]
	S227N	Increase α2,6 binding and decrease α2,3 binding	[78]
	G228S	Increase α2,6 binding	[79]
NA	Deletion in stalk	Functional balance with H5N1 by decreasing enzyme activity of H5N1	[80, 81]

1.1.3.2 Polymerase complex

Viral RNA polymerase is crucial for avian influenza viruses, since these polymerases have relatively poor activity in mammalian cells. Several amino-acid substitutions in the ribonucleoprotein complex are known to contribute to the host-range restriction of influenza viruses and increase replication in the mammalian host. High virus replication in the upper respiratory tract is critical for airborne transmission since decreased replication abolished airborne transmission between mammals [82]. In the study of Herfst *et al.* [83], the airborne-transmissible H5N1 virus possessed the E627K amino-acid substitution in PB2. However, it has yet to be elucidated if this residue is crucial for airborne transmission and whether it can be substituted by functionally equivalent mutations. The airborne-transmissible H5N1 viruses of Herfst *et al.* [83] possess several additional substitutions in the polymerase genes, which may have contributed to airborne transmission. A K627E substitution was found to reduce transmission in a direct contact transmission model for the highly pathogenic avian influenza (HPAI) H5N1 virus. Introduction of D701N in combination with the K627E substitution resulted in more efficient transmission in mammals, a phenotype more similar to that of the wild type viruses, suggesting that this residue can

compensate for the absence of 627K [84]. In the context of a human H3N2 virus, introduction of K627E resulted in less efficient transmission in guinea pigs [84]. Studies on the A(H1N1)pdm09 virus demonstrated that this virus was transmitted efficiently via the airborne route between ferrets [85]. Nevertheless, acquisition of the D701N substitution in A(H1N1)pdm09 virus resulted in more severe disease and increased transmission [86]. These data indicate that amino-acid positions 627 and 701 in PB2 are critical determinants of airborne transmission between mammals in diverse virus backgrounds. There is also evidence that the PB1 gene from an avian source promotes avian polymerase activity in mammalian cells [87]. Two mutations in PB1 (473V and 598P) were identified as increasing the polymerase activity of viruses carrying PB2 627E in mammalian cells [88]. More recently, it was found that mutations in NEP are also involved in host adaptation. The adaptive mutation M16I (and others) in the NEP proteins of certain human H5N1 isolates can increase the relatively low polymerase activity of avian viruses in mammalian cells [89]. These NEP mutations are more common in human H5N1 isolates carrying the PB2 627E mutation than in human H5N1 viruses possessing PB2 627K, which suggests that NEP can act as an important determinant of host adaptation by promoting efficient polymerase activity in human cells. Summary of mutations which are involved in increased polymerase activity and show in Table 1.2.

Table 1.2 Amino acid mutations involved in increased polymerase activity

Protein	Mutation	Adaptive mechanism	Reference
PB1	L473V	Increase polymerase activity of H5N1 and 2009pH1N1	[88]
	L598P	Increase polymerase activity of H5N1	[88]
PB2	Q591K	Increase polymerase activity of H5N1 and 2009pH1N1	[90]
	E627K	Increase polymerase activity of H5N1	[84, 91]
	D701N	Increase polymerase activity of H5N1 and H7N7	[92]
NEP	M16I	Increase polymerase activity of H5N1	[93]

1.1.3.3 Reassortment

Previously, it was believed that avian influenza viruses may not cause the next influenza pandemic directly, as pigs were considered a necessary intermediate host to facilitate reassortment between avian, swine and human influenza viruses. In addition, pigs were thought to serve as a critical host for initial mammalian adaptation. However, the role of pigs as mixing vessel for avian and human influenza viruses may not be unique, as humans can be infected with avian influenza viruses directly from an avian reservoir. Reassortment of the H5N1 virus with contemporary human influenza viruses did not easily yield an airborne-transmissible virus between mammals [94]. However, more recently, it was shown that several reassortant H5N1 virus variants were transmitted via the airborne route between guinea pigs [95]. This H5 virus, which revealed dual specificity for avian and human receptors, required the PA and NS genes of the A(H1N1)pdm09 virus to acquire airborne transmissibility between guinea pigs. In addition, the NP, M and NA genes from A(H1N1)pdm09 virus were important to enhance airborne transmissibility between mammals. These results appear to be in contrast to the study of Imai *et al.* [96] in which a reassortant virus with a mutant H5 HA with human receptor specificity in a A(H1N1)pdm09 virus backbone failed to transmit via the airborne route between ferrets. This difference may be explained by the use of different lineages of H5 HAs. In addition, it is unclear how the guinea pig and ferret models compare with respect to H5 virus transmission studies. However, as mentioned above, the avian-human reassortant influenza virus in the study of Imai *et al.* [96] transmitted via the airborne route after passaging in ferrets, when a few additional genetic changes in HA were acquired. These two studies thus demonstrated that different airborne-transmissible H5N1 strains can emerge upon reassortment between human and avian influenza viruses, as was previously also shown for avian H9N2 virus.

Fortunately, at present, reassortment of avian H5, H7 and H9 viruses with contemporary human influenza viruses has not been detected in nature. This may in part be explained by the relatively low number of human cases of avian influenza virus infections, and the low probability of double infections with human influenza viruses in a single host. In addition, influenza viruses have to infect the same cell, and similar timing of infection is necessary to initiate gene reassortment. However, co-infections of avian and human influenza viruses in humans or pigs may provide

new opportunities for reassortment, and evidence from pandemics of the last century indicates that the likelihood of such reassortment is not negligible.

The emergence of the A(H1N1)pdm09 virus demonstrated that pigs can be the direct source of pandemic influenza. Reassortment was responsible for the unique constellation of virus genes, which was shown to be a critical determinant of airborne transmission between ferrets [85], in particular the Eurasian swine-origin gene segments [97]. The emergence of H1N2 and H3N2 swine viruses underlines that swine populations should be monitored closely for the emergence of influenza viruses with pandemic potential. When the airborne transmissibility of these viruses was assessed, the H1N2 virus acquired substitutions in HA (D222G) and NA (S315N) during a single ferret passage that resulted in airborne transmission among ferrets. Reverse genetics studies further indicated that these amino-acid substitutions contributed substantially to the airborne transmissibility [98]. The viral RNA polymerase was also shown to promote airborne transmission [99]. Moreover, four swine H3N2v viruses, collected from 2009 until 2011, also possessed the capacity to spread between cohoused ferrets, and the 2010 and 2011 H3N2 viruses transmitted efficiently to naive ferrets via the airborne route [100]. These findings support the continuous threat of swine influenza viruses to humans, and the need for continued surveillance.

1.1.3.4 Unknown determinants of transmission

The role of other viral proteins in airborne transmission has so far remained elusive. The study of Zhang *et al.* [95] demonstrated that the PA, NS, M, NA and NP genes are important to confer airborne transmission; however, the key amino-acid substitutions remain unknown. In addition, it has been suggested that H5N1 viruses that acquire a long stalk NA through reassortment may be more likely to be transmitted among humans [101]. Although it is known that influenza virus morphology affects virus production, the relative contribution of spherical and more elongated versions of influenza virus to transmission is still unclear. Early work showed that most influenza virus strains isolated from humans are predominantly filamentous and, upon continued passage in egg or tissue culture, adopt a more spherical morphology, which correlated with increased virus titers [102]. It is possible that increased levels of influenza virus production by spherical strains will results in more efficient influenza virus transmission [97]. The contribution of substitutions in

the M gene segment on virus morphology and transmission warrants further investigation.

1.2 The non-structural (NS1) protein

NS1 protein is widely regarded as a multifunctional virulence factor, and is expressed at high levels in virus-infected cells [19]. It is not a structural component of the virion [103]. During infection, NS1 performs a plethora of activities that each contribute to efficient virus replication: Temporal regulation of viral RNA synthesis [104], enhancement of viral mRNA translation [58], regulation of virus particle morphogenesis [46], and suppression of the host immune/apoptotic responses [47] The protein-protein and protein-RNA interactions that mediate these functions are detailed below.
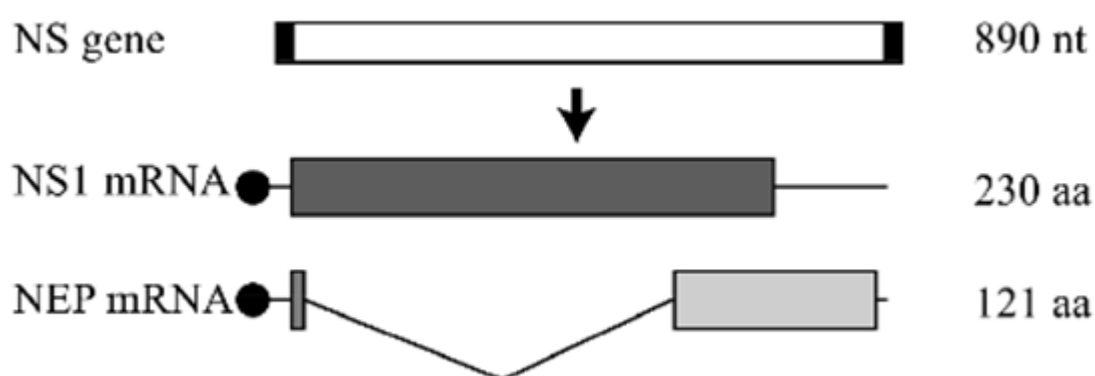
Fig. 1.8 Generation of the NS1 and nuclear export protein (NEP) mRNAs of the influenza A virus. The intact NS gene is represented as a white box flanked by black squares that represent the non-coding regions of the gene. Thin lines at the ends of the mRNAs represent untranslated regions. The 5' cap structures (black circles) and poly(A) tails in the mRNAs are shown. The open reading frame of the NS1 protein is represented as a gray box. The specific NEP open reading frame is shown as a hatched box. The NEP mRNA derived from the NS gene is a spliced product of the NS1 mRNA, as indicated by the V-shaped line. Reproduced from Garcia-Sastre *et al*. [103]

1.2.1 Synthesis of NS1 protein

The smallest genomic segment of influenza A virus (segment 8) is transcribed into two separate mRNAs, which encode the non-structural (NS1) and nuclear export (NEP) viral polypeptides [19] (Fig 1.8). A co-linear mRNA transcript directly codes for NS1, whilst NEP is translated from spliced mRNA [19]. Both mRNA species share a

56-nucleotide viral leader sequence, which contains the AUG initiation codon and encodes nine N-terminal amino acid residues common to NS1 and NEP [105]. Removal of the 473-nucleotide intron in order to form NEP mRNA means that after the 9 shared residues, translation of NEP continues in the +1 ORF relative to NS [106]. Thus, after the splicing site, the NS1 and NEP ORFs overlap by the equivalent of ~70 residues [106]. In infected cells, the steady-state amount of spliced NEP mRNA is only ~10% that of unspliced NS1 mRNA [107].

1.2.2 Sub-cellular localization of NS1 protein

The sub-cellular localization of NS1 protein appears to be dependent on several factors, including virus strain, expression level of NS1, cell-type used, state of cell-polarity and time post-infection [108]. Experimental detection of NS1 within cells is also determined by the fixation procedure used, as some fixatives (such as acetone) have been suggested to preferentially extract small proteins like NS1 from the cytoplasm [109]. At early work identified the NS1 protein in crystalline cytoplasmic inclusions that could be isolated from cells late in infection. NS1 proteins contain one or two nuclear localisation sequences (NLSs; NLS1 and NLS2), which mediate their active nuclear import via binding to cellular importin α-molecules [110]. As such, translocation of NS1 from cytoplasmic ribosomes to the nucleus is thought to be extremely rapid. NLS1 in NS1 is monopartite, and involves arginine-35, arginine-38, and lysine-41, residues also involved in dsRNA-binding [110]. This NLS is well-conserved among all known influenza A virus NS1 proteins [110]. In contrast, the bipartite NLS2 comprises specific amino-acids at the C-terminus of only some NS1 proteins (lysine-219, arginine-220, arginine-231 and arginine-232) [110].

Concurrent with NLS2 is a functional nucleolar localization signal (NoLS), which requires additional basic residues (usually arginine and lysine, respectively) at positions 224 and 229 [110]. Thus, although the NS1 proteins of most strains appear predominantly nuclear during virus infection, only a subset that contain a functional NoLS localise into nucleoli [110]. The nucleolar function of NS1 is unknown, however a mutant influenza A virus (A/Udorn/72 strain) expressing a truncated NS1 protein unable to localise into nucleoli was not attenuated for replication under tissue-culture conditions [110]. Therefore, it has been suggested that any nucleolar function of NS1

may only be necessary for the in vivo pathogenesis of some viruses [110]. As NLS2 is absent from the majority of pathogenic and non-pathogenic influenza A virus strains, it is difficult to ascribe a critical function to this sequence with regards viral replication/pathogenesis. Thus, many regulatory signals are responsible for the varied distribution of NS1 during infection (i.e. nuclear, nucleolar or cytoplasmic). Such varied localizations presumably contribute to the reported ability of NS1 to perform a number of different functions as detailed below (Fig 1.9).
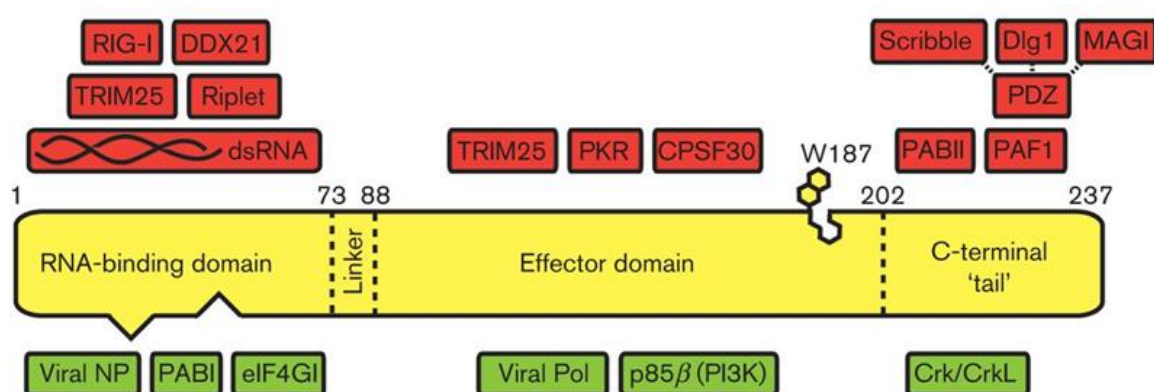
Fig. 1.9 Linear schematic of the NS1 domain layout and interactions. NS1 (yellow) can be divided into four distinct regions: the N-terminal RNA-binding domain (RBD), the linker region (LR), the effector domain (ED) and the C-terminal 'tail' (CTT). Interaction sites for NS1 to form homo-multimers are present in both the RBD (triangular cut-outs) and ED (W187). Both the LR and the CTT vary in length among strains: the longest total NS1 length reported is 237 aa, but 230 residues are common. NS1 interacts with many viral and cellular factors during infection, and some well-described examples are indicated: red-coloured factors are targeted by NS1 to inhibit cellular antiviral defences, while green-coloured factors are stimulated by NS1 to enhance virus replication (RIG-I, retinoic acid inducible gene I; DDX21, DEAD box helicase 21; TRIM25, tripartite motif containing 25; PKR, double stranded RNA activated protein kinase; PABII, poly(A) binding protein II; PAF1, RNA polymerase II associated factor; PABI, poly(A) binding protein I; eIF4GI, eukaryotic translation initiation factor 4 gamma, 1; Pol, polymerase). (Adapted from Hale BG [111])

1.2.3 NS1 and viral RNA synthesis

The NS1 protein has been reported to control the temporal synthesis of both viral mRNAs and vRNAs [56]. The highly conserved (>95%) isoleucine-123 and methionine-124 residues in the C-terminal effector domain of NS1 have been implicated in this activity as the substitution of these two residues for alanine resulted in the increased synthesis of all viral mRNAs and vRNAs early in infection [104]. In

particular, both HA and M1 (usually only synthesised in the "late" phase of infection) were synthesised "early" in the context of a mutant virus encoding NS1 with amino-acid substitutions at isoleucine-123 and methionine-124 [104]. The mechanism by which NS1 might regulate switches in viral vRNA, mRNA, and protein synthesis is unclear, but is not thought to involve PKR, a cellular protein bound by NS1 that can regulate translation (see below) [104]. One possibility is that NS1 functionally interacts with the viral polymerase complex to affect these processes [57].

1.2.4 NS1 and viral mRNA translation

As an RNA-binding protein, NS1 has been shown to interact in vitro with a variety of RNA species: dsRNA [112], viral genomic RNA [113], viral mRNA [59], poly(A)-containing RNAs [114] and snRNAs (small nuclear RNAs) derived from the U6 promoter [115]. As described below, the interactions of NS1 with putative viral dsRNA, viral genomic RNA and cellular poly(A)-containing RNAs (as well as the cellular proteins that may bind these ligands) likely play predominant roles in countering the host antiviral response [116]. Moreover, the possible interaction of NS1 with the 5'UTR (untranslated region) of viral mRNAs [59] has been linked to the ability of NS1 to directly enhance the translation initiation of viral mRNAs [117].

Other than possibly binding the 5'UTR of viral mRNAs, NS1-mediated enhancement of viral protein synthesis may also require its interaction with host-cell proteins. NS1 can form an RNA-protein complex consisting of the eukaryotic translation initiation factor eIF4GI, poly(A)-binding protein I (PABI) and viral mRNAs [58, 118]. The RNA-independent binding of NS1 to eIF4GI requires the N-terminal 113 residues of NS1 [118], whilst the RNA-independent interaction with PABI requires residues in the N-terminal 81 amino acids of NS1 [58]. Thus, mutant NS1 proteins unable to bind eIF4GI are also defective in enhancing viral mRNA translation [117].

In addition, NS1 interacts with hStaufen, a dsRNA-and tubulin-binding protein that is related to PKR [119]. The interaction is independent of RNA and appears to be mediated by the C-terminal effector domain of NS1 and the dsRNA-binding domains of hStaufen [119]. It has been speculated that the interaction between NS1 and hStaufen may also promote efficient protein synthesis from viral mRNAs [119].

Indeed, a proportion of both NS1 and hStaufen has been found to co-fractionate with cytoplasmic polysomes in influenza A virus infected cells [117]. Thus, in order to promote efficient viral protein synthesis, NS1 may interact with cellular hStaufen, eIF4GI and PABI to specifically recruit viral mRNAs to multi-protein translation-initiation complexes. The additional contribution of NS1 to viral protein synthesis by inhibiting PKR is discussed below.

1.2.5 NS1 and the host immune response

The innate interferon (IFN) response of the host-cell is a potent antiviral mechanism that can limit the replication and spread of viruses (reviewed in [120]). IFNs (such as IFNα or IFNβ) are soluble cytokines synthesised by cells in response to viral infection. Secreted IFNs act in both an autocrine and paracrine fashion to upregulate >300 genes and thereby induce an "antiviral state" within target host cells.

A number of studies have demonstrated, at the molecular level, how NS1 functions to limit both the production and downstream effects of IFN. As described below, it is becoming increasingly apparent that the mechanisms by which NS1 achieves this are likely to be strain and/or cell-type specific [121, 122].

1.2.5.1 Limitation of IFN production by NS1

Studies on the NS1 protein of influenza PR8 (H1N1) virus show that it can specifically prevent dsRNA-and virus-mediated activation of the transcription factors interferon regulatory factor-3 (IRF-3), NFκB and c-Jun/ATF-2, and thus limit induction of IFNβ [123]. This inhibition appears to occur pre-transcriptionally, and has been attributed to two residues in the dimerised RNA-binding domain of PR8/NS1: arginine-38 and lysine-41, which both mediate efficient RNA-binding [124]. Furthermore, recent work indicates that the mechanism of IFN inhibition may actually involve PR8/NS1 forming a complex with retinoic acid-inducible gene product I (RIG-I) [116]. Studies using the human H3N2 virus A/Udorn/72 (Ud) have revealed that Ud/NS1 can limit IFNβ induction by preventing the global post-transcriptional processing of cellular pre mRNAs [125]. For this, the C-terminal effector domain of Ud/NS1 binds directly to two zinc-finger regions in the 30 kDa subunit of cleavage and polyadenylation specificity factor (CPSF30) and also binds poly(A)-binding

protein II (PABII) [126]. NS1 binding to CPSF30 prevents the cellular protein from binding pre-mRNAs, thus inhibiting the correct cleavage and polyadenylation of host mRNAs [127]. NS1 binding to PABII is thought to block the nuclear export of mRNAs that might partially escape from the inhibition of 3'-end formation [128]. Retention of cellular pre-mRNAs within the nucleus of infected cells usually leads to their rapid degradation.

1.2.5.2 Inhibition of host-cell mRNA processing by NS1

It has been shown that the NS1 can also form a complex with components of the mRNA nuclear export machinery: NXF1, p15, Rae1, E1B-AP5 and to some extent Nup98 [47]. The complex formation between NS1 and NXF1, Rae1, and E1B-AP5 requires residues in both the RNA-binding and C-terminal effector domains of NS1, whilst the interaction with p15 appears to be mediated solely by the C-terminal effector domain [47]. In addition to inhibiting the 3'-end processing of host-cell pre-mRNAs (and thereby mRNA export) by binding CPSF30 and PABII, NS1 can act directly at the level of nuclear mRNA export transporters in order to prevent host protein synthesis.

Yeast two-hybrid studies also identified a novel ~70 kDa NS1-binding protein (subsequently termed NS1-BP) [129]. It has been proposed that the interaction between NS1 and NS1-BP may contribute towards the inhibition of host-cell mRNA processing, although a role for the interaction in regulating viral mRNA splicing cannot be ruled out [129].

1.2.5.3 Inhibition of IFN-inducible enzymes by NS1

The ability of some NS1 proteins to efficiently limit IFN and tumor necrosis factor α (TNFα) stimulated gene expression, has a beneficial effect on virus replication and pathogenicity [122]. However, NS1 also specifically blocks the activation of two cytoplasmic IFN-inducible anti-viral proteins. Firstly, 2'-5'-oligoadenylate synthetases (2'-5'-OAS) is activated by double-stranded RNA (dsRNA) (a putative by-product of RNA virus replication) that acts as co-factor to activate 2'-5'-OAS, which is then able to polymerizeadenosine triphosphate (ATP) into 2'-5'-oligoadenylate (2'-5' oligo(A)) chains (reviewed in [19]). These 2'-5' oligo(A) chains in turn cause dimerisation and activation of the latent ribonuclease RNaseL that inhibits viral replication (translation)

by degrading single-stranded RNAs, such as mRNAs and ribosomal RNAs (reviewed in [19].

Secondly, dsRNA also activates protein kinase-R (PKR). PKR is activated by dsRNA. PKR can be activated by the protein PACT or by heparin. PKR contains an N-terminal dsRNA binding domain (dsRBD) and a C-terminal kinase domain that gives pro-apoptotic functions. NS1 can binds to specific motifs within the N-terminal domain of PKR, and thereby releases its conformational induced auto inhibition of both cellular and viral protein synthesis (reviewed in [130]). PKR also play roles in upregulating gene expression of IFNβ from IRF-3 and NFκB responsive promoters (reviewed in [130]), and is involved in initiating the apoptotic response. Thus, it is beneficial for virus to block both 2'-5'-OAS and PKR as they play important roles in limiting virus replication.

1.2.5.4 NS1 and the adaptive immune response

Studies on human-derived primary dendritic cell (DCs) have revealed that the influenza A virus NS1 protein is able to prevent the correct maturation of DCs in response to virus infection, and thereby limits host T-cell activation [131]. Specifically, infection of DCs with PR8delNS1 virus (PR8 lacking the ability to express full-length NS1) leads to the secretion of higher amounts of IFNα, IFNβ, TNFα, and IL-6, as compared to the WT virus [131]. Expression of WT NS1 also specifically limited the virus-induced expression of several genes involved in DC maturation and migration, including: MHC, IL-8, IL-12, p35, IL-23, p19, IRF-7, RANTES, TRIF, MIP-1β and CCR7 [131]. Thus, DCs infected with influenza A viruses expressing WT NS1 are unable to mature, and thereby fail to stimulate the secretion of IFNγ from T-cells [131]. This effect of NS1 would clearly have a profound inhibitory effect on the adaptive immune response to infection.

1.2.6 Effect of NS1 on other cell signaling pathways

The NS1 proteins from five different human and avian influenza A virus strains can associate with NS1-I, a human protein highly homologous to the porcine 17β-estradiol dehydrogenase precursor protein, which may mediate steroid hormone levels [132]. Although the function of this interaction is not well understood,

overexpression of NS1-I in 293 cells specifically reduces the expression of influenza A virus proteins, suggesting that NS1-I has antiviral activity that may be inhibited by NS1 [132]. Moreover, large-scale sequence analyses of avian influenza A viruses have also revealed two other putative protein binding motifs within NS1: a Src-homology 3 (SH3) binding motif (residues 212-216) [133] and a PDZ domain ligand. These containing SH3 or PDZ domains often coordinate the assembly of a diverse array of localized signaling complexes. *In vitro* studies have shown that the PDZ domain ligand of highly pathogenic avian influenza virus NS1s (including those from H5N1 and 1918 strains) can bind over 30 different human PDZ-proteins [134].

1.2.7 NS1 and the host apoptotic response

During infection, influenza A viruses induce cell death by both apoptosis [135] and necrosis [136]. Most infected cells undergo apoptosis by intrinsic mechanisms, however influenza A virus can induce apoptosis in neighbouring, uninfected cells by triggering the release of extracellular cytokines that act in a paracrine fashion [137].

The exact function of NS1 with regard to virus-induced apoptosis/cell-death is unclear, and may be dependent upon specific host-cell factors or virus strains. For example, Ud/NS1 on its own appears to be extremely toxic to MDCK cells, but not in HeLa cells [138] and Ud/NS1 (but not PR8/NS1) inhibits the processing of cellular pre-mRNAs, a process likely to be toxic to the cell [139]. However, in the context of virus infection, NS1 appears to have anti-apoptotic functions, which have been linked largely to its ability to limit the production and/or downstream effects of IFN [140]. As such, catalytically active PKR is reported to play an important role in influenza A virus-mediated induction of apoptosis [141], thus the direct binding and inhibition of PKR by NS1 may contribute to cell-death suppression [142]. The same may be true for the pro-apoptotic functions of 2'-5' OAS/RNaseL [143]. In addition, by limiting the production of IFN and other cytokines, NS1 might reduce paracrin-mediated (extrinsic) apoptosis induction in neighbouring uninfected cells [144]. Overall, there may be a temporal role for NS1 in contributing to both "early" (active) suppression of apoptosis, and "late" (toxic) induction cell-death during infection.

1.3 NS1 protein and host range

During infection, the host innate immune response is elicited to counteract virus replication. Influenza A viruses limit this cellular defense mechanism in infected cells by producing the NS1 protein from genomic segment 8. In recent years, it has become increasingly apparent that a number of NS1 functions are virus strain-specific. All NS1 proteins appear to bind and neutralize RIG-I ligands (such as 5′triphosphated RNAs) as part of their antagonism of RIG-I signaling [63]. However, another mechanism by which NS1 proteins can inhibit RIG-I activation is by preventing the ubiquitination of RIG-I by both TRIM25 or Riplet ubiquitin E3 ligases and this function appears to vary between strains [64]. Studies suggest that an avian-type H5N1 NS1, but not human/swine-type NS1s, can bind efficiently to chicken TRIM25 to suppress IFN production in chicken cells. In contrast, all NS1s tested so far (including avian, swine, and human) appear to interact with human TRIM25. Interestingly, the avian H5N1 NS1 protein used in the above study failed to interact with human Riplet, while human-type NS1 proteins bind human Riplet and inhibit its RIG-I activating function [64]. It remains to be determined precisely whether the various different NS1-TRIM25/Riplet binding specificities contribute to avian-mammalian transmission.

The interaction of NS1 with CPSF30 is also strain-dependent. The viruses isolated after 1998 carry out mutations residues 103 and 106 on NS1 of H5N1 viruses, which acquiring the ability to bind human CPSF30 and thereby better suppress the human IFN response [65].

Sequence analyses have revealed several features of NS1 that are potentially relevant to host adaptation. Firstly, the NS1 gene can be divided into two major alleles: A and B [20]. Allele A NS1s are found in both avian and human viruses, while allele B NS1s are only found in avian viruses [67, 68]. Viruses with allele A NS1s appear to have a replication advantage over those with allele B NS1s in mammalian cells, suggesting that those avian H5N1 influenza viruses carrying allele A NS1 genes may already have acquired functions adapted to replicate in mammals. In NS1 feature revealed by sequencing is the presence of strong or weak PDZ-ligand domain consensus motifs located at the C-terminus of NS1. Such motifs have been

identified as virulence determinants [69]. NS1 proteins with avian-like PDZ-ligand domains (including H5N1) are associated with high virulence in mammals [70], which may result from binding of these 'strong' PDZ-ligand domains to several human PDZ-containing proteins [73]. Therefore, it is possible that switching from avian-type ('strong') to human-type ('weak') PDZ-ligand domain motifs is required during full avian-to-mammal adaptation as a virus reaches equilibrium with its host and virulence is compromised. The C-terminus of NS1 is thought to be unstructured [74], and is highly variable in length between strains [68, 75]. Different variants may have different host-specific preferences relating to cellular binding partners, which will include cellular PDZ-domain containing proteins as well as other proteins. Whether the C-terminal length variability of NS1 proteins contributes to host adaptation remains to be thoroughly examined.

1.4 Aims

Highly pathogenic avian influenza viruses (HPAIV) with reassorted NS segments from H5 (GD; A/Goose/Guangdong/1/1996) and H7 (A/Mallard/NL/12/2000) type avian virus strains placed in the genetic background of A/FPV/Rostock/34 HPAIV (FPV-H7N1) were generated by reverse genetics (FPV-NS^{GD} and FPV-NS^{MA}). Virological characterisation demonstrated that growth kinetics of the reassortant viruses differed from the wild type FPV and depended on cells of mammalian or avian origin. Surprisingly, molecular analysis revealed that the different reassortant NS segments were not only responsible for alterations in the anti-viral host response, but also affected viral genome replication and transcription. Polymerase reconstitution experiments demonstrated the effects on accumulation of viral RNA species depended on the specific NS-segment. IFN-beta expression and the induction of apoptosis were found to be inversely correlated with the magnitude of viral replication. Based on the above results, especially based on the fact that the NS-GD and NS-MA proteins only differ in eight amino acids, and NS-GD and NS-MA in the FPV genetic background lead to dramatically different propagation characteristics of reassortant viruses. I therefore aim to analyze which amino acids or which combination of amino acids are implicated in

      I.   an effect on the viral polymerase regarding viral genome replication, transcription.

      II.   viral propagation (growth rate) and transmission.

      III.   the effect of the NS protein on the global of cellular transcription profile in mammalian host.

Chapter 2

Materials and Methods

2.1 Materials

2.1.1 Instruments

Abbocath-T (26Gx19mm)	Hospira
Bio Imaging Analyzer (BAS 2000)	Fuji Film
BioMax TranScreen HE Intensifying Screen	Kodak
BioMax Cassette	Kodak
Cell culture incubator	Heraeus; Nuaire
Cell culture microscope	Hund
Confocal laser scanning microscope (TCS SP5)	Leica
Culture Hood (HB2448)	Heraeus
Developing machine	Optimax, Protec
Disposable Razor Med Comfort	AMPri GmbH
Electrophoresis apparatus system	Institute for Medical Virology
Electrophoresis power supply (EPS500/400)	Pharmacia
ELISA reader (Type LP 400)	Diagnostic Pasteur
FACScan	Becton Dickinson, USA
Fine scale (Mettler PM460)	Mettler Waagen GmbH
Heat block	Jumotron
Luminex^{TM} Reader	Biorad
Magnetic stirrer	IKA Labortechnik
Megafuge 1.0 R	Heraeus
Microwave oven	Quelle
Mini centrifuge	Biofuge 13, Heraeus
Neubauer chamber	Optik Labor
Omincan 50	Braun Medical
pH meter (Type 632)	Metrohm
Shaker (Type 3013)	MSGV GmbH
Scale (P1200)	Mettler
Scanner Canonscan 9900F	Canon

SDS-PAGE gel system	Invitrogen, Germany
Sonicator (Type HD70)	Bondelin Sonoplus
Spectrophotometer (DU-70)	Beckman
Sterile needles	BD Microlance 3 BD
Syringe (microliter, serial 700)	Hamilton
Syringe 20ml single use	Braun, Melsungen AG
Tissue Ruptor	Qiagen
Vortex (Vibrofix VF1)	IKA Labortechnik
Water bath (SW-20C)	Julabo

2.1.2 Reagents and general materials

1 kb DNA ladder mix	PEQLAB
10X restriction enzyme buffer 1, 2, 3 and 4	NEB
10X AccuPrime Pfx DNA polymerase buffer	Invitrogen
Acrylamide	Bio-Rad
Ammonium persulfate (APS)	Serva
AccuPrime dNTPs (3 mM)	Invitrogen
Accutase	PAA
Acetic acid	Roth
Agar high-gel strength	Serva
Agarose ultra pure	Roth
Aprotinin	Roth
β-mercaptoethanol (MetOH)	Roth
Benzamidin	Sigma
Blotting papers (GB004)	Scheicher & Schuell
Bradford reagent	Bio-Rad
Bromophenol blue	Merck
Boric acid	Roth
BSA (Solution, 30%)	MP Biomedicals
BSA (Powder)	Roth
Casein Bacto-Casitone	Difco Laboratories
Chloroform	Roth
Coomassie brilliant blue R 250	Merck

Cryotubes	Nunc
Cuvette	Bio-Rad
DAB Peroxidase substrate	
(3,3'-Diaminobenzidine)	Sigma
DAPI (stock 1mg/ml)	Sigma
DEAE Dextran (MW: 500,000)	Pharmacia Biotech
1,4-Diazabicyclo [2,2,2]octane (DABCO)	Merck
Dimethylsulfoxid (DMSO)	Sigma
1,4-Dithiothreit ($C_4H_{10}O_2S_2$) (DTT)	Roth
DNA loading buffer (6X)	PeqLab
Eppendorf tube	Eppendorf
Ethanol (absolute)	Roth
Ethidium bromide	Roche
Ethylenediamine tetraacetic acid (EDTA)	Fluka
Glycerol	Sigma
Glycine	Roth
Hydrochloride (HCl)	Roth
Isopropanol	Roth
Kodak® BioMax™ MS film (20cm×25 cm)	Sigma
Leupeptin	Sigma
Magnesium chloride ($MgCl_2$)	Merck
Microtiter plate (96 wells)	Greiner
Mowiol 40 – 88	Aldrich
Methanol	Roth
Oxoid Agar	Oxoid
Paraformaldehyde (PFA)	Merck
Pefablock	Roth
Peptone from meat trypsin-digested	Merck
Potassium chloride (KCl)	Roth
Precision Plus Protein Standards (All Blue)	Bio-Rad
Potassium dihydrogen phosphate (KH_2PO_4)	Roth
Propidium Iodide	Sigma
PVDF-Membrane Immobilon-P transfer membrane	Millipore
Rainbow marker	Amersham

Roti-Free, ready-to-use Stripping Buffer	Roth
Scientific Imaging film BioMax MR	Kodak
Sodium chloride (NaCl)	Roth
Sodium dodecyl sulfate (SDS)	Merck
Sodium-β-glycerophosphate	Sigma
Sodium hydroxide (NaOH)	Merck
Sodium hydrogen carbonate (NaHCO$_3$)	Fluka
Sodium orthovanadate	Sigma
Sodium pyrophosphate	Sigma
TEMED (N,N,N',N'-Tetramethyl-ethylene diamine)	Serva
TLC plates (20 x 20 cm Silica gel 60)	Merck
TranIT2020	Mirus
Trypsin-EDTA (10X)	PAA
Tris-HCl	Roth
Triton X-100 (t-Octylphenoxypolyethoxyethanol)	Sigma
Trizol Reagent	Invitrogen
Tween 20	Roth
Trypan blue	Gibco
Urea	Sigma
Whatman 3MM Paper	Schleicher & Schüll

2.1.3 Monoclonal and polyclonal antibodies

Antibody	Company	Dilution
Anti-flu A NP mouse monoclonal IgG	SantaCruz Biotechnology	1:500
Anti-flu A NS1 mouse monoclonal IgG	SantaCruz Biotechnology	1:2000
Anti-flu A GST-NS1 mouse monoclonal IgG	Kind gift from Dr. T. Wolff, Berlin, Germany	1:2000
HRP conjugated goat anti-mouse IgG	SantaCruz Biotechnology	1:1000
HRP conjugated goat anti-rabbit IgG	SantaCruz Biotechnology	1:1000
Anti-flu A NP (FPV) mouse (clone 1331)	Biozol–Biodesign Internat.	1:5000
Anti-influenza A PR/8/34 rabbit polyclonal IgG	Biomol-US Biological	1:1000
Alexa 594 anti-mouse	Invitrogen	1:200
Alexa 594 anti-rabbit	Invitrogen	1:200

2.1.4 Materials for cell culture

Chicken Serum	Sigma
Dulbecco's Modified Eagle's medium (DMEM)	Invitrogen
Fetal calf serum (FCS)	PAN
HIMF10	Invitrogen
L-Glutamine 100X	Invitrogen
Minimum Essential Media (MEM) (10X)	Invitrogen
Penicillin-streptomycin solution (100X)	PAA
TPCK-treated Trypsin (10X)	PAA
Tissue culture dish	Becton Dickinson
Tissue culture flask	Nunc
Tryptose Phosphate Broth	Sigma
Bovine Albumin (30% BSA)	PAA

2.1.5 Enzymes

AccuPrime Pfx DNA Polymerase	Invitrogen
GoTaq flexi DNA polymerase	Promega
Platinum^R Pfx DNA polymerase	Invitrogen
SuperScript ^{TM} III reverse transcriptase	Invitrogen
T4 Ligase	NEB
T4 polynuleotide kinase (10,000 units/ml)	NEB

2.1.6 Kits

AEC staining kit	Sigma
Bradford Protein Assay Kit	
ECL (enhanced chemiluminescence) solution Kit	Amersham/GE
High pure PCR product purification Kit	Roche
In situ cell death detection Kit, fluorescein	Roche
NucleoPond Xtra Maxi Kit for DNA plasmids prep	Macherey-Nagel
pcDNA^{TM} 3.1 directional TOPO expression Kit	Invitrogen
QIAprep Spin Miniprep Kit (250)	Qiagen
QIAamp Viral RNA Mini Kit (250)	Qiagen
Qiagen plasmid Maxi Kit	Qiagen
Nucleotide removal Kit TOPO XL PCR cloning Kit	Qiagen
Caspase-3 activity	Abcam
Rapid DNA ligation Kit	Roche
QuikChange® Site-Directed Mutagenesis Kit	Stratagene
Human Interferon beta Kit	PBL Assay Science

2.1.7 *E. coli* strain, recombinant viruses and cell lines

E. coli strain

XL1-Blue	Stratagene
TOP 10	Invitrogen

Recombinant influenza viruses

A/FPV/Rostock/34 (H7N1) (FPV-WT)	Rescued at the Institute of Medical Virology, Giessen
FPV-NS^{GD}	Rescued at the Institute of Medical Virology, Giessen
FPV-NS^{MA}	Rescued at the Institute of Medical Virology, Giessen
FPV-NS$^{MA\_P3S}$	Rescued at the Institute of Medical Virology, Giessen
FPV-NS$^{MA\_R41K}$	Rescued at the Institute of Medical Virology, Giessen
FPV-NS$^{MA\_D74N}$	Rescued at the Institute of Medical Virology, Giessen
FPV-NS$^{MA\_I98M}$	Rescued at the Institute of Medical Virology, Giessen
FPV-NS$^{MA\_D153S}$	Rescued at the Institute of Medical Virology, Giessen
FPV-NS$^{MA\_M166V}$	Rescued at the Institute of Medical Virology, Giessen
FPV-NS$^{MA\_P213S}$	Rescued at the Institute of Medical Virology, Giessen
FPV-NS$^{MA\_R224K}$	Rescued at the Institute of Medical Virology, Giessen

FPV-NS^{MA_P3S+R41K}

Rescued at the Institute of Medical Virology, Giessen

FPV-NS^{MA_P3S+R41K+D74N}

Rescued at the Institute of Medical Virology, Giessen

FPV-NS^{MA_P3S+R41K+D74N+I98M}

Rescued at the Institute of Medical Virology, Giessen

FPV-NS^{MA_P3S+R41K+D74N+I98M+D153S}

Rescued at the Institute of Medical Virology, Giessen

FPV-NS^{MA_P3S+R41K+D74N+I98M+D153S+M166V}

Rescued at the Institute of Medical Virology, Giessen

FPV-NS^{MA_P3S+R41K+D74N+I98M+D153S+M166V+P213S}

Rescued at the Institute of Medical Virology, Giessen

FPV-NS^{MA_P3S+R41K+D74N+I98M+D153S+M166V+P213S+R224K}

Rescued at the Institute of Medical Virology, Giessen

FPV-NS^{GD/MA}

Rescued at the Institute of Medical Virology, Giessen

FPV-NS^{MA/GD}

Rescued at the Institute of Medical Virology, Giessen

Cell lines

A549 (Human Alveoar Epithelial cells)	ATCC
MDCK-II (Madin-Darby canine kidney cells)	Cell-collection of the Institute of Medical Virology, Giessen
293T (Human embryonic kidney cells)	Cell-collection of the Institute of Medical Virology, Giessen
QT6 (quail fibroblast cells)	Kind gift from the Institute for Virology, Marburg

2.1.8 Plasmids

pPolI-FPV-PB1 (A/FPV/Rostock/34 (H7N1))	Kind gift from the Institute for Virology, Marburg
pPolI-FPV-PB2 (A/FPV/Rostock/34 (H7N1))	Kind gift from the Institute for Virology, Marburg
pPolI-FPV-PA (A/FPV/Rostock/34 (H7N1))	Kind gift from the Institute for Virology, Marburg
pPolI-NP (A/FPV/Rostock/34 (H7N1))	Kind gift from the Institute for Virology, Marburg
pPolI-FPV-HA (A/FPV/Rostock/34 (H7N1))	Kind gift from the Institute for Virology, Marburg

pPolI-FPV-NA (A/FPV/Rostock/34 (H7N1))   Kind gift from the
                                           Institute for Virology,
                                           Marburg

pPolI-FPV-M (A/FPV/Rostock/34 (H7N1))   Kind gift from the
                                           Institute for Virology,
                                           Marburg

pPolI-FPV-NS (A/FPV/Rostock/34 (H7N1))   Kind gift from the
                                           Institute for Virology,
                                           Marburg

pCI-GD-NS (A/Goose/Guangdong/1/96 (H5N1)) Kind gift from the
                                           Institute for Virology,
                                           Marburg

pPolI-MA-NS (A/Mallard/NL/12/2000 (H7N3)) Kind gift from the
                                           Institute for Virology,
                                           Helsinki

pPolI-Ma-NS$^{GD/MA}$ (A/Mallard/NL/12/2000 (H7N3)) Kind gift from the
                                           Institute for Virology,
                                           Helsinki

pPolI-Ma-NS$^{MA/GD}$ (A/Mallard/NL/12/2000 (H7N3)) Kind gift from the
                                           Institute for Virology,
                                           Helsinki

pHMG-PA (A/Puerto Rico/8/34(H1N1))   Kind gift from the
                                           Institute for Virology,
                                           Zurich

pHMG-PB1 (A/Puerto Rico/8/34(H1N1))   Kind gift from the
                                           Institute for Virology,
                                           Zurich

pHMG-PB2 (A/Puerto Rico/8/34(H1N1))   Kind gift from the
                                           Institute for Virology,
                                           Zurich

pHMG-NP (A/Puerto Rico/8/34(H1N1))   Kind gift from the
                                           Institute for Virology,
                                           Zurich

pPolI-CAT-RT (Human Pol promoter)	Kind gift from the department of microbiology, Mount Sinai School of Medicine, New York
pcDNA3.0-GD-NS1(A/Goose/Guangdong/1/96 (H5N1))	Constructed at the Institute of Medical Virology, Giessen
pcDNA3.0-MA-NS1(A/Mallard/NL/12/2000 (H7N3))	Constructed at the Institute of Medical Virology, Giessen
pcDNA3.0-MA-NS1^{D74N}(A/Mallard/NL/12/2000 (H7N3))	Constructed at the Institute of Medical Virology, Giessen
pcDNA3.0-MA-NS1$^{P3S/R41K/D74N}$ (A/Mallard/NL/12/2000 (H7N3))	Constructed at the Institute of Medical Virology, Giessen
pcDNA3.1-FPV-NP (A/FPV/Rostock/34 (H7N1))	Constructed at the Institute of Medical Virology, Giessen
pcDNA3.0-FPV-PB1(A/FPV/Rostock/34 (H7N1))	Constructed at the Institute of Medical Virology, Giessen
pcDNA3.0-FPV-PB2(A/FPV/Rostock/34 (H7N1))	Constructed at the Institute of Medical Virology, Giessen
pcDNA3.0-FPV-PA(A/FPV/Rostock/34 (H7N1))	Constructed at the Institute of Medical Virology, Giessen

2.1.9 Medias, buffers and solutions

Avicel Medium (100 ml)

10	ml	10X MEM
33	ml	ddH$_2$O
1	ml	Penicillin/Strepromycin liquid (100X)
1	ml	BSA solution (35%)
50	ml	Avicell Stock (2.5%)
1	ml	DEAE-Dextran (1%)
4	ml	NaHCO3 (7.5%)

Avicel Stock (2.5%)

5	g	Avicel-Powder
200	ml	ddH$_2$O

Cell culture medium for QT6 cells (500 ml)

425	ml	HAM's-F10 media
5	ml	Penicillin/Strepromycin liquid (100X)
5	ml	L-Glutamine
50	ml	Fetal Calf Serum (FCS)
5	ml	Chicken Serum
10	ml	Tryptose Phosphate Broth

Cell fixing buffer (100 ml)

95	ml	PBS++
4	ml	Formaldehyde (PFA) (37%)
1	ml	Triton X-100 (t-Octylphenoxypolyethoxyethanol)

DMEM/BA (500 ml)

492	ml	DMEM
5	ml	Penicillin/streptomycin (100X)
3	ml	Bovine Albumin (BA) (30%)

2X DMEM/BA for Plaque-Assay (500 ml)

100	ml	MEM (10X)
10	ml	Penicillin/Streptomycin (100X)
20	ml	$NaHCO_3$ (7.5%)
6	ml	Bovine Albumin (BA) (30%)
354	ml	ddH_2O

Luria-Broth (LB) medium

Extract of yeast powder (0.5%) (w/v)

Peptone from meat trypsin-digested (1%) (w/v)

adjust pH to 7.5 with NaOH and total volume to 1 L with ddH_2O, autoclaved

for plates, add agar high-gel strength (1.5%) (w/v), autoclaved

Infection media (for MDCK, A549 and 293T) (100 ml)

98.5	ml	DMEM (1X)
1	ml	Penicillin/Strepromycin liquid (100X)
500	ul	BSA (30%)

Infection media (QT6) (100 ml)

95.5	ml	HAM's-F10 media
1	ml	Penicillin/Strepromycin liquid (100x)
1	ml	L-Glutamine
2	ml	Tryptose Phosphate Broth
500	µl	BSA (30%)

Mowiol mounting medium

Mowiol 4-88

Glycerol

Tris-HCl (0.2 M, pH 8.5)

DABCO (1,4-diazabicyclo-[2,2,2]-octane)

SDS-PAGE stacking gel (1 gel)

2.9	ml	ddH_2O
1.25	ml	Tris-HCl, pH 6.8 (0.5 M)
50	µl	SDS (10%)
750	µl	Polyacrylamide (PAA) (30%)
50	µl	APS (10%)
4	µl	TEMED

SDS-PAGE resolving gel (10%) (1 gel)

4	ml	ddH_2O
2.5	ml	Tris-HCl, pH 8.8 (1.5 M)
100	µl	SDS (10%)
3.3	ml	Polyacrylamide (PAA) (30%)

SM medium

Gelatin (0.01%)

NaCl 250 mM

$MgSO_4$ 8.5 mM

Tris–HCl 50 mM, pH 7.5

SOC Medium

Tryptone (2%) (w/v)

Yeast extract (0.5%) (w/v)

NaCl 10 mM

$MaCl_2$ 10 mM

Glucose 20 mM

Prepare a solution containing the first four reagents, sterilize at 121°C, then add sterile $MgCl_2$ and Glucose

6%, 7M urea polyacrylamide gel

21	g	Urea
5	ml	10X TBE
7.5	ml	Acrylamide (40%)

Fill up the tube to 50ml with sterile water

0.5	ml	APS (10%)
0.05	ml	TEMED

Blocking buffer and antibody diluting solution

Non-fat dry milk (5%) (w/v) in 1XTBS-T (see below)

Lysis buffer

10	ml	TLB buffer (see TLB buffer)
10	µl	Pefablock (200 mM)
10	µl	Aprotinin (5 mg/ml)
10	µl	Leupeptin (5 mg/ml)
100	µl	Sodium orthovanadate (100 mM)
50	µl	Benzamidine (1 M)

1XPBS^{++} buffer (500 ml)

495	ml	1XPBS (autoclaved)
5	ml	Ca^{2+}/Mg^{2+} solution (100X)

PBS/Ca^{2+}/Mg^{2+}/BA/antibiotic (200ml)

20	ml	10X PBS (see above)
174.8	ml	ddH_2O (sterile)
2	ml	Penicillin/Streptomycin (100X)
1.2	ml	BSA (30%)
2	ml	Ca^{2+}/Mg^{2+} (100X)

SDS-PAGE loading buffer (2X) (Laemmli Buffer)

100	mM	Tris-HCl, pH 6.8
200	mM	DTT (dithiothreitol)
		SDS (4%)
		Glycerol (20%)
		Bromophenol blue (0.2%)

SDS-PAGE running buffer (5X) (1000 ml)

1	g	SDS
6	g	Tris-HCl
28.8	g	Glycin

adjust total volume to 1 L with ddH$_2$O

SDS-PAGE transfer buffer (1000 ml)

5.8	g	Tris-HCl
2.9	g	Glycin
0.17	g	SDS
200	ml	Methanol

adjust to total volume to 1 L with ddH$_2$O

TAE buffer (10X) (1000 ml)

48.5	g	Tris
11.4	ml	Glacial acetic acid
20	ml	0.5 M EDTA (pH 8.0)

TAE buffer (1X)

Dilute stock solution 10X (10:1) in ddH$_2$O

1XTAE buffer contain

40	mM	Tris
20	mM	Acetic acid
1	mM	EDTA

TLB buffer

20	mM	Tris-HCl, pH 7.4
137	mM	NaCl
		Glycerol (10%) (v/v)
		Triton X-100 (1%) (v/v)
2	mM	EDTA
50	mM	Sodium-β-glycerophosphate
20	mM	Sodiumpyrophosphate

Tris-Buffered Saline (10X TBS) (1000 ml)

24.2	g	Tris-HCl
80	g	NaCl

dissolve by adding 900 ml ddH$_2$O

adjust pH to 7.6 and total volume to 1 L with ddH$_2$O

TBS/Tween (0.05%) (1XTBS-T) (1000 ml)

100	ml	10X TBS
900	ml	ddH$_2$O
0.5	ml	Tween 20

2.2 Methods

2.2.1 DNA cloning and sub-cloning

2.2.1.1 Preparation of competent cells for DNA transformation

10 μl glycerol stock of *Escherichia coli* XL1-Blue (or DH5α) strain was transferred into 10 ml LB medium. Cells were grown overnight at 37°C on the incubator shaker with moderate shaking (200 rpm). 10 ml overnight culture was transferred into 1 L LB medium. Cells were grown for additional 3-4 h at 37°C until the OD_{595} reached 0.5-0.8. After cooling down on ice for 30 min, cells were transferred into four sterile 250 ml centrifugation tubes and pelleted by centrifugation for 10 min at 10,000 rpm (Biofuge 13, 16,000 g), 4°C. Then cells were sequentially resuspended in 500ml of chilled 1 mM HEPES (pH 7.0), pelleted again by centrifugation and resuspended in 250 ml of chilled 1 mM HEPES (pH 7.0), pelleted by centrifugation again as above. The cells were resuspended in 50 ml chilled 10% glycerol in ddH_2O, centrifuged again as above and resuspended in 2.5-3 ml 10% (v/v) glycerol. Competent cells were aliquoted in 100 μl on ice. The tubes containing the competent cells were placed into fluid nitrogen to be frozen, and then stocked immediately at -70°C.

2.2.1.2 Transformation cells by heat sock

10 µl of plasmid DNA (10 ng/µl) or 20 μl of desalted ligation mixture was mixed in 100 μl of rapidly thawed competent cells by stirring gently with the pipette tip. After a short incubation in ice, a mixture of chemically competent bacteria and DNA is placed at 42°C for 45 seconds (heat shock) and then placed back in ice. SOC media is added and the transformed cells are incubated at 37°C for 30 min with agitation, Afterward, the cells and SOC medium mixture was centrifuged shortly after incubation, then only 100 µl medium was kept in the eppendorf tube, rest of supernatants were discarded. The cell pellet was resuspended in the 100 µl liquid as mentioned and spread onto a pre-warmed LB plate containing 100 µg/ml ampicillin. The plates were incubated overnight at 37°C (plasmid transformed bacteria are selected on LB plates with ampicillin). After 16 h incubation, the single colony was picked and inoculated in LB medium with ampicillin and shaken overnight at 37°C. The bacteria culture was then used for preparing plasmid DNA and frozen glycerol stocks by mixing 850 µl bacteria culture with 150 µl autoclaved 100% glycerol.

2.2.1.3 Preparation of plasmid DNA

Plasmid DNA maxi preparation was performed using QIAprep plasmid midi or maxi Kit. The culture of bacteria containing plasmids was grown in 100 ml of LB media overnight in 37°C incubator with shaking at 200 rpm. The bacteria were collected by centrifuging the overnight culture at 6,000 rpm (Beckman JA14, 7,500 g) and 4°C for 15 min. Then after the bacterial pellet was resuspended in 10 ml of buffer P1 and 10 ml buffer P2 was added. The whole mixture was mixed gently and incubated at room temperature for 5 min. 10 ml of chilled buffer P3 was added, mixed immediately and incubated on ice for 20 min. The mixture was centrifuged at 4,000 rpm (Megafuge 1.0R, 5,400 g) for 30 min at 4°C. The supernatant was applied to an equilibrated QIAGEN-tip 500 and allowed to enter the resin by gravity flow. The QIAGEN-tip was washed twice with 30 ml buffer QC. DNA was eluted with 15 ml buffer QF. The DNA is precipitated by adding 0.7 volumes (10.5 ml) of isopropanol and centrifugation at 12,000 rpm (Beckman JA20, 21,000 g) for 30 min at 4°C. The resulting pellet was washed twice with 70% ethanol and air-dried at room temperature. The pellet is then carefully resuspended in certain volume of TE buffer depending on the size of DNA pellet. The concentration of plasmid DNA was photometric measured and adjusted to 1 µg/µl. The plasmid DNA can be stored at 4°C for a short time only or at -20°C over a longer period.

2.2.1.4 Measurement of plasmid DNA concentration

The DNA concentration is determined by using a picodrop (Xipha Biotech) at wavelength of 260 nm and 280 nm. The absorption of at 260 nm corresponds to the concentration of DNA and 280 is corresponds to the protein. First of all an appropriate DNA dilution (normally 1:10 or 1:100) was made, 5 µl of DNA suspension was transferred into a picodrop, which has been calibrated before to the solvent (either H_2O or TE buffer). The absorbent ratio between 260/280 should lie in between 1.8-2 to ensure high purity of DNA.

2.2.1.5 Restriction endonuclease digestion

Digestion of DNA with restriction endonuclease was performed by pipetting DNA sample, 10X restriction buffer, restriction enzyme, and distilled and deionized water (ddH_2O) in a 1.5 ml eppendorf tube. The reaction mixture was incubated at the

recommended temperature (usually at 37°C). Normally 1 or 5 Units of restriction enzyme were used to digest 1 µg DNA.

2.2.1.6 Agarose gel electrophoresis

The agarose (1-3%) was melted in 1X TAE buffer using a microwave oven, and cooled to about 55°C. Before the gel was poured into a casting platform, ethidium bromide (4 µl of 10 mg/ml in 100 ml solved agarose) was added. DNA samples were mixed with appropriate amount of 6X loading buffer before loaded into the wells. Normally, the gel was run with 100-120 V and 300-400 mA. DNA was visualized by placing gel on a UV light source and picture was photographed directly by a photo system.

2.2.1.7 Preparation of DNA fragments

DNA bands were excised from gel and subsequently purified with a High pure PCR product purification Kit (Roche). The preparation was performed according to the manufacturer's instruction. After purification, 5 µl of the purified DNA was run on agarose gel for determine the DNA amount for ligation.

2.2.1.8 Ligation

Ligations were done with a rapid DNA ligation Kit (Roche). Each 4 µl of linearized vector DNA and purified DNA fragment were used. The exact operation was performed according to the manufacturer's instruction. The ligation products were purified with high pure PCR product purification Kit according to the manufacturer's instruction, before they were used for heat shock transformation.

2.2.2 QuikChange® Site-Directed Mutagenesis

QuikChange® Site-Directed Mutagenesis is a four-step procedure (Fig. 2.1), and is used for introduction of point mutations, switching of amino acids, and deletion or insertion of amino acids residues. The method uses a double stranded DNA vector and two oligonucleotide primers containing the desired mutation. The primers are complementary to each other and to the double stranded template DNA. After denaturation of the vector DNA, the mutagenic primers anneal complementary to opposite strands of the vector. Elongation by *Pfu* DNA polymerase results in a mutated plasmid with staggered nicks. After the thermal cycling, the PCR product is

treated with *DpnI* endonuclease. *DpnI* has the target sequence 5'-G^{m6}ATC-3', and is used to digest hemimethylated and methylated parental DNA, leaving the non-methylated, newly synthesized DNA intact for further use. After *DpnI* treatment, the plasmids are transformed into competent *E. coli* XL blue, where the cells DNA repair machinery seals the nick.
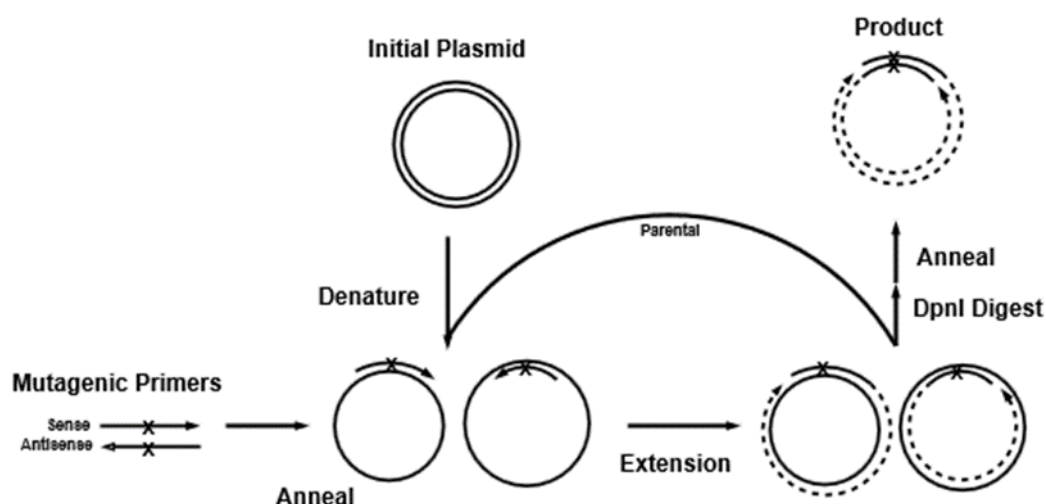
Fig. 2.1 An illustration of the four steps of the QuikChange® Site-Directed Mutagenesis protocol. In step one the plasmid is isolated for the mutagenesis reaction. Step two involves the mutagenic PCR. The third step is digestion of the template with *DpnI*, leaving only the mutated PCR products. The final step is transformation of the mutated plasmid. Figure from http://www.stratagene.com/manuals/200516.pdf.

All the work was carried out as suggested by the QuikChange® Site-Directed Mutagenesis protocol, but with small alterations to the reaction mix, which was as follows:

2.2.2.1 Primers:

All primers were designed by Primer X software (www.bioinfirmatics.org/primerx)

Primers	Sequence (5'->3')	Tm (˚C)
P3S-F	GACAAAGACATAATGGATTCCAACACGATAACCTCG	68,3
P3S-R	CGAGGTTATCGTGTTGGAATCCATTATGTCTTTGTC	68,3
R41K-F	CTCCGAAGAGACCAAAAGGCATTAAAGGGAAGAG	69,5
R41K-R	CTCTTCCCTTTAATGCCTTTTGGTCTCTTCGGAG	69,5
D74N-F	CTGAAGAGTGAAACAAATGAAAACCTCAAAATAG	63,4
D74N-R	CTATTTTGAGGTTTTCATTTGTTTCACTCTTCAG	63,4
I98M-F	GAGCATAGAGGAGATGAGCCGAGAATGGTAC	69,5
I98M-R	GTACCATTCTCGGCTCATCTCCTCTATGCTC	69,5
D153S-F	GAGGGCATTCACAGAAAGTGGTGCTATTGTGGCTG	71,8
D153S-R	CAGCCACAATAGCACCACTTTCTGTGAATGCCCTC	71,8
D74N-WT-F	GATTCTGGAGGAAGAATCCAATGAGGCACTTAAAATGAC	69,5
D74N-WT-R	GTCATTTTAAGTGCCTCATTGGATTCTTCCTCCAGAATC	69,5

2.2.2.2 Reaction mix

0.5	µl	forward primer, 2.5 pmoles/µl
0.5	µl	reverse primer, 2.5 pmoles/µl
0.25	µl	40 mM dNTP mix, (10 mM each)
1.25	µl	10X PfuUltra Buffer (contains Mg++)
1.0	µl	Template DNA, 2 ng/µl
0.25	µl	PfuUltra Hotstart (Stratagene)
8.75	µl	Sterile H$_2$O
0.625	µl	DMSO
8.125	µl	Total

2.2.2.3 PCR program setup for site directed mutagenesis

1.   5 min, 95 °C

2.   Repeat 18X   (a) 50 s, 95 °C

                        (b) 50 s, 60 °C

                        (c) 1 min+1 min/1 kb template, 68 °C

3.   7 min, 68 °C

2.2.2.4 Control of amplification DNA by gel electrophoresis (1%)

 For this assay, 50 ml of 1X TAE buffer was measured, 0.5 g of agarose powder weighed and microwaved for 2.5 minutes. The solution was then allowed to cool for a few minutes then 2 µl of Ethidium bromide was added. This solution was then poured in a gel plate and an 8 lane comb inserted in it to form the grooves/wells. The solution was then allowed to solidify at room temperature. The samples were then loaded at ran at 200 V in TAE buffer.

2.2.2.5 Transformation of XL1-Blue competent cells

XL1-Blue cells were obtained from Stratagene, 0.85 µl of the β-mercaptoethanol provided was then added to 50 µl of the cells, 1 µl of the DNA plasmid obtained after PCR quick change added, the tube was incubated on ice for 30 minutes, heat pulsed at 42 °C (water bath) for 45 seconds, incubated on ice for 2 minutes again, 0.5 ml SOC solution to the tube and then the tube incubated at 37 °C for 1 h (rotation speed 200 rpm). After the incubation, 50 µl of the solution was applied to LB agar plate containing 250 mg/ml ampicillin. The plates were then incubated at 37 °C overnight. The next day, a single colony from an agar plate was picked up, added to a culture tube containing 5 ml LB media contain 250 mg/ml ampicillin added and allowed to rotate at 200 rpm at 37 °C overnight. The next day, the amplified DNA had to be extracted.

2.2.3 Working with cell cultures

2.2.3.1 Maintenance of mammalian and avian cell culture

MDCK, A549 and 293T were maintained in Dulbecco modified Eagles medium (DMEM) containing phenol red as a pH-indicator, supplemented with 10% heat inactivated fetal calf serum (FCS) and Penicillin/Strepromycin (P/S). The cells were

incubated at 37°C with 5% CO_2 and 95% humidity. They were routinely cultured to a 100% confluence than passaged according to the need. QT6 were maintained in HAM's-F10 media containing 1% L-Glutamine, supplemented with 8% heat inactivated fetal calf serum (FCS), 2% Chicken Serum, 2% Tryptose phosphate broth and P/S. The cells were incubated at 37°C with 5% CO_2 and 95% humidity. They were routinely cultured to a 100% confluence than passaged according to the need.

2.2.3.2 Storage of cell cultures

For freezing; cells were washed with 1X PBS and 5 ml of 1X trypsin-EDTA was then added. The cells were then incubated at 37°C with 5% CO_2 and 95% humidity and left until cell detachment, after which 5ml complete media was added. Cell suspensions were then centrifuged at 1200 rpm, 4°C for 5 min. The cells pellet were gently resuspended with 1 ml freeze medium (90% complete DMEM and 10% DMSO) and transferred into cryotubes. These were set into a styropore box and left to freeze gradually in the -80°C freezer. The DMSO prevents ice crystal formation and allows the cells to remain intact. After 24 hours, cells were transferred into liquid nitrogen where they can be kept for a longer period of time.

For thawing; cells were removed from liquid nitrogen and immediately transferred into a 37°C water bath until complete thawing. Cells were then resuspended carefully and transferred into a cell culture flask filled with complete DMEM (15 ml). After 24h cells were replaced with complete DMEM (15 ml) and continue culture until the cells have reached 100% confluence and should be passaged for further propagation.

2.2.3.3 Infection of cells

The virus inoculum was prepared by adding the according amount of virus stock to a certain volume of PBS/BA depending on the desired multiplicity of infection (moi) used for experiment. Confluent cells in 3.5 cm dishes were washed with 1x PBS[++] and 500 µl of virus inoculum was laid on top of cell surface, rolling the plate to ensure the virus inoculum were equally distributed. The cells were further incubated at room temperature for 1 h, after which the inoculum was removed by aspiration, then wash the cell one time with 1X PBS, and 2ml of infection media was added. Cells were then further incubated at 37°C with 5% CO_2 for the desired time points.

The calculation of moi was done as follows:

$$\frac{1000\ \mu l}{\text{Virus titer [PFU]}} = \frac{X\ \mu l\ \text{virus}}{\text{moi x cell amount in the culture}}$$

2.2.3.4 Preparation of cell lysates for Western blot analysis

At a certain time point after infection and/or treatment, cells (from 3.5 cm dishes) were washed with cold 1X PBS^{++}. An extra 1 ml of cold 1X PBS^{++} was added to the cells with which they were scraped off and transferred into eppendorf tube. This was then centrifuged at 13000 rpm for 1 min and the cell pellet carefully resuspended in 75 µl lysis buffer by pipetting up and down. The lysis was performed by incubating cells for 25-30 min on ice and vortexing at 5 min intervals. The lysed cells were then centrifuged at 13000 rpm, 4°C for 15 min. The supernatant was finally transferred into new eppendorf tube and stored at -70°C until further requirement.

2.2.4 Cell viability (cytotoxicity) analysis

In order to determine whether the concentration of inhibitors used for experiments would affect cell viability, MTT-assay was performed. This assays measure the activity of mitochondrial dehydrogenase in the living cells. 3-(4,5-dimethylthiazole-2-yl)-2,5-diphenyl tetrazolium bromide (MTT) or (4-(3-(-iodophenyl)-2-(4-nitrophenyl)-2H-5tetrazolio)-1,3-benzene disulfoonate) (WST-1) is taken up by cells and can be reduced either enzymatically (by mitochondrial dehydrogenase/reductase enzymes) or through direct interaction with NADH, which is reduced to NADPH. This reaction only takes place when enzymes are active in living cells and therefore conversion is directly related to number of viable cells and can be analyzed photometrically in an enzyme-linked immunosorbent assay (ELISA) reader. This reaction produces blue formazan crystals (MTT) in living cells.

2.2.4.1 MTT-assay

MDCK, A549, and QT6 cells were seeded in 96well cell culture plates (150 ul/well) and grown in complete DMEM media overnight at 37°C with 5% CO_2 so that they were confluent on the day of the experiment. After addition of the inhibitors (mixed in DMEM/BA), cells were incubated further for 4, 6, 8, 10, 24 and 48 hours. Cell media

was then replaced with 150 µl of complete DMEM media and incubated for 1 h to allow for cell proliferation. 7 µl of 5mg/ml MTT stock (diluted in complete DMEM media) solution was diluted in 193 µl complete DMEM media (175 µg/ml final concentration) and added into each well after aspirating the old media. Cells were incubated for a further 90 min and subsequently fixed with 4% paraformaldehyde (PFA, in 1X PBS) at room temperature for 30 min. The fixing solution was aspirated and the plates were dried under the hood for 10-15 min. The tetrazolium crystal was dissolved by adding 200 µl of isopropanol to each well and the plates left shaking for 10 min on a 96-well plate shaker. The plates were analyzed photometrically at 550 nm excitation in an enzyme-linked immunosorbent assay (ELISA) reader.

2.2.5 DNA-transfection of eukaryotic cell cultures

2.2.5.1 Transfection of adherent 293T cells

The day before transfection, 293T were split 1:2 into a new flask to promote cell growth. The next day the cells were seeded in 3.5 cm dishes to grow to approximately 90% confluence over night for the transfection. DNA and TranIT2020 mix were prepared as follows: DNA (in µg) was diluted in OPTI-MEM reduced serum medium (final volume is 100 µl) and mixed gently. TranIT2020 (2 µl of TranIT2020 per µg DNA) was mixed and diluted in OPTI-MEM (final volume is 100 µl), mixed gently and incubated for 5 min at room temperature. The diluted TranIT2020 was added to the tube containing the diluted DNA, then mixed gently and incubated for 45 min at room temperature to allow forming of the DNA-TranIT2020 complexes. During complex formation, cells were washed with OPTI-MEM and refreshed with 800 µl of new medium without antibiotics (DMEM+10% FCS) was added. The DNA-Plus-TranIT2020 Reagent complexes (total 200 µl volume) were added dropwise into the dish containing fresh medium. The cells were incubated at 37°C at 5% CO_2 for 6 h. Thereafter, the media containing DNA-Plus-TranLT2020 Reagent complexes was removed and replaced with 2 ml of complete DMEM media. The cells were further incubated at 37°C at 5% CO_2 for 24-48 h.

2.2.5.2 RNP reconstitution assay

2.2.5.2.1 Transfection of adherent cells to performed CAT assay after RNP reconstitution

1.2 µg of DNA mixture of four expression plasmids encoding the PB1, PB2, PA and NP proteins (in the ratio of 1:1:1:2) from FPV virus, and 2.0 µg of pPolI-CAT-RT (carrying the human pol-I-promoter), together with either empty vector pcDNA 3.0 (4.0 µg) or pcDNA-NS1 (4.0 µg) from GD, MA, and MA mutant virus respectively were transfected according to section 2.2.5.1.

2.2.5.2.2 Chloramphenicol Acetyl Transferase (CAT) assay

The principle for CAT assay is shown in Fig 2.2.

2.2.5.2.3 Preparation of cell extracts

Cells were washed with 1X PBS^{++} scraped off in 500 µl 1X PBS^{++} and transferred into a new eppendorf tube (on ice). Cells were centrifuged at 3000 rpm in a microcentrifuge (Heraeus, Germany) at 4°C for 1 min. Pellet was resuspended in 100 µl of 0.25 M Tris-HCl (pH-7.4). Resuspended pellet was incubated for 2 min in liquid nitrogen followed by 5 min incubation at 37°C in water bath. This process was repeated for two more times and cells were centrifuged at 3000 rpm for 1 min at 4°C. 100 µl supernatant, which is the enzyme extract, was transferred into a new eppendorf tube on ice and was used for CAT assay (Invitrogen, USA) or was stored at -70°C.

2.2.5.2.4 Determination of relative protein amount

A 5 µl sample from the cell lysate was taken to measure the relative protein amount and mixed as followed:

5	µl	Sample
200	µl	Bradford protein buffer
800	µl	ddH2O

The relative concentration of protein was calculated by the measurement of the absorbance at the wavelength 595 nm in a DU-70 spectrophotometer (Beckman). According to the indicated absorbance, the protein concentration of different samples could be calculated by stand curve derived from BSA standards or compared between samples by normalizing the lowest concentration to 1.
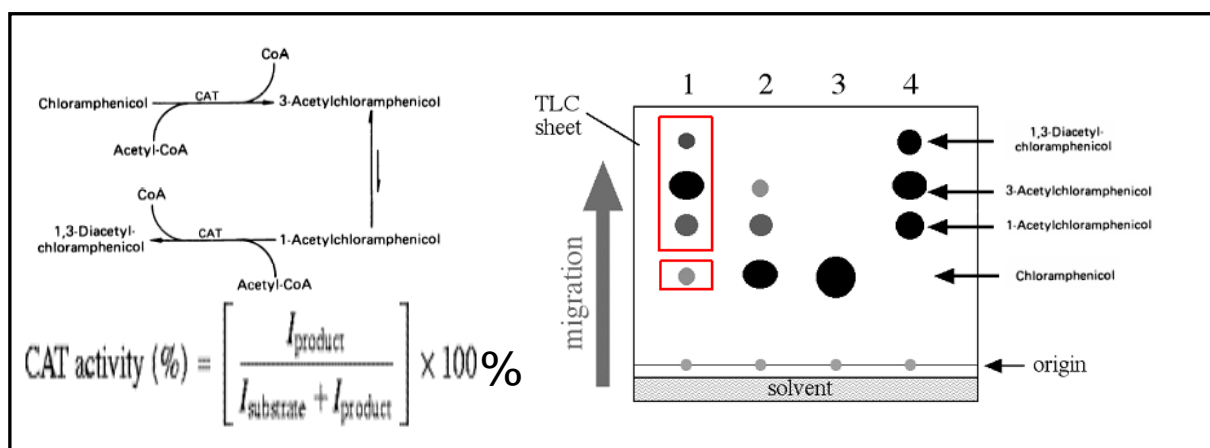
Fig. 2.2 The principle of CAT assay. CAT, a bacterial gene, which neutralizes the antibiotics chloramphenicol by acetylating the drug at one or two hydroxyl groups. Cell lysates containing CAT enzyme are simply incubated with the fluorescent substrate and acetyl-CoA at 37°C, ethyl acetate is added to terminate the reaction and to extract the fluorescent substrate and its acetylated derivatives, which are then resolved by thin layer chromatograph (TLC, Invitrogen). Brightly fluorescent, well-separated spots can be visualized with a hand-held UV lamp. To quantify CAT activity, a laser scanner typoon (GE healthcare) is used.

2.2.5.2.5 Chloramphenicol reaction

Running chamber was set up one day before Chloramphenicol reaction. 26 ml of methanol and 174 ml of chloroform (13:87) was mixed as running buffer, and then the running buffer was poured into the chamber and covered with a lid overnight to generate a stable air gas phase. 50 μl of each pre-diluted enzyme (1:10, 1:100 and 1:1000) extract was incubated with 20 μl (4mM) AcCoA and 5 μl BODIPY (Invitrogen). Everything was mixed properly and this 75 μl reaction mixture was incubated at 37°C for two and a half hours in a water bath. Thereafter, 500 μl of ethyl acetate was added and mixed, the mixture was vortexed vigorously for 5 min and then centrifuged at 13000 rpm for another 5min resulting in two phases including the upper ethyl acetate layer (450 μl) and lower water layer. Ethyl acetate layer was transferred into new eppendorf tube (with holes made in the lid) and were vacuum dried with speed vac machine (Savant) for 25 min.

2.2.5.2.6 Loading samples on TLC plate

The dried pellet was dissolved with 20 μl ethyl acetate and was loaded in the form of little dots on TLC plate (Silica gel, Sigma Aldrich) with the help of air supply. Air supply helps minimizing spread of ethyl acetate on TLC plate during sample loading. The dots were loaded a little higher than the level of pre-equilibrated running buffer.

TLC plate was plated into the running chamber in an inclined position. The spots migrated up by capillary action until the solvent reached the top of the TLC plate (around 30 min). Then it was stopped by removing the plate and allowing the plate to dry. Later, the products (acetylated chloramphenicol) and the unacetylated substrate were visualized as a light green colour spot on the chromatogram in UV-light (as Fig. 2.3). The plates were scanned by Typhoon 9200 (GE Healthcare) and the spots were quantified and calculated (as Fig. 2.2) by GenQuant software (GE Healthcare).

2.2.6 Generation, amplification and purification of NS reassortant of H7-type highly pathogenic avian influenza virus

293T cells in 3.5 cm diameter dishes were transfected with 12 plasmids (5 µg DNA in total) according to section 2.2.5.1. For the generation of wt FPV, 1.2 µl (1 µg/µl) of the protein expression plasmids (pHMG-PB1, pHMG-PB2, pHMG-PA and pHMG-NP) were transfected in a ratio of 1:1:1:2 along with 3.8 µl (1 µg/µl) of the pol-I plasmids (pPol-I-FPV-PB1, FPV-PB2, FPV-PA, FPV-NP, FPV-HA, FPV-NA, FPV-M and FPV-NS) in a ratio of 1:1:1:1:2:2:1:1. To generate the reassortant viruses carrying different NS segments (NS-GD, NS-MA and NS-MA mutants), the pPol-I-FPV-NS plasmid was substituted by the pPol-I-NS plasmids of NS-GD, MA and MA- mutants. At 24 h after transfection, the transfection mixture was removed and the cells were incubated with 2 ml of fresh medium. The harvested medium from transfected dishes was screened for rescued influenza virus by observation of cytopathic effect (CPE) and plaque assay on MDCK cells according to the section 2.2.7.1. The progeny viruses were amplified on MDCK cells in 75 mm flask and continued for 3 round of plaque purification according to the section 2.2.7.3. The purified viruses were then amplified and titrated on MDCK cells by foci assay according to section 2.2.7.2 and stored at -70°C. The generation of all viruses was carried out using biosafety level 3 procedures.

2.2.7 Analysis of infectious virus titers

2.2.7.1 Standard plaque assay

MDCK cells were seeded on 3.5 cm dishes one day before and grew to 100% confluence. The cells were washed once with 1X PBS++, then 100 µl of virus dilution (10 time serial dilute) was laid on the cells. The cells were incubated at RT for 1 h.

During the incubation, 2 ml Oxoid (2%) agar was melted and incubated alongside at 42°C in a water bath. DMEM medium was also incubated in a 37°C water bath. After one hour, the inoculum was removed from the dishes, 2 ml Oxoid (2%) agar was mixed with DMEM (and the other solutions, as described in section 2.1.9.). 2 ml mixture was given immediately to every plate using a sterile plastic pipette. When the agar became solid, the dishes were inversely laid in a 37°C, 5% CO_2 humidified incubator. After 2 days plaques were seen on the dishes. The cells were fixed with 3.7% formaldehyde for 1h at room temperature. Then the agar was removed from the dishes with a spatula. Cells were stained with 1.25% coomassie brilliant blue (1 ml/3.5 cm plate) at room temperature for 5 min, and then the plates were washed gently with tab water. Plaques were counted at different dilutions and the total amount of plaques was calculated by the following formula:

$$PFU/ml = number\ of\ plaques \times volume\ factor \times dilution\ factor$$

Volume factor: PFU (Plaque forming unit) is related to 1 ml. If a dish was infected with 100 µl viral dilution solution, the factor is 10.

2.2.7.2 Immunohistochemistry (Avicel Foci assay)

Virus dilutions were made in the 96 well microtiter plates with U-form bottom. First 180 µl of virus dilution solution was pipetted into each well and 20 µl of the virus stock was added into the wells of the first row. The virus dilution (200 µl) was mixed by up and down pipetting and 20 µl of it was transferred into wells of the second row. The same steps were repeated up to the last row (A-H) to get 10^{-1} to 10^{-8} dilution series. MDCK cells were seeded in 96-well plates and grown over night at 37°C with 5% CO_2 so that they were 90% confluent on the day of infection. The cells were washed once with 1X PBS++, then infected with 50 µl of virus dilution and incubated at room temperature for 1 h. Virus inoculum was aspirated and 150 µl Avicel media (See in section 2.1.9) was added into each well. The plate was placed at 37°C with 5% CO_2 for 30 or 48 h depending on the virus strain. After the incubation, avicel media was removed by aspiration. Cells were washed twice with 1X PBS++ and fixed, as well as permeabilized, with 330 µl/well of 4% PFA/1% TritonX-100 in 1X PBS++ overnight at 4°C or alternatively for 1 h at RT. Afterwards cells were washed and three times with 1X PBS/0.05% Tween20 and incubated with 50 µl of primary

antibody (anti NP-mAb, 1:6000 diluted in PBS^{++}/3% BSA) for 1 h at room temperature. After aspirating the primary antibody dilution, cells were again washed three times with PBS/0.05% Tween20, followed by secondary antibody incubation (Horse Radish Peroxidase (HRP)-conjugated anti mouse, 1:1000 diluted in PBS^{++}/3% BSA) for 45 min at room temperature. Cells were washed and 40 µl of AEC staining Kit solution (section 2.1.10) was added into each well and placed at room temperature for 30-60 min. The AEC (3-Amino-9-ethylcarbazole) staining Kit is used for staining peroxidase labelled compounds in immunohistochemistry or immunoblotting techniques. AEC produces an insoluble end-product which has a red colour. Red stained foci were observed under microscope, wells were washed with normal water to remove the rest of salts and air dried at room temperature. After drying, the plates were scanned using the Canon scan 9900F (Canon) at 1600 dpi and virus foci counted. The viral titre was determined as follows:

FFU/ml = number of foci x volume factor x dilution factor

Volume factor: FFU (Foci forming unit) is related to 1 ml. If a dish was infected with 50 µl viral dilution solution, the factor is 20.

One foci was considered when more than 3-5 adjacent cells were stained in one particular area, as opposed to single cell staining which would probably mean, that the cell had not produced an infectious virus.

2.2.7.3 Influenza virus plaque purification

MDCK cells were seeded on 3.5 cm dishes one day before and grew to 100% confluence. The cells were washed once with 1X PBS^{++}, then 100 µl of virus dilution (10 time serial dilute) was laid on the cells. The cells were incubated at RT for 1 h. During the incubation, 2 ml Oxoid (2%) agar was melted and incubated alongside at 42°C in a water bath. DMEM medium was also incubated in a 37°C water bath. After one hour, the inoculum was removed from the dishes, 2 ml Oxoid (2%) agar was mixed with DMEM (and the other solutions, as describe in section 2.1.9.). 2 ml mixture was given immediately to every plate using a sterile plastic pipette. When the agar became solid, the dishes were inversely laid in a 37°C, 5% CO_2 humidified incubator. After 2 days plaques were seen on the dishes. A single plaque was picked

using a sterile Pasteur pipette. The plug was incubated overnight in SM buffer to release the viral particles from the agarose.

2.2.8 Haemagglutination (HA) Assay

Red blood cells should be taken from Specific Pathogen Free (SPF) chickens. If SPF chickens are not available, blood may be taken from normal chickens that are shown to be free from antibodies to (avian) influenza viruses. Firstly about 20-30 ml fresh chicken blood was transferred to a 50 ml sterilized falcon centrifugation tube containing 10 ml of 3.7% sodium citric acid. The RBCs was washed by filling the tube to 50 ml with cooled 1X PBS^{++} and centrifuged at 1,500 rpm (Megafuge 1.0R, 700 g) at 4°C for 10 min. The supernatant above the RBC-fraction containing serum, white blood cells and fat was carefully removed by aspiration, and then RBCs pellet was washed again with cooled 1X PBS^{++} and centrifuged as mentioned above. This washing step was repeated twice. Finally the pellet of RBCs was diluted to 0.5% (v/v) with cooled 1X PBS^{++} for haemagglutination assay. 50 µl 1X PBS^{++} was dispensed into each well of a plastic V-bottomed microliter plate (96 wells), then 50 µl virus suspension (for example cell culture supernatant) was placed in the first well. Two-fold dilutions of 50 µl volumes of the virus suspension were made from well #1-#12 in each row (left to right), subsequently 50 µl of 0.5% chicken RBCs was dispensed to each well. The mixture of every well was mixed by tapping the plate gently and then the RBCs were allowed to settle for about 30-60 min at 4°C. The Haemagglutinating Units (HAU) are: 2^x, where X is the number of the last well without tear-shaped streaming.

2.2.9 Confocal laser scanning microscopy and immunofluorescence assay (IFA)

Confluent cells were trypsinized by 1X trypsin-EDTA, reseeded in the 3.5 cm dish containing sterile glass cover-slips (12 mm) and incubated at 37°C with 5% CO_2. On the next day, the cells were confluent. After infection or transfection, the growth medium was removed from the culture dish at the indicated time points, and the cells were washed once with 1X PBS^{++}, then the cells were fixed with 1 ml 4% PFA in 1X PBS^{++} over night at 4°C. After fixation, cells were washed twice with 1X PBS^{++} and subsequently incubated with 1 ml 1% Triton X-100 for 45 min. Cells were then

washed 3X with 1X PBS^{++} and incubated with 20 µl of the primary mouse anti-Flu A NP mouse (clone 1331) (1:200 dilution in PBS^{++}/3% BSA) or rabbit anti-GST-NS1 polyclonal antibody (1:1000 in PBS/3% bovine serum albumin), kindly provided by T. Wolff, (Berlin, Germany) for each cover-slip for 1 h at room temperature. Afterwards cells were washed three times as before, and further incubated with 20 µl of the secondary Alexa 594 goat anti-mouse IgG (1:200 diluted in PBS^{++}/3% BSA) or goat anti-rabbit IgG (1:200 diluted in PBS^{++}/3% BSA) for 1 h at room temperature. The cells were then washed again three times and incubated with 20 µl DAPI (10 mg/ml in PBS/3% bovine serum albumin, Roth) for 5 minutes. After a further three washes (as above) and an extra wash with ddH$_2$O, the glass cover slip was fixed on a glass slide with Mowiol/DABCO overnight. Fluorescence was visualised using a TCS-SP5 confocal laser-scanning microscope (Leica).

2.2.9.1 Mowiol/DABCO mounting medium

Add 2.4 g of Mowiol 4-88 to 6 g of glycerol. Stir to mix. Add 6 ml of H$_2$O and leave for several hours at room temperature. Add 12 ml of 0.2 M Tris-HCl (pH 8.5) and heat to 50°C for 10 min with occasional mixing. After the Mowiol dissolves, clarify by centrifugation at 5,000 g for 15 min. For fluorescence detection, add DABCO to 2.5% to reduce fading. Aliquot in airtight containers and store at −20°C. Stock is stable at room temperature for several weeks after thawing.

2.2.10 Western blotting (Semi-dry)

2.2.10.1 Measurement of protein concentration (Bio-Rad protein assay)

The Bio-Rad protein assay is based on the observation that when Coomassie Brilliant Blue G250 binds to the protein the absorbency maximum shifts from 450 nm to 595 nm. 5 µl of cell lysate (as described in 2.2.4. section) was added into diluted Bio-Rad Dye Reagent (1:5 dilution of Dye Reagent concentrate in ddH$_2$O). Mix well and after a period of 10 min, the relative protein content was determined by measuring the absorption at wavelength 595 versus reagent blank (containing the lysis buffer only). This was done to apply an equal protein amount of all samples onto the SDS-PAGE gel.

2.2.10.2 Sodium dodecyl sulfate polyacrylamide gel electrophoresis (SDS-PAGE)

The electrophoresis apparatus was assembled according to manufacturer's (Bio-Rad) instruction, and the resolving gel was poured in between the two glass plates. Leave a space about 1 cm plus the length of the teeth of the comb. Isopropanol or 100% ethanol was added to the surface of the gel for an even distribution along the gel surface. After the resolving gel was polymerized, isopropanol was removed and the stacking gel was poured on top of the resolving gel. Insert the comb and let the gel polymerise. Mixed 75 µl total of containing protein sample (after determining the protein concentration) with 35 µl laemlli buffer containing 10% β-mercaptoethanol to reduce disulphide bonds were incubated for 5 min at 95°C and cooled on ice for 1 min, then shortly centrifuged and the calculated sample amount was loaded into wells of gel. Rainbow protein marker (Roche, 2 µl marker + 8 µl laemlli buffer) was loaded as control. After running buffer was added to the chamber, a cover was placed over the gel chamber. Gels should be run at about 20 V/cm gel length. The negatively charged SDS-proteins complexes migrate in the direction of the anode at the bottom of the gel. Small proteins move rapidly through the gel, whereas large ones stay at the top. Proteins that differ in mass by about 2% can be distinguished with this method. The electrophoretic mobility of many proteins in SDS-polyacrylamide gels is proportional to the logarithm of their mass.

2.2.10.3 Transfer membrane in "Semi-dry" electroblotter

After the cell extracts were subjected to SDS-PAGE, the proteins were transferred by electroblotting onto a PVDF-Membrane, which was incubated before in 100% Methanol for 2-3 min, and washed three times (5 min each) in ddH_2O, then equilibrated in the transfer buffer for 2-3 min. On a layer of 2 blotting papers soaked with transfer buffer the PVDF-Membrane was laid. The polyacrylamide gel and again 2 blotting papers soaked with transfer buffer were then placed on the PVDF-Membrane, making a "sandwich" (without any bubbles), and laid in "Semi-dry" electroblotter. The current was set to 0.8 mA/cm^2 for 90 min for transfer.

2.2.10.4 Immunodetection of proteins

After transferring the proteins, the PVDF-Membrane was washed for 5 min in 1X TBS-T buffer, then the membrane was blocked in blocking buffer (5% non-fat milk in TBS-T) for 1 h at room temperature or overnight at 4°C. There after the membrane was washed for 5 min in 1X TBS-T buffer, then incubated with the primary antibody (e.g. anti-Flu A-NP monoclonal antibody, 1:500 dilution in blocking buffer or anti-NS1 monoclonal antibody) for 1 h at room temperature or overnight at 4°C. After washing three times (5 min each) in 1X TBS-T buffer, the membrane was incubated with the secondary antibody solution (e.g.: HRP-conjugated anti mouse monoclonal antibody, 1:1000 dilution in blocking buffer) for 1 h at room temperature.

2.2.10.5 Enhanced chemiluminescence (ECL) reaction

As mentioned above the membrane was washed three times (5 min each) in 1X TBS-T buffer and once in 1X TBS, then incubated for 1 min in ECL (enhanced chemiluminescence) solution, which was prepared according to the manufacture (Amersham) between a glass plate and a clear plastic membrane. After 1 min, everything was laid into a photo cassette, and then a light sensitive film was placed on top of the membrane and exposed for 1.5-5 min or longer. The film was then developed.

In order to detect the beta-actin protein (as a loading control), the attached antibody was stripped from membrane by incubating the membrane in a 1:10 diluted "strong stripping solution" (Re-Blot Plus Western Blot Recycling Kit, Chemicon) for 45-60 min at 37°C. After washing with 1X TBS-T buffer for 5 min, the membrane was incubated in blocking buffer for 1 h at room temperature. Then it was washed for 5 min in 1X TBS-T buffer and incubated with the anti-beta-actin monoclonal antibody (1:10000 dilution in blocking buffer) solution for 1 h at room temperature. Subsequently the membrane was washed three times in 1X TBS-T buffer and washed once in 1XTBS, then incubated for 1 min in ECL solution and proceeded as mentioned above.

2.2.10.6 Quantification of protein bands

Protein bands exposed on the film were scanned (Canon scan LiDE 30/N1240U) at 800 dpi, and the picture was saved in grey scales as TIFF file. The intensity of protein bands was densitometrically determined by means of PC-BAS software. These steps were done for the specific bands of the protein to be detected (e.g. NP

or NS1) as well as beta-actin bands. The lowest value of beta-actin band, which was set to one, was divided by each value of beta-actin bands to get a factor for each according specific protein band value. This calculation was done to normalize the amount of specific protein by the amount of beta actin protein loaded.

2.2.11 Primer extension

2.2.11.1 Isolating RNA (Trizol Method)

To isolated total RNA from infected cells, confluent MDCK cells in 35 mm dishes were infected with different recombinant virus at MOI=2 in triplicates. The total cellular RNA was extracted with Trizol reagent (Invitrogen) at different time point post infection (2 h p.i., 4 h p.i., 6 h p.i. and 8 h p.i.) as followed: The medium from transfected or infected cells in 35 mm dishes was aspirated and 1 ml of Trizol was added into the dishes, after 5 min incubation at room temperature, Trizol was stirred with P1000 tip until all the cells are suspended. Then the solution was transferred into an reaction tube and was incubated at room temperature for 10 min. To each reaction tube 200 µl of chloroform was added and mixed properly and incubate for 5 min at room temperature with occasional shaking. Later the tubes were centrifuged for 20 min at 4°C at 13,000 rpm. The upper phase (app. 0.6 ml) was transferred later into fresh RNAase free reaction cup. 0.5 ml isopropanol was added to this upper phase supernatant and mixed properly and incubated at room temperature for 10 min. Afterwards centrifuge at 13,000 rpm for 20 min at 4°C. The supernatant was removed carefully and 1 ml of ethanol was added to the pellet and centrifuged at 13000 rpm for 5-10 min at 4°C. Without dislodging the pellet, alcohol content was discarded and pellet was air dried for 5-10 min and dissolved in 30 µl of RNAase free H_2O (Life Technologies) and used directly for the experiment or frozen at -70°C.

2.2.11.2 Primer labeling

The gene-specific primers used were as followed: NP mRNA and cRNA 5'-ACCATTCTCCCAACAGATGC 3' (expected size of cRNA 121 nt and mRNA, 135 nt). NP vRNA: 5' ATGATGGAGAGTGCCAGACC 3' (expected size of band 181 nt. On receiving, the primers should be diluted into the concentration of 10 pmol/µl in RNAase free ddH$_2$O. Mixed well with other components of labeling reaction and incubated at 37°C for 1 h in PCR thermoblock.

Labeling reaction:	Primer 10 pmol/µl	1	µl
	DPEC H$_2$O	6	µl
	10X PNK Buffer (Roche)	1	µl
	[γ-^{32}P]ATP (6000 Ci/mmol, 10 µCi/µl)	1	µl
	PNK (T4 polynucleotide kinase, 10 U/µl)	1	µl

----

10 µl

After 1 h incubation, This 10 µl mixture was transferred into new 1.5 ml RNAase-free reaction cup and further 450 µl PN-buffer (Qiagen Nucleotide removal Kit) was added, mixed well and placed over the Qiagen Nucleotide removal column with the help of a pipette. The column was spin for 1 min at 6,000 rpm and the collection was discarded. The column was washed 2 times with 500 µl PE-buffer. Further spin down for 1 min at 6000 rpm and the collection was discarded followed by one more time spinning down for one minute at 13,000 rpm to remove residual alcohol content in the column. Fresh 1.5 ml RNAase free eppendorf tube was labelled clearly and the column was placed onto it. 40 µl EB-buffer or RNAase free H$_2$O was added on the column and incubated for 2 min at room temperature. Finally the tube was centrifuged for 1 min at 13000 rpm and eluted (40 µl) was collected in the eppendorf. This can be stored at -20°C in isotope room.

2.2.11.3 DNA-marker labelling

Labeling reaction:	autoclaved ddH$_2$O	6.0	µl
	1 Kb DNA Ladder (Roche marker IV)	1.0	µl
	10X PNK Buffer (Roche)	1.0	µl
	[γ-^{32}P]ATP (6000 Ci/mmol, 10 µCi/µl)	1.0	µl
	PNK (T4 polynucleotide kinase, 10 U/µl)	1.0	µl

----

10 µl

Mixed well and incubated at 37°C for 1h in PCR thermoblock. After 1 h incubation, This 10 µl mixture was transferred into new 1.5 ml RNAase-free eppendorf tube and further proceeded with Qiagen Nucleotide removal Kit as mention above and stored at -20°C in isotope room. Before gel loading, add the phosphorylated markers directly

to the Loading Dye, heat at 95°C for 10 minutes and then immediately load the markers onto the denature running gel.

2.2.11.4 Reverse transcriptase

Labelled primer-mix: mix the primers as follows according to the no. of samples to be analyzed and always make surplus than the need.

For one sample:

^{32}P labelled Primer for vRNA (10 mmol/µl)	0.25 µl
^{32}P labelled primer for cRNA and mRNA (10 mmol/µl)	0.25 µl
^{32}P labelled primer for 5s rRNA100 (10 mmol/µl)	0.25 µl
Primer for 5s rRNA100 (cold) (10 mmol/µl)	0.25 µl
DEPC ddH$_2$O	3 µl
Total	4 µl

For one reaction, 1.0 µl (10 µg) of Trizol-purified RNA was mixed with 4.0 µl of primer mixture. After 3 min running at 95°C in PCR block, the tubes were placed on ice for 5 min. During 5 min incubation time, the superscript mixture was prepared as followed:

For one sample :

5X RT buffer (Invitrogen)	2.0 µl
100 mM DTT (Invitrogen)	1.0 µl
10 mM dNTP (sigma)	0.5 µl
DEPC ddH$_2$O	1.25 µl
Superscript II (Invitrogen, 10 U/µl)	0.25 µl
Total	5 µl

Superscript master mix was prepared as mentioned above, and then pre-incubated at 45°C alongside with the primer-RNA mixture in a PCR block. When the RNA-primer samples reached to 45°C, 5 µl of the Superscript mix was aliquoted into the RNA mix, then incubated for 1 h at 45°C (for reverse transcriptase reaction), followed by incubation at 70°C for 10 min (to inactivate the Superscript) and cooled to 4°C.

2.2.11.5 Running the 6% 7M urea polyacrylamide gel

During reverse transcriptase reaction, the 6% 7M urea polyacrylamide gel should be prepared as follows:

Urea	21.0 g
10X TBE	5. 0 ml
40% acrylamide	7. 5 ml

Autoclaved ion free water to	50 ml

The above solution was mixed very well until the powder is dissolved. When the gel apparatus is ready, 0.5 ml 10% APS and 0.05 ml TEMED is added to the falcon tube and mixed quickly. The gel mixture was poured into the apparatus followed by 1 h incubation at RT and was fixed in the gel tank. Then pre-run at 50W for 1 h until the temperature of gel rise to 50°C. 8 µl of formamide mix (10 mM EDTA, xylene cyanol (Sigma No: X-2751XC), Bromophenol blue (Sigma, sodium salt), ACS reagent, No: B-7021BPB)) was added to each samples and mixed, and heated to 95°C. 10 µl of each sample was loaded on the gel. The gel was run at 50 W until the blue dye is approximately 3 cm away from the bottom of the plate. When the gel run was finished, the glass plates were separated very carefully and the gel should stick to one of the glasses. The gel on the glass plates was transferred to wattman-paper and was wrapped in Clingfilm (plastic foil side at the top). Then the gel was dried in vacuum drier for 60 min. When the gel was dried, it was placed in the screen cassettes together with a image plate phosphor (Fuji Photo Film Co. Ltd.) the gel side should be facing towards the white side of screen) overnight. Next day the screen was scanned on a typhoon 9200 (GE Healthcare) and the bands were quantified using the "Quantity One" software package (BioRad). The Increases of vRNA, mRNA and cRNA level were compared to the strain-specific RNA level at 2 h p.i..

2.2.12 Tunel assay (*in situ* cell death detection Kit)

Extensive DNA degradation is a characteristic event which occurs in the late stages of apoptosis. Cleavage of the DNA may yield double-stranded, low molecular weight

DNA fragments (mono- and oligo-nucleosomes) as well as single strand breaks ("nicks") in high molecular weight DNA. Those DNA strand breaks can be detected by enzymatic labeling of the free 3'-OH termini with modified nucleotides (X-dUTP, X = biotin, DIG or fluorescein). This method is called "Terminal deoxynucleotidyl transferase dUTP nick end labeling" (Tunel).

A549 cells grown on 6 well plate were infected with recombinant viruses at MOI=1 for 10 h. Cells were washed with 1X PBS, then cells were trypsinized and transferred to eppendorf tube. Afterward cells were fixed with 4% paraformaldehyde (PFA) in 1X PBS (pH 7.4) over night at 4°C. The samples were then washed twice with 1X PBS, centrifuge at 6,000 rpm for 5 min. Cell pallets were permeabilized with 1% Triton X-100 in 0.1% sodium citrate on ice for 20 min. Cells were washed and incubated with 50 µl reaction mixture (provided in *in situ* cell death detection Kit, Invitrogen) or the "no enzyme" control in 50 µl label solution (provided in *in situ* cell death detection Kit, Invitrogen) for 1 h in the dark. After 3 washes with 1X PBS, cells were incubated with DAPI (10 mg/ml in 1X PBS containing 3% bovine serum albumin) for 10 min in the dark. Finally, cells were washed twice and were fixed in 3.7% formaldehyde in 1X PBS. Fluorescence was visualised using FAC analysis.

2.2.13 IFN-beta enzyme linked immunosorbent assay (ELISA)

IFN-beta concentrations were assessed using the human IFN-beta ELISA Kit (PBL) according to the manufacturer's protocol. Briefly, confluent A549 cells in 3.5 cm dishes were infected with the different recombinant virus at an MOI of 0.01, and at 24 h p.i., 36 h p.i. and 48 h p.i. 100 µl of supernatant was taken and added into 96-well plates coated with human IFN-beta IgG Fab fragments, together with standards, and incubated for 1 h with shaking at RT. After 2 times washes with washing solution (human IFN-beta ELISA Kit), the human HRP-labelled IFN-beta antibody (human IFN-beta ELISA Kit) was added and incubated for 1 h with shaking at room temperature. After 3 times washes, the substrate solution (human IFN-beta ELISA Kit) was added to develop the colour, followed by the stop solution (0.5 M H_2SO_4) and the OD at 450 nm was measured.

2.2.14 Microarray

The microarray experiment were performed to compare the mRNA expression profiles of A549 cells infected which variant Influenza virus FPV-NS (MOI=2, 6 h p.i.) to A549 cells mock-infected with 1X PBS with 2 biological replicates. Six hours after infection, total RNA was isolated using the RNeasy mini Kit (QIAGEN, Hilden) following the manufacturer's protocol. Quality control and quantification of total RNA was assessed using a NanoDrop1000 UV-Visspectrophotometer (Kisker) and an Agilent 2100 Bioanalyzer (Agilent Technologies). The microarray analysis was performed using single-color hybridizations. RNA labeling was done with the Low RNA Input Linear Amplification Kit PLUS (Agilent Technologies). In brief, mRNA was reverse transcribed and amplified using an oligo-dT-T7 promoter primer, and cyanin-3 labelled cRNA was subsequently generated by T7 RNA-polymerase. After precipitation and purification, 1.25 µg of of each labelled cRNA was fragmented and hybridized to AgilentSurePrint G3 Human GE v2 8x60K Microarrays (Agilent Design ID 039494) according to the supplier's protocol. Microarrays were scanned with 2 µm resolution using an Innoscan 900 scanner (Innopsys) and images were gridded with Mapix 6.5.0. Data were analyzed in R using limma. Signal intensities were quantified. Normalized log signal intensities of replicated spots were averaged before further processing. Genes were considered as up or down regulated relative to mock infected cells if they showed more than 2-fold different in average signal intensities and were statistically significant at the p≤0.01 level using ANOVA. Gene set tests were performed for the KEGG pathways and Gene Ontologies using the gene Set Test function from limma on the moderated t-statistics. (According to Microarray Service by Dr. J. Wilhelm, ECCPS, Giessen).

2.2.15 RNA analysis by qRT-PCR

A549 cells were infected with recombinant viruses at MOI of 3. To analyze the primary viral transcription, cycloheximide (100 µg/ml) was added to the infection media. At 6 h p.i., cells were collected in Trizol and RNA was purified according to the manufacturer's protocol. To measure the accumulation levels of viral mRNA and vRNA, quantitative RT-PCR (qRT-PCR) was performed. Total RNAs were subjected to reverse transcription using SuperScript III reverse transcriptase (Invitrogen) with either oligo-dT (50 pmol) or 5'-GACGATGCAACGGCTGGTCTG-3' (10 pmol) primer

for synthesizing cDNA from segment 5 (NP) mRNA, or vRNA, respectively. The synthesized single-stranded cDNA were subjected to real-time quantitative PCR analysis (MX3000P; Stratagene) using Power SYBR® Green PCR Master Mix (Invitrogen) and a set of specific primers (NP) (see below). The levels of these RNAs were normalized by the amount of cellular beta-actin mRNA measured using specific primers (see below). The results shown are averages from three independent experiments with standard deviations. The level of significance was determined by Student's *t*-test (unpaired).

beta-actin-F	GACGATGCAACGGCTGGTCTG
beta-actin-R	GGTCATCTTCTCGCGGTT
NP-F	GACGATGCAACGGCTGGTCTG
NP-R	AGCATTGTTCCAACTCCTTT

2.2.16 Mice infections

C57BL/6J mice were obtained from Janvier, France and maintained under specific pathogen free conditions in a BSL3 facility at the Helmholtz Centre for Infection Research, Braunschweig, according to the German animal welfare law. The protocol used in these experiments has been approved by an ethics committee (Permit Number: 33.9.42502-04-051/09). Female mice (10-12 weeks of age) were anaesthetized by intra-peritoneal injection with ketamin-xylazines olution (85% NaCl (0.9%), 10% ketamine, 5% xylazine; 200 µl per 20 g body weight) and then infected intra-nasally with a dose of $2X10^4$PFU of the respective virus in 20 µl sterile 1X PBS. Body weight was monitored every day. Mice showing more than 30% of body weight loss were euthanized.

2.2.17 *In silico* analysis of NS1 protein flexibility at different temperatures

3D models for NS1 of GD, MA and MA mutant were generated using Phyre2 Protein structure prediction on the web: a case study using the Phyre server [145], based on PDB structure 3F5T [X-ray structure of NS1 from a highly pathogenic H5N1 influenza virus [146]. The molecules were minimized and solvated in a neutralized water box of 14x14 Å using NAMD [147-150]. Scalable molecular dynamics with NAMD [150] and vmd [151]. After equilibration and heating to the target temperature for ~0.7

nanoseconds, the molecular dynamics simulations were performed using the CHARMM22 force-field [152] for 20 nanoseconds.

2.2.18 Statistical analysis

Each point corresponds to the mean +/- S.D. of the indicated experiments. The statistical significance of differences between the indicated groups was tested using the unpaired Student's t test with a threshold of p: significant * < 0.5; very significant ** <0.01 and very very significant *** < 0.001.

Chapter 3

Results

In order to cross the species barrier to mammals, AIV must gain adaptive mutations to overcome host specific restrictions for an efficient viral replication in the new host [89]. Beside amino acid (aa) changes in viral hemagglutinin (HA) to overcome the poor HA-binding to the cellular receptors of the new host [71, 74, 76, 77, 153, 154] and adaptations of the NS1 to escape the host immune response [155-157], the viral RNA-dependent RNA polymerase (RdRp) plays a central role in IAV replication and is known to undergo adaptive changes when IAV transmits between species. It was reported that the change E627K in PB2 of AIV is responsible for enhancing viral polymerase activity in mammalian cells, but not in avian cells [158]. However, the E627K substitution is not the only mammalian-adaptive mutation that can arise in the polymerase. Indeed, a large proportion of H5N1-type AIV strains isolated from humans possess a PB2:627E, suggesting that other adaptive aa substitutions must exist in order to counterbalance the generally low polymerase activity in human cells. Along this line, it was also reported that PB2:591K/R and PB2:701N can compensate for a lack of PB2:627K, thereby ensuring efficient polymerase activity in mammalian cells [90, 92]. Furthermore, there is evidence that the PB1 gene from an avian source promotes polymerase activity of human IAV in mammalian cells [87]. Two aa in an AIV PB1 (473V and 598P) were identified to further increase the polymerase activity of human IAV carrying PB2:627E in mammalian cells [88]. Besides adaptive mutations in the polymerase subunits PB1, PB2, and PA and the nucleoprotein (NP) also changes in the nuclear export protein (NEP) have been found to be involved in the viral host adaptation [89].

In the recent years, it has become increasingly apparent that the NS1 gene is another factor likely to be responsible for enhancing IAV polymerase activity. NS1 has been highlighted in an important interaction with the ribonucleoprotein (RNP) complex that regulates viral genome replication [56, 104, 117, 159]. In this respect it was shown that the NS1 protein interacts with the RNP complex *in vivo* [117] and that truncated NS1 affected the production of viral RNA (vRNA) but not of cRNA and mRNA in infected Madin-Darby canine kidney II (MDCK-II) cells, implicating a role of

NS1 in the regulation of viral genome replication [56]. Among many functions the NS1 protein of a human IAV was also shown to inhibit the activity of the cellular anti-viral acting PKR and to regulate the time course of viral RNA synthesis during infection in mammalian cells for review [19] and [104]. The NS segment of an H5N1-type AIV could greatly improve the replication efficiency of the reassortant avian strain FPV (H7N1) in mammalian but not in avian cells by altering the production of viral RNA species [160]. NS1 also interacts with CPSF30, a host RNA polymerase II (Pol II)-associated factor involved in the 3'-end processing of host mRNAs, in a macromolecular complex also containing viral polymerase and NP [161]. In this regard, these findings provide substantial evidence that NS1 is capable to modulate viral genome replication and able to confer a significant replicative advantage during mammalian adaptation of AIV. However, it remains to be determined, which specific part and/or which aa of NS1 are involved in modulating viral polymerase activity, providing a rationale for this study.

In this report, I demonstrate that the specific aa changes D74N and/or P3S+R41K+D74N in the NS1 protein are sufficient for mammalian adaption of AIV. I provide a detailed characterization of the phenotypic changes caused by these residues and I report the importance of these specific residues for strongly enhanced mRNA production as well as viral protein production in mammalian cells. At the same time these adaptive changes are not disadvantageous in avian cells. My study also suggest that the D74N and/or P3S+R41K+D74N substitutions are involved in the temperature adaptation of the AIV polymerase from birds to mammals, as the adaptive changes enhanced the production of viral RNAs synthesis at temperatures representative for the human upper respiratory tract (33-37°C), whereas no affect occurred at avian temperature (41°C). Furthermore, these substitutions enable a strictly AIV to replicate in mice and cause disease. Together, the adaptive mutation D74N and/or P3S+R41K+D74N in NS1 protein allow AIV to establish successful infections in mammalian cells.

3.1 Identification mammalian adapted amino acid on NS1-GD

A previous report by Wang and co-workers [160] has shown that different NS segments of highly pathogenic avian influenza virus (HPAIV) strains

A/Goose/Guandong/1/1996 (GD, H5N1) and A/Mallard/NL/12/2000 (MA, H7N3) in the genetic background of the HAPIV strain A/FPV/Rostock/34 (FPV, H7N1), resulted in altered viral replication characteristics including alteration of the RdRp activity. The reassortant virus FPV-NS^{GD} replicates to high titer, while FPV-NS^{MA} replication efficiency was impaired in mammalian cells [160]. However, in avian cell culture systems, both reassortant viruses replicate to similar extent. These results suggested that the NS1-GD contributes to mammalian adaptation. The two different NS segments of strain GD and MA belong to the same NS allele (allele A). These differ by only eight amino acids (Fig. 3.1A). In order to determine specific aa or aa combinations in the NS1-GD that might be responsible for improved replication of FPV-NS^{GD} in mammalian cells, I utilize two chimera NS segments cloned into an according vRNA expression vector provided by our collaboration (Kalle Saksela, Finland). The first one, containing the N-terminal half of the NS-GD fused with the C-terminal half of NS-MA (NS-GD/MA). The second one, containing the N-terminal half of NS-MA fused with the C-terminal half of NS-GD (NS-MA/GD) (Fig. 3.1B).

To investigate the effect of mutations on viral replication, both vRNA expressing vectors for both NS chimeras were used to generate recombinant reassortant viruses in the backbone of a FPV by reverse genetics. The identity of the viruses was confirmed by RT-PCR and sequences analysis. I then determined the replicative properties of these reassortant viruses. For this I infected cells at a MOI of 0.01 and examined the kinetics of viral growth (Fig. 3.2A). The obtained results show that the reassortant virus harboring NS-GD/MA, grew similar to FPV-NS^{GD}. In contrast, the reassortant virus harboring NS-MA/GD showed impaired replication in mammalian cells similar to FPV-NS^{MA}. This result is reflected in the individual plaque size of the according viruses. I found that the reassortant virus harboring NS-GD/MA yielded large plaques (Fig. 3.2B), comparable to FPV-NS^{GD}, while the reassortant virus harboring NS-MA/GD yielded small plaques. These results indicate that the residue difference between NS1-GD and NS1-MA of S3, K41, N74, V98 and S153, which are located in N-terminal part of NS1-GD, are contributing to the mammalian adaption of the respective reassortant virus in my experimental setting. However, its NS1 protein did not have any known high pathogenicity-associated determinants [90,156,162,163].

A

```
NS-GD   1   MDSNTITSFQ VDCYLWHIRK LLSMRDMCDA PFDDRLRRDQ KALKGRGSTL GLDLRVATME   60

NS-MA   1   MDPNTITSFQ VDCYLWHIRK LLSMRDMCDA PFDDRLRRDQ RALKGRGSTL GLDLRVATME   60

NS-GD  61   GKKIVEDILK SETNENLKIA IASSPAPRYI TDMSIEEMSR EWYMLMPRQK ITGGLMVKMD  120

NS-MA  61   GKKIVEDILK SETDENLKIA IASSPAPRYI TDMSIEEISR EWYMLMPRQK ITGGLMVKMD  120

NS-GD 121   QAIMDKRIIL KANFSVLFDQ LETLVSLRAF TESGAIVAEI SPIPSVPGHS TEDVKNAIGI  180

NS-MA 121   QAIMDKRIIL KANFSVLFDQ LETLVSLRAF TEDGAIVAEI SPIPSMPGHS TEDVKNAIGI  180

NS-GD 181   LIGGLEWNDN SIRASENIQR FAWGIRDENG GPSLPPKQKR YMAKRVESEV  230

NS-MA 181   LIGGLEWNDN SIRASENIQR FAWGIRDENG GPPLPPKQKR YMARRVESEV  230
```

B
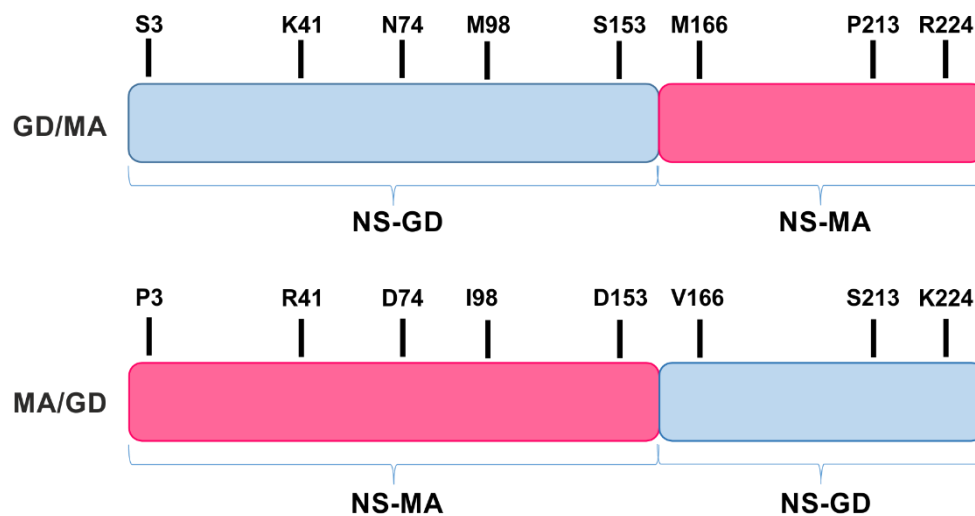
Fig. 3.1 Structural and functional comparison of NS-MA and NS1-GD protein. (A) Comparison of the NS1 amino acid sequences of A/Goose/Guangdong/1/1996 (GD) to A/Mallard/NL/12/2000 (MA). Sequences were aligned with CLUSTAL W. The different amino acid positon among of them are indicated, blue; GD and red, MA. **(B)** Schematic representation of chimeric NS1 containing the N-terminal sequence of A/Goose/Guangdong/1/1996 (GD) and the C-terminal sequence of A/Mallard/NL/12/2000 (MA) "GD/MA" and the chimeric NS1 containing the N-terminal sequence of A/Mallard/NL/12/2000 (MA) and the C-terminal sequence of A/Goose/Guangdong/1/1996 (GD) "MA/GD".

A

B
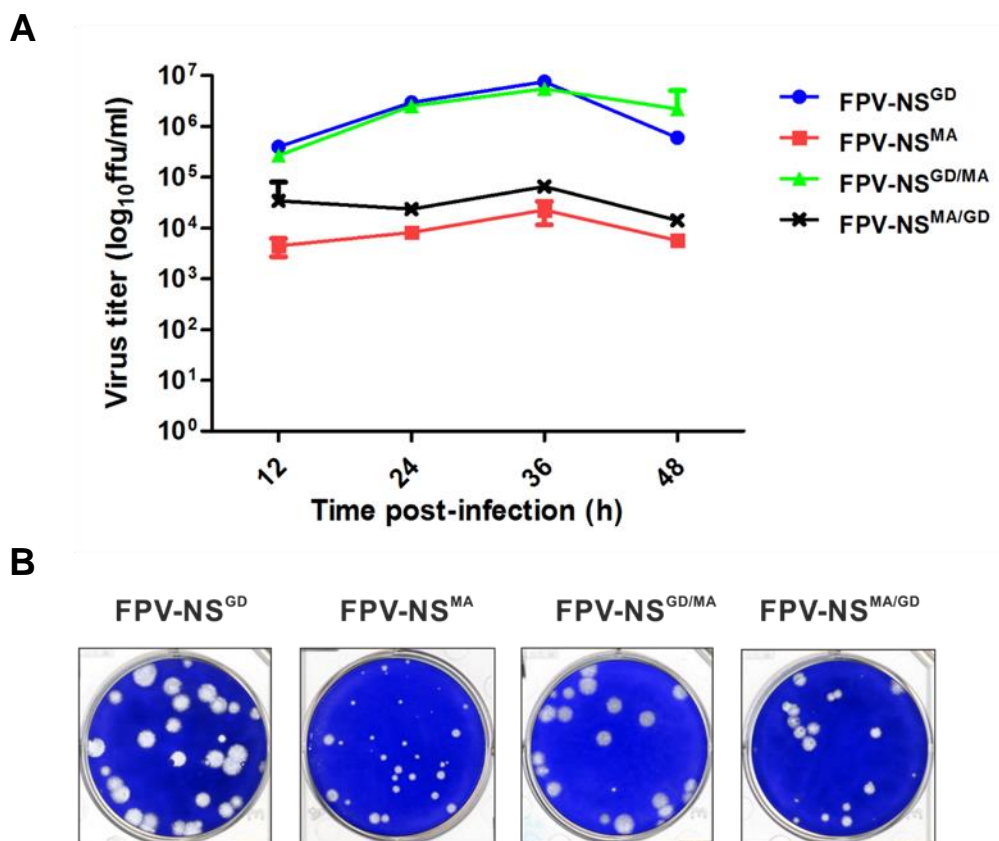
Fig. 3.2 Growth kinetic of virus infected cells. **(A)** Replication kinetic, A549 cells were infected with wild type and mutant virus containing chimeric NS1 expression plasmid at MOI of 0.001. Supernatant of cells inoculated at a MOI of 0.001 were harvested at 12 h interval until 48 h post infection. The virus titers were determined by foci assay on MDCK cells. **(B)** Plaque assay, MDCK cells were inoculated with wild type and mutant virus expressing chimeric NS1. At 48 h p.i., cells were washed, fixed with 3.7% formaldehyde and stained with 1.25% Coomassie blue in 0.25% methanol. Error bars represent standard deviation (n=3).

To further confirm the relevance of the five aa of NS1-GD (S3, K41, N74, V98 and S153) for mammalian adaptation, the codon of each of these aa was introduced into NS1-MA sequence in the corresponding vRNA expressing vector by site directed mutagenesis, replacing those found in the NS1-MA gene to yield five different mutated NS1-MA segments. In addition the codons for the aa combinations P3S+R41K, P3S+R41K+D74N, P3S+R41K+D74N+I98V and P3S+R41K+D74N+I98V+D153S were introduced in the same way. To investigate the effect of the adaptive mutations on viral replication, FPV-NS^{MA} virus variants expressing the different NS1-MA proteins were generated by reverse genetics. As mentioned in section 2.2.7, 293T cells were transfected with 4 plasmids expressing polymerase proteins, NP and 7 plasmids expressing vRNA of FPV-PB1, FPV-PB2,

FPV-PA, FPV-NP, FPV-HA, FPV-NA, FPV-M, together with plasmids expressing vRNA of FPV-NS of the wild type A/chicken/FPV/Rostock/34 (FPV-WT, H7N1) or with other NS segments from A/Goose/Guangdong/1/96 (GD, H5N1), A/Mallard/NL/12/2000 (Ma, H7N3) and NS-MA mutants. At 24 h after transfection of 293T cells, the harvested medium from transfected dishes was screened for rescued influenza virus by observation of liquid CPE and plaque assay on MDCK cells. After three rounds of plaque purification, the recombinant viruses were confirmed by restriction enzyme digestion of RT-PCR products obtained from the NS vRNA. Additionally, the NS, HA, NA and PB2 segments from different recombinant viruses were amplified by RT-PCR and sequenced by GATC corp. The results showed that after three passages, the NS, HA, NA and PB2 were not changed (data not show).

After generation by reverse genetics, all nine possible FPV-NS^{MA} variants were characterized. The replication kinetics were studied and compared to FPV-NS^{GD} and FPV-NS^{MA} in different host cell species: human A549 and avian QT6 cells. Given the titres achieved for each reassortant in human A549 cells (Fig. 3.3) the recombinants containing either the single substitution in NS1-MA (FPV-NS$^{MA\_D74N}$) (Fig. 3.3iv) or the triple substitutions in NS1-MA (FPV-NS$^{MA\_P3S+R41K+D74N}$) (Fig. 3.3viii) show similar or even higher virus replication compared to FPV-NS^{GD}, respectively. Interestingly, FPV-NS$^{MA\_D74N}$ and FPV-NS$^{MA\_P3S+R41K+D74N}$ show comparable replication efficiency on avian QT6 cells (Fig. 3.4). This result revealed that the single substitution D74N and the triple substitutions P3S+R41K+D74N in NS1-MA protein implicated an important functional role for enhanced replication of an AIV in mammalian cells.

I further asked the question whether P3S plus D74N or R41K plus D74N is needed for mammalian adapted virus strain. Results are presented in Fig 3.5. The growth kinetic (Fig. 3.5A) and plaque size (Fig. 3.5B) confirmed that the substitution P3S, R41K together with D74N or D74N alone can improve virus replication independently. Nevertheless, only the triple combination shows an optimal result.
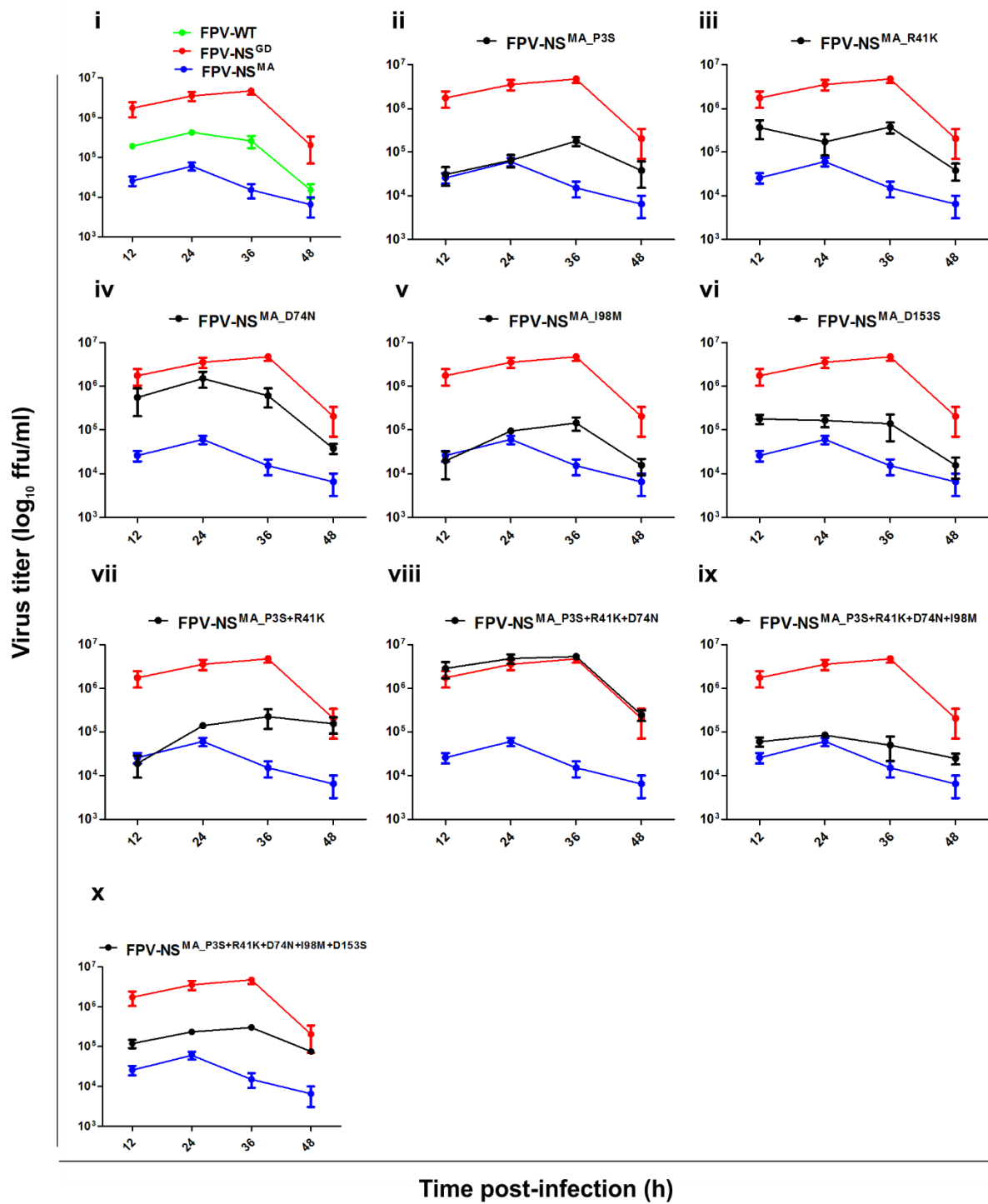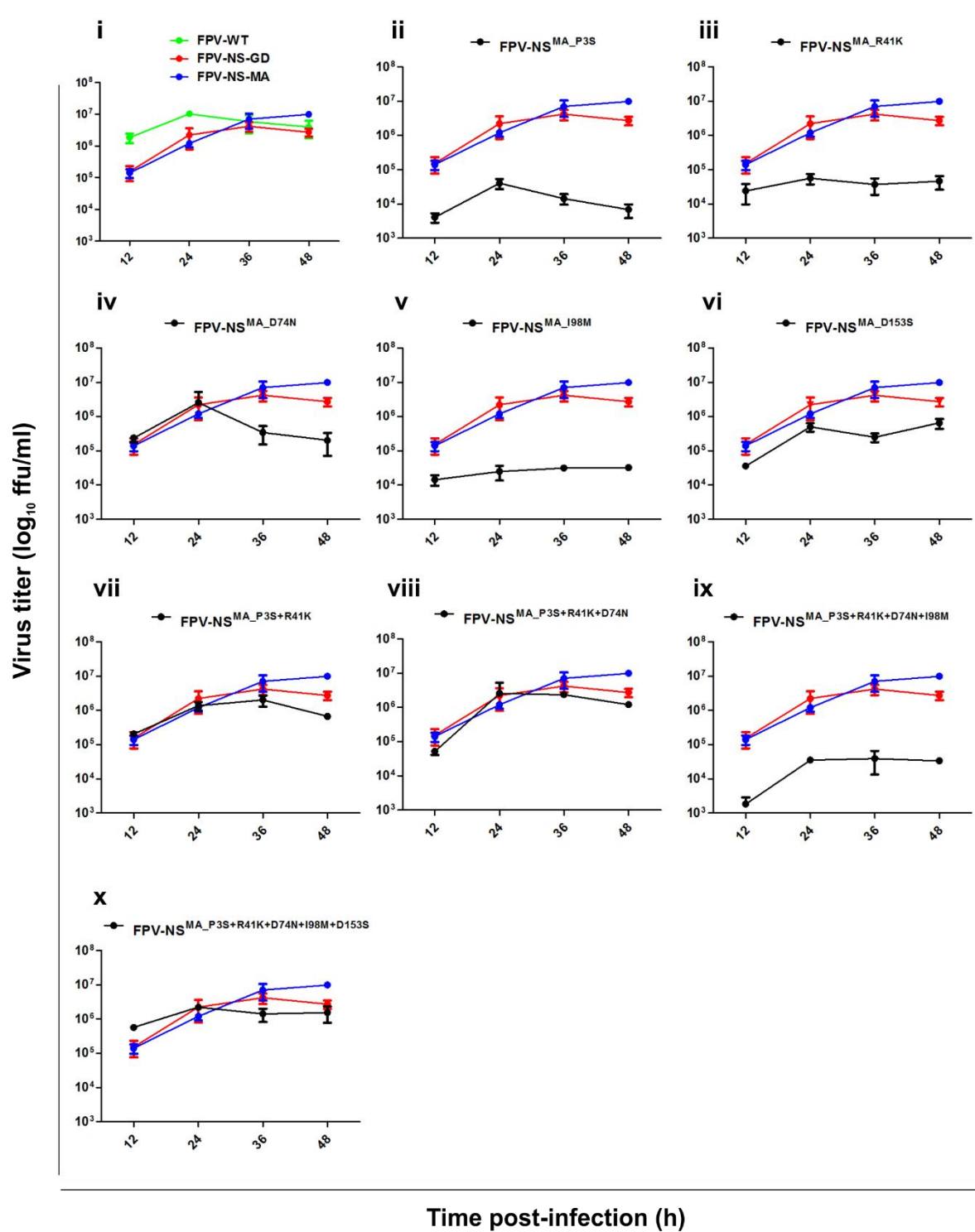
Fig. 3.3 Growth kinetic of viruses in infected A549 cells. A549 cells were infected with wild type or different mutant virus at MOI of 0.001. Supernatant were harvested at 12 h interval until 48 h post infection. The virus titrations were determined by foci assay on MDCK cells. Error bars represent standard deviation (n=3).

Time post-infection (h)

Fig. 3.4 Growth kinetic of viruses in infected QT6 cells. QT6 cells were infected with wild type or different mutant virus at MOI of 0.001. Supernatant were harvested at 12 h interval until 48 h post infection. The virus titrations were determined by foci assay on MDCK cells. Error bars represent standard deviation (n=3).

.

A

B

FPV-NS^{GD}	FPV-NS^{MA}	FPV-NS$^{MA\_P3S+D74N}$	FPV-NS$^{MA\_R41K+D74N}$	FPV-NS$^{MA\_P3S+R41K+D74N}$
0.38±0.04	0.12±0.02	0.22±0.02	0.24±0.02	0.36±0.03
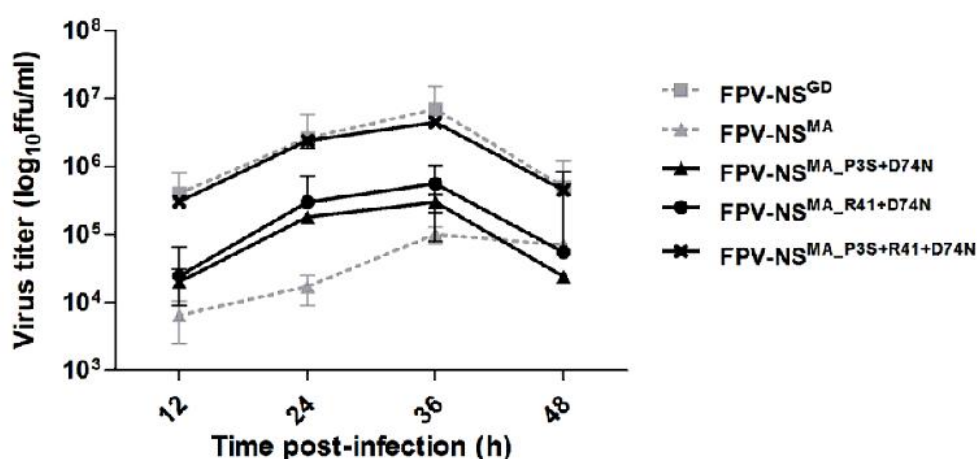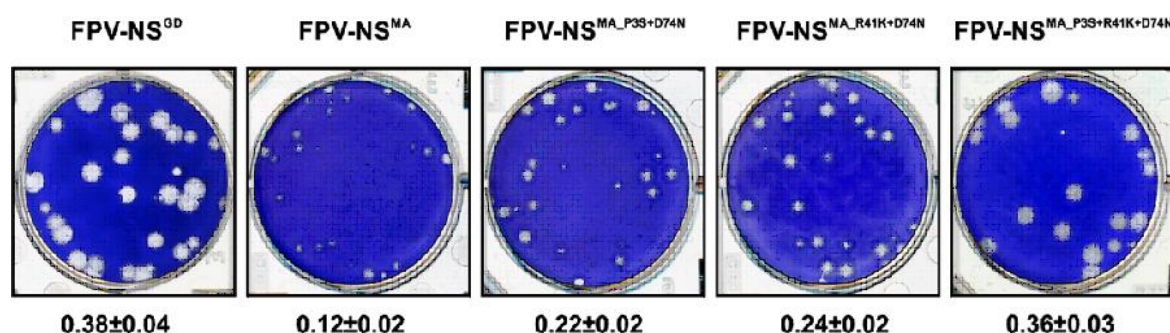
Fig. 3.5 Replication kinetics and plaque analysis. (A) A549 cells were infected with FPV-NS^{GD}, FPV-NS^{MA} or different mutant virus at MOI of 0.001. Supernatant were harvested at 12 h interval until 48 h post infection. The virus titrations were determined by foci assay on MDCK cells. **(B)** Plaque assay, MDCK cells were inoculated with FPV-NS^{GD}, FPV-NS^{MA} or different mutant. After 48 h p.i., cell were washed, fixed with 3.7% formaldehyde and stained with 1.25% Coomassie blue in 0.25% methanol. The diameters of plaques were measured in total 50 plaques. The results represent the averages from three independent experiments.

3.2 Specific effect of the amino acid substitutions in the NS^{MA} on the plaque phenotype of reassortant FPV viruses

In order to investigate whether the specific amino acid substitutions in the NS^{MA} altered the replication speed of the wt FPV virus, I performed *in vitro* replication of the recombinant FPV-NS variants with harboring adaptive mammalian mutation by measuring plaque size upon infection of MDCK cells. At 48 h post infection, cells

were fixed and stained with 1.25% comases blue in methanol and acetic acid and the diameter of 50 plaques in duplicates was quantified. The results are presented in Fig. 3.6. The MDCK cells infected with FPV-NS$^{MA\_P3S+R41K+D74N}$ yielded plaques that were comparable to those observed for FPV-NS^{GD}. However, plaques of cells infected with FPV-NS$^{MA\_D74N}$ resulted in slightly increased size compared to FPV-NS^{MA}, but the FPV-NS$^{MA\_D74N}$ yielded plaques smaller than those observed for FPV-NS^{GD} and FPV-NS$^{MA\_P3S+R41K+D74N}$. This suggests that the adaptive mammalian substitutions P3S+R41K+D74N in the NS1 protein contribute to enhanced speed of virus replication in mammalian cells as shown by big plaque size, but it is not the case for single substitution D74N
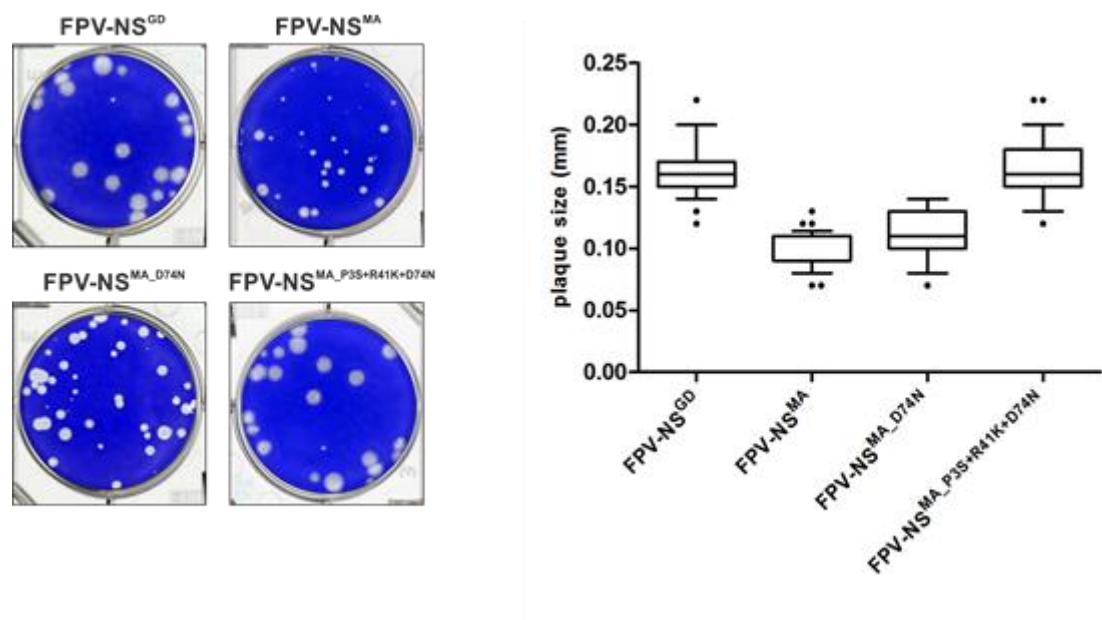
Fig. 3.6 Plaque assay. MDCK cells were inoculated with FPV-NS^{GD}, FPV-NS^{MA} as control and FPV-NS^{MA} containing the indicated substitutions. At 48 h p.i., cell were washed, fixed and stained. The diameters of the plaques were measured (total 50 plaques in duplicates) (**left panel**). The size of individual plaques was plotted using boxplots indicating the median value and quartiles (**right panel**). Differences between individual groups were significant (p<0.01) in Student's t-test.

3.3 Substitution D74N and P3S+R41K+D74N in the MA-NS1 protein alters RNP export in mammalian cells

Efficient nuclear export of RNPs is important for the production of infectious virus [164,165]. In order to investigate whether the substitution D74N and P3S+R41K+D74N in the NS1-MA protein affected viral RNP export patterns, NP localization was analyzed by immunofluorescence using an anti-NP antibody (Fig.

3.7). At 6h p.i., A549 cells infected with recombinant FPV-NS^{GD} showed most NP protein predominantly in the cytoplasm, while FPV-NS^{MA} showed a more nuclear localization. However, in cells infected with FPV-NS$^{MA\_D74N}$ and FPV-NS$^{MA\_P3S+R41K+D74N}$ most NP protein was located in the cytoplasm in similar pattern as FPV-NS^{GD}, indicating that the substitution D74N and P3S+R41K+D74N in the MA-NS1 protein can alter RNP export dynamic. Interestingly, QT6 cells infected with different recombinant viruses showed analogues viral RNP export patterns. This indicates that the substitution D74N and P3S+R41K+D74N in the MA-NS1 protein do not influence RNP export dynamics in avian cell. It seems possible that the substitution D74N and P3S+R41K+D74N in the MA-NS1 protein contribute to rapid RNP export and higher infectious virus titres in mammalian host.
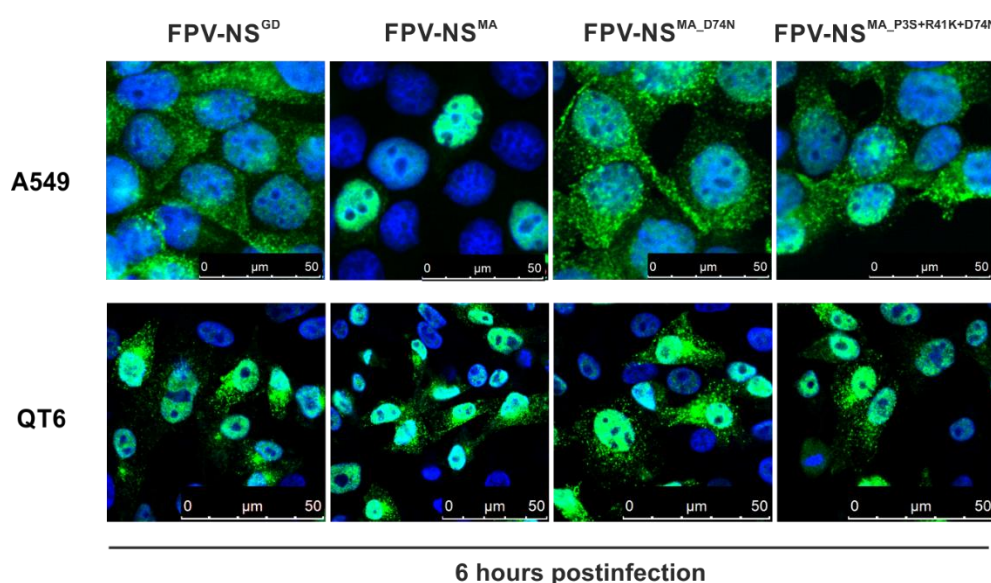
Fig. 3.7 RNP localization in infected cells. Immunofluorescence showing RNP export of the different recombinant viruses. A549 and QT6 cells were infected with recombinant viruses at an MOI of 3 and at 6 h p.i. stained with an anti-NP antibody (green) and DAPI (blue) for the nuclei. The results represent one out of three independent experiments.

3.4 Substitutions D74N and P3S+R41K+D74N in the NS1-MA protein do not alter NS1 protein localization and do not correlate with infectious viral titre

NS1 contains two nuclear localization signals (NLS) and one nuclear export signal (NES), which are responsible for the bi-directional transport of the protein between the nucleus and the cytoplasm. The NS1 protein can therefore localizes either in the

nucleus or in the cytoplasm or in both compartments [166, 167]. The aa sequence comparison showed that the sequence of both, the NLS1 (34-39 aa) and NLS2 (216-220 aa) are conserved between the two NS1 proteins of GD and MA. However, the mammalian adaptive substitutions D74N and P3S+R41K+D74N in the NS1-MA protein are located close to the NLS1 region, possibly influencing its intra-cellular localization. Therefore, I investigated the localization of the NS1 proteins of the different reassortant viruses (FPV-NS^{GD}, FPV-NS^{MA}, FPV-NS$^{MA\_D74N}$, FPV-NS$^{MA\_P3S+R41K+D74N}$) in infected A549 and QT6 cells. At all times points of the infection I found that the NS1 proteins of all viruses were predominantly cytoplasmic in A549 infected cells (Fig. 3.8A), while all viruses infected QT6 cells showed a cytoplasmic and nuclear NS1 localization (Fig. 3.8B). Hence, the substitutions in the NS1-MA protein do not alter its intra-cellular localization, and therefore the infectious titre of the respective FPV-NS^{MA} variants in A549 cells does not correlate with intra-cellular localization of the different NS1 proteins.

A

A549

| FPV-NS^{GD} | FPV-NS^{MA} | FPV-NS^{MA_D74N} | FPV-NS^{MA_P3S+R41K+D74N} | h.p.i. |

B

QT6

| FPV-NS^{GD} | FPV-NS^{MA} | FPV-NS^{MA_D74N} | FPV-NS^{MA_P3S_R41K_D74N} | h.p.i. |
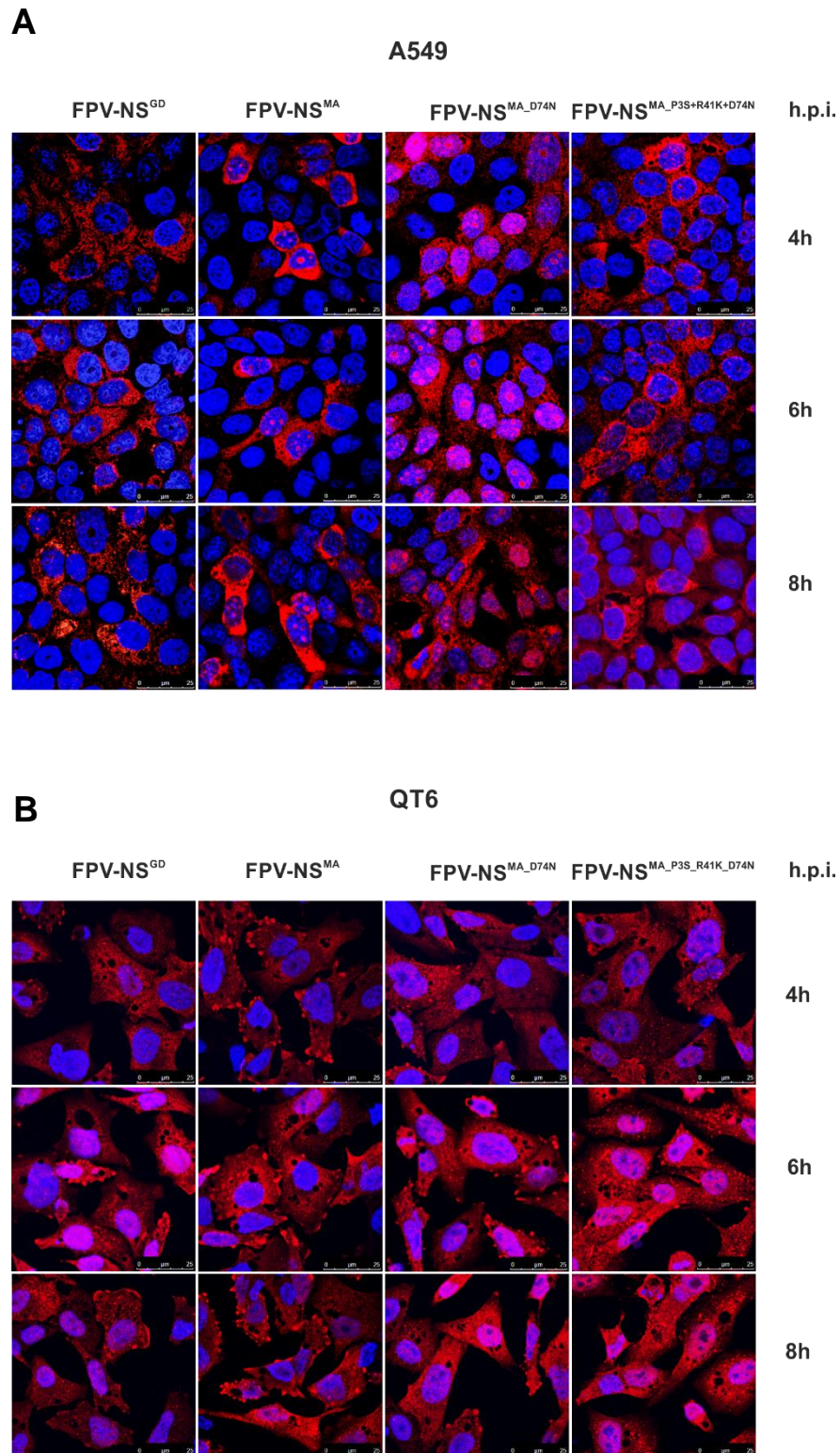
Fig. 3.8 The NS1 localization in infected cells. A549 **(A)** and QT6 **(B)** cells were infected with wild type and mutant virus at MOI of 3. At the indicated time points post infection, cells were fixed and stained using a rabbit polyclonal anti-NS1 primary, and Alexa 594 anti-rabbit (red) as well as DAPI (blue) to localize NS1 and the nucleus, respectively. Representative images are shown (taken using a 63x oil immersion objective). The results represent one out of three independent experiments.

3.5 The contribution of D74N and P3S+R41K+D74N in the MA-NS1 protein enhances viral protein synthesis in mammalian cells

To determine the consequences of the aa substitutions in the NS1-MA at the level of the viral protein production, cells were infected with either FPV-NS^{GD} or the mutant FPV-NS^{MA} viruses and viral protein production was determined during a single-infection cycle. For this, infected A549 cells (MOI=2) were lysed at the indicated time points p.i. and the viral proteins were detected after SDS-PAGE by Western blot using NS1- and NP-specific antibodies. The results are presented in Fig. 3.9A. Apparently, NS1 and NP synthesis in human A549 cells was strong over the entire time course of the FPV-NS^{GD} infection. In contrast, I observed a delay in the synthesis as well as a low overall amount of these viral proteins during FPV-NS^{MA} infection. However, compared to viral protein production in cells infected with FPV-NS^{MA}, I observed a higher accumulation of the viral proteins over the entire time course of the infection in cells infected with FPV-NS$^{MA\_D74N}$ and FPV-NS$^{MA\_P3S+R41K+D74N}$. Here, the amounts of NS1 and NP were comparable to those of the FPV-NS^{GD} (Fig. 3.9A). The delay in viral protein synthesis as well as the low level of viral protein production observed for FPV-NS^{MA} could be due to slower kinetics of viral RNA replication, viral transcription, or both. However, this defect was rescued in FPV-NS$^{MA\_D74N}$ and FPV-NS$^{MA\_P3S+R41K+D74N}$ virus-infected cells, suggesting that these substitutions in the NS1-MA protein might contribute to kinetics of viral RNA replication, viral transcription or both. The situation in avian QT6 cells was different (Fig. 3.9B). I found that the kinetic and also the amount of viral protein synthesis are undistinguishable between the different viruses in all infections. This could be due to equal mRNA or vRNA accumulation in these avian cells, and might be a possible explanation for the high production of viral proteins in the QT6 cells. To investigate these assumptions, I next set out to determine the accumulation of viral vRNA, mRNA and cRNA in cells infected with the different viruses.

A

B
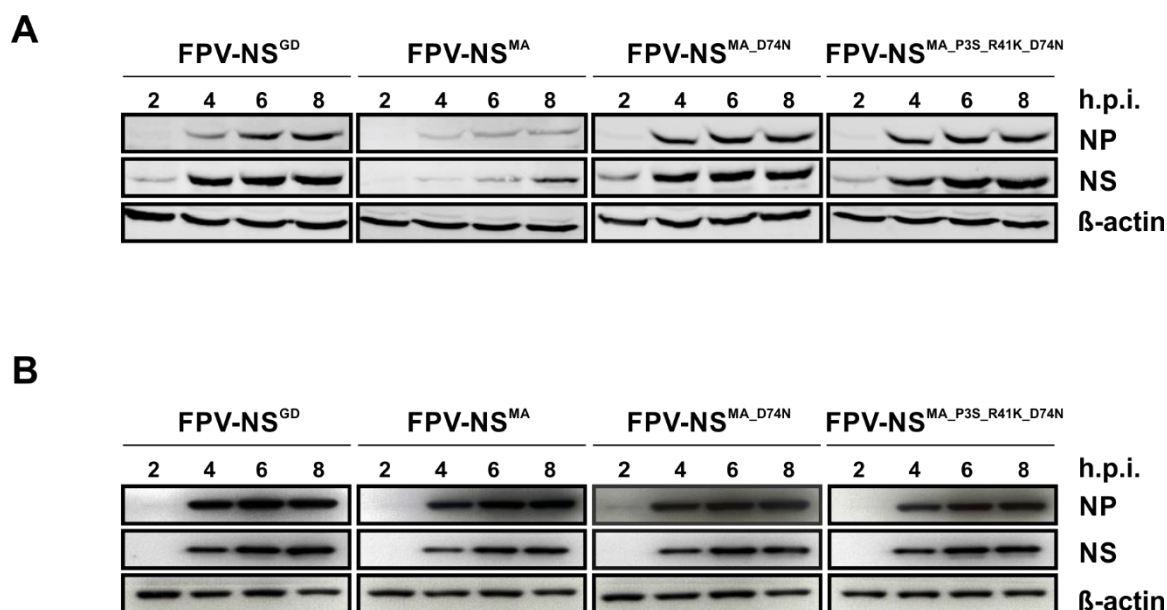
Fig. 3.9 Viral protein synthesis in infected cells. A549 **(A)** and QT6 **(B)** cells were infected with wild type and mutant viruses at MOI of 3. Cells were lysed at the indicated time points, and the lysates were analyzed for the viral proteins NS1 and NP by immunoblotting under identical conditions. Cellular actin was detected as a loading control. The results represent one out of three independent experiments.

3.6 Substitutions D74N and P3S+R41K+D74N in the MA-NS1 protein enhanced viral polymerase activity in a RNP reconstitution assay

The NS1 protein has been shown to be involved in viral RNA replication [16, 56, 160, 168], translation of viral mRNA [57, 169] and also the temporal regulation of vRNA synthesis was affected in NS1 mutant viruses [104]. Furthermore, the NS1 protein has been shown to interact directly with the viral polymerase complex [159]. In addition, NS1 also seems to interact with the 5′ untranslated region (5′-UTR) of viral mRNAs, enhancing their translation [57].

To test the hypothesis that the single substitution D74N or the combination of P3S+R41K+D74N in the MA-NS1 protein might affect the viral polymerase activity, I utilized a RNP reconstitution assay that recreates functional influenza virus RNPs by transfecting cells with plasmids that separately express the three polymerase proteins PB1, PB2, PA, NP and NS1 and a (-) vRNA segment encoding a CAT gene. To determine polymerase complex function, CAT activity [22] was used as a marker of mRNA transcription. The principle of the *in vitro* RNP reconstitution assay is shown in Fig. 3.10. The results are presented in Fig. 3.11. In 293T cells, the polymerase

complex of FPV co-transfected with NS1-GD was significantly more active than that of wild-type NS1-FPV or NS1-MA (P<0.001, Student's t-test). However, when the FPV polymerase complexes were co-transfected with NS1-MA^{D74N} or NS1-MA$^{P3S+R41K+D74N}$, the reverse pattern was observed. The substitutions D74N in NS1-MA resulted in a 2.5-fold increase in CAT activity as compared to the NS1-MA and 2-fold compared to the wild-type NS1-FPV. Whereas, substitutions P3S+R41K+D74N in NS1-MA yielded a 4.5-fold increase in CAT accumulation compared to those induced by the NS1-MA and 4-fold compared to the wild-type NS1-FPV. Remarkably, the triple substitutions P3S+R41K+D74N in NS1-MA resulted even in a 1.5-fold increases as compared to NS1-GD.
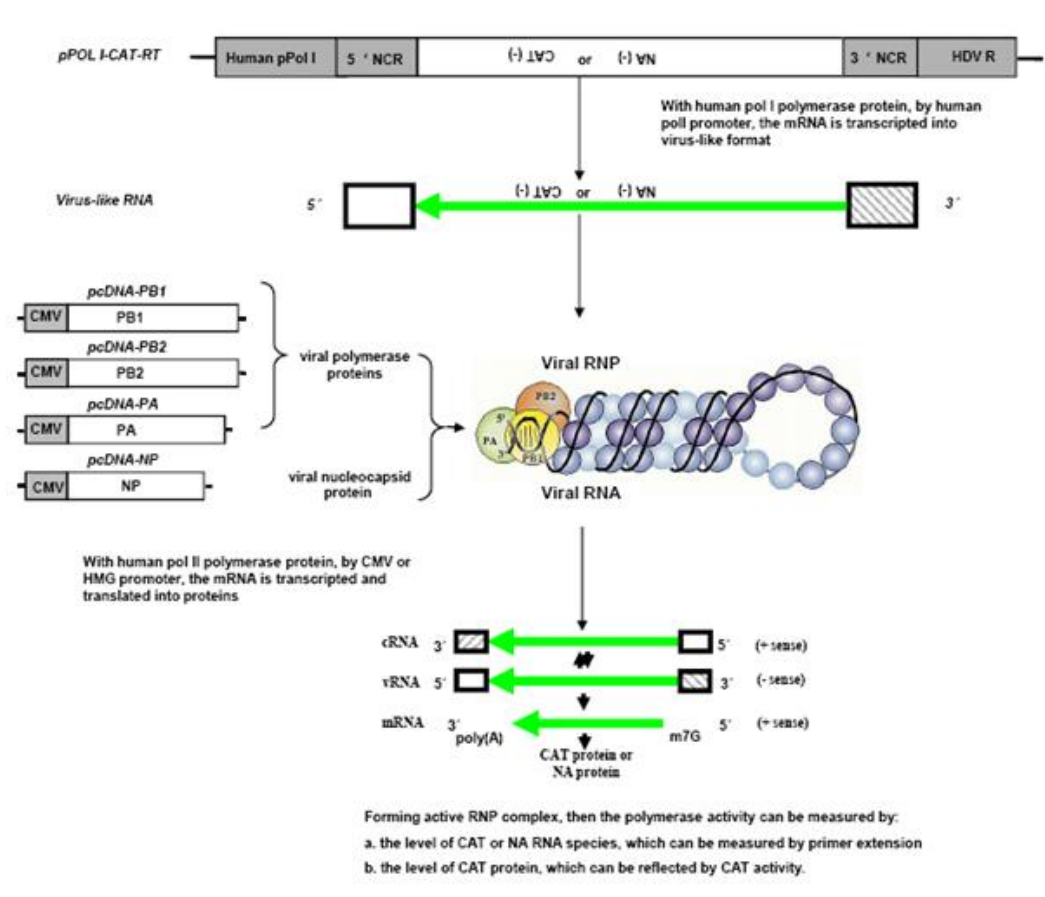
Fig. 3.10 Principle of RNP reconstitution assay (CAT assay). The plasmid pPOLI-CAT-RT contains the CAT open reading frame in minus sense flanked by the noncoding regions of the NS RNA segment of influenza A/WSN/33. Expression of the influenza virus-like RNA is driven by a truncated human RNA pol-I promoter and ended by a sequence derived from the hepatitis delta virus genomic ribozyme (R). The other four plasmids express viral PB1, PB2, PA, and NP proteins with a CMV promoter. These proteins are able to amplify and transcribe the influenza virus-like RNA expressed by pPOLI-CAT-RT into mRNA, resulting in the detection of CAT activity in transfected human 293 cells. The represented regions in the plasmid constructs are not drawn to scale [22].

My data thus show that the different NS1 proteins can affect the viral polymerase activity of avian FPV virus, and that this effect is greater in mammalian cells when NS1 possess amino acid residues D74N and P3S+R41K+D74N. This observation raises the possibility that yet unknown molecular features in the NS1 contribute to high level of polymerase activity of avian FPV virus in mammalian cells.
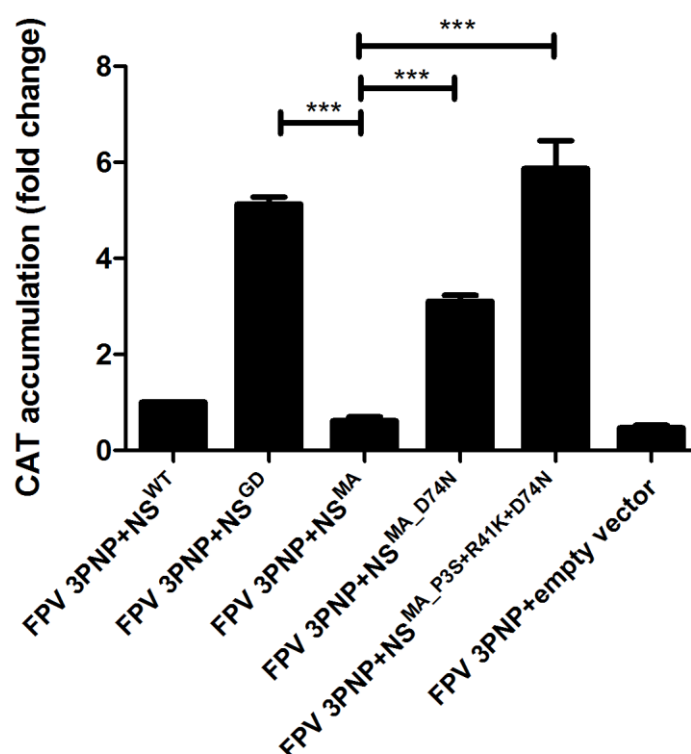
Fig. 3.11 Effects of the substitutions in the NS1-MA protein on viral polymerase activity using RNP reconstitution assay. Relative CAT activity (normalized against FPV 3PNP+NS^{WT}) after reconstitution of the avian FPV polymerase (FPV+3PNP) in 293T cells and co-transfection of plasmids encoding the different MA-NS1 variants (NS^{GD}, NS^{MA}, NS$^{MA\_D74N}$ and NS$^{MA\_P3S+R41K+D74N}$) or empty plasmid vector (control). Error bars represent standard deviation (n=3).

3.7 Substitutions D74N and P3S+R41K+D74N in NS1 protein enhances viral genome synthesis

To study the activity of the viral polymerase in more detail I investigated the amount of vRNA, cRNA and mRNA produced during the time course of a viral infection, by primer extension assays (The principle of primer extension is shown in the Fig 3.12) using total cellular RNA isolated from virus infected A549 and QT6 cells. At various time points after infection with MOI=2 using FPV-NS^{GD}, FPV-NS^{MA}, FPV-NS$^{MA\_D74N}$,

and FPV-NS$^{MA\_P3S+R41K+D74N}$ viruses, all three RNAs species were detected and quantified.
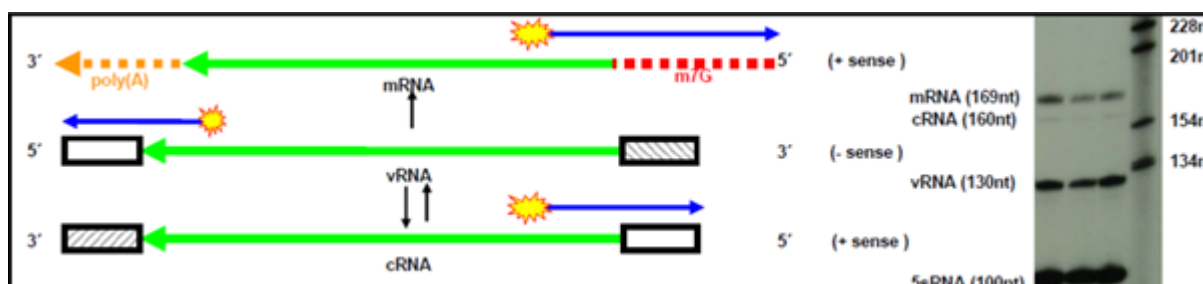
Fig. 3.12 Primer extension for detection of viral replication and transcription. As mentioned before, viral vRNA is replicated by a cRNA (full length copy) into more vRNA (replication) and transcribed into viral mRNA primed by cellular 5' cap primer from vRNA (transcription). These three viral RNAs are different in their ends. If two radioactivity labelled primers are used for reverse transcription (RT) reaction to detect vRNA and cRNA/mRNA, they will give products of different length. After separation on the 7M urea 6% PAGE sequence gel, the RT products can be quantified to show the amount of viral RNA species.

The results are presented in Fig 3.13A. Compared to FPV-NS^{GD}, FPV-NS^{MA} synthesized apparently lower amounts of all viral species in A549 cells. However, in infection with FPV-NS$^{MA\_D74N}$ and FPV-NS$^{MA\_P3S+R41K+D74N}$ virus infected cells led to elevated levels of all three viral RNA species similar to FPV-NS^{GD}, predominantly increasing the amount of vRNA and cRNA, while marginally changing the mRNA quantity. Notably, infection with FPV-NS$^{MA\_D74N}$ resulted in a minor increase in the level of vRNA and cRNA, while in a significant increase of the mRNA levels at early time points (2-4 h p.i.), but then significantly decreasing at late time points of infection (6-8 h p.i.). These results are compatible with the data obtained by *in vitro* reconstitution of recombinant RNPs (Fig 3.11). In contrast, in all virus-infected QT6 cells no difference in the amounts of viral RNAs (Fig. 3.13) was observed. Here, production of all RNA species showed similar kinetics over the entire course of the infection, suggesting that the efficiency of polymerase activity of FPV-NS^{GD}, FPV-NS^{MA} and FPV-NS^{MA} mutants remained constant. From these results, I conclude that the single substitution D74N and the triple substitution P3S+R41K+D74N in MA-NS1 increases mRNA production is based on transcription activity (mRNA levels) only or also in part on replication activity of the RdRp (vRNA, cRNA-level).

A A549

B QT6
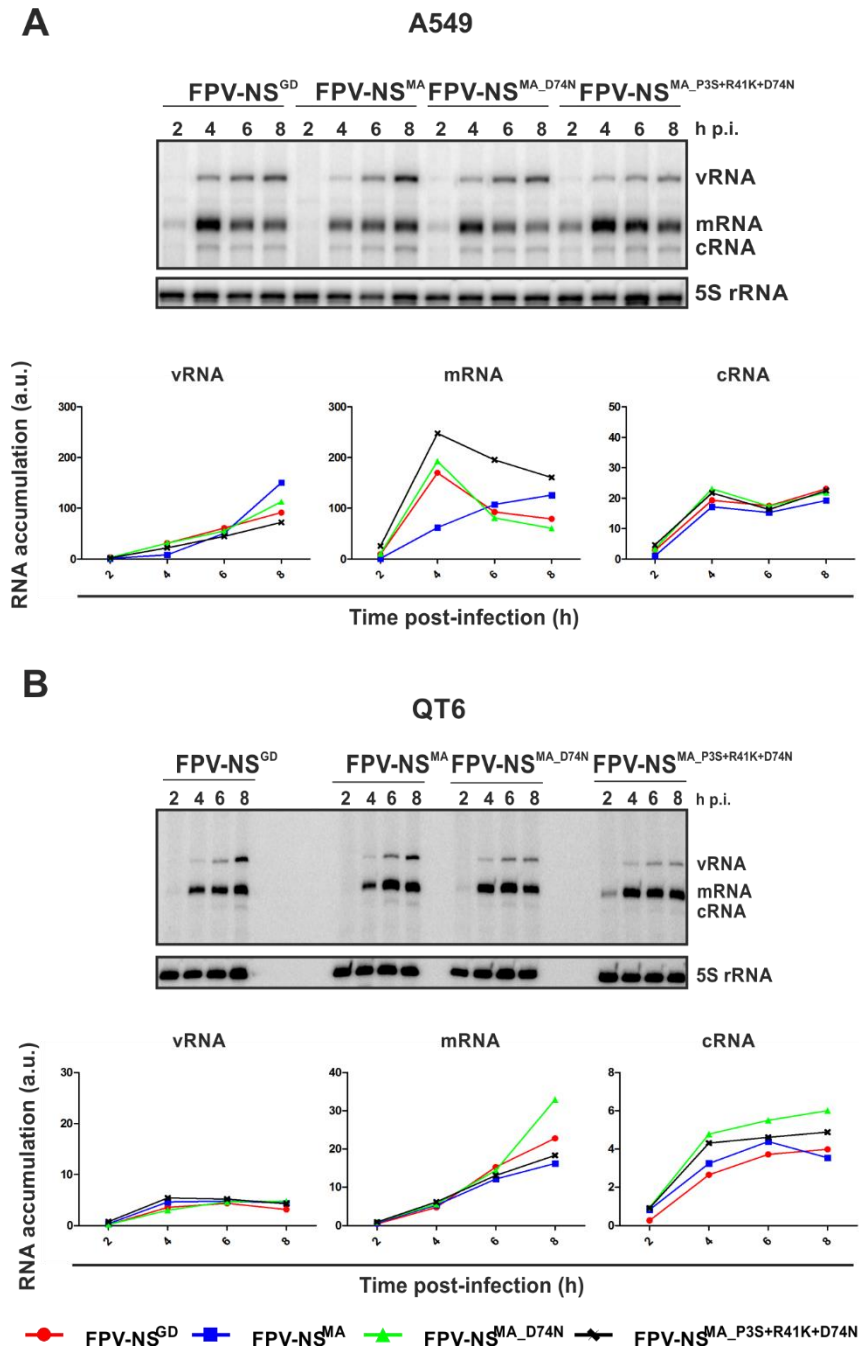
Fig. 3.13 Effects of the mutations in the NS1-MA protein on viral RNA synthesis. A549 **(A)** and QT6 **(B)** cells were infected (MOI of 2) with FPV-NS^{GD}, FPV-NS^{MA}, FPV-NS$^{MA\_D74N}$ and FPV-NS$^{MA\_P3S+R41K+D74N}$. At the indicated time p.i. the accumulation levels of vRNA, cRNA and viral mRNA were determined by primer extension (shown in the upper panels), and the amount of these RNAs were normalized to that of cellular 5S rRNA (shown in the lower panels). Increase in the levels of vRNA, cRNA and mRNA at 4, 6, 8 h p.i. of each viruses were set in relation to the strain-specific RNA levels at 2 h p.i.. This experiment is represent one out of at least three independent experiments.

3.8 Viral transcription are affected by the substitutions D74N and P3S+R41K+D74N

Based on the results mentioned above the level of viral RNA synthesis and the increase of virus protein synthesis in the presence of MA-NS1 with either the single substitution D74N or the triple substitution P3S+R41K+D74N (Fig. 3.13) could be caused by the viral genome amplification and/or the viral genome transcription.

To elucidate whether the substitutions affect genome replication (cRNA and vRNA synthesis) and/or transcription (viral mRNA synthesis) activities, I measured the primary transcription activity, i.e. transcription directed by the incoming parental RNPs in the absence of viral RNA amplification using cycloheximide (CHX), a potent inhibitor of protein synthesis. It was previously shown that CHX suppresses (viral) protein synthesis and thereby leads to the degradation of newly replicated viral genomic RNA, but not of viral mRNA since formation of new vRNPs was repressed [170-172]. I utilized this method to measure the primary transcription activity that depends only on the incoming vRNPs excluding effects of the secondary genome replication process. Therefore, the levels of viral mRNA and vRNA in the absence or presence of CHX were determined after cells were transfected with different plasmid encoding NS1 and superinfect with different viruses. As the primer extension technique showed not to be suitable for this purpose, probably due to the overall low levels of viral RNAs in the infected cells, I performed qRT-PCR and the viral transcription activity was calculated as the ratio of viral mRNA/vRNA (Fig. 3.14). The results show that the difference of the mRNA/vRNA ratio for the NP segment of the FPV-NS^{GD} is significantly higher than in the FPV-NS^{MA} infected cells in the absence or presence of CHX (Fig. 3.14A and 3.14B). Interestingly, the difference of the mRNA/vRNA ratio between cells infected with FPV-NS$^{MA\_D74N}$ or FPV-NS$^{MA\_P3S+R41K+D74N}$ compared to cells infected with FPV-NS^{MA} is also higher in the absence and presence of CHX (Fig. 3.14A and 3.14B). These data indicate that either D74N alone or the combined P3S+R41K+D74N substitutions in the NS1-MA protein has an affect on transcription activity.

A   **B**
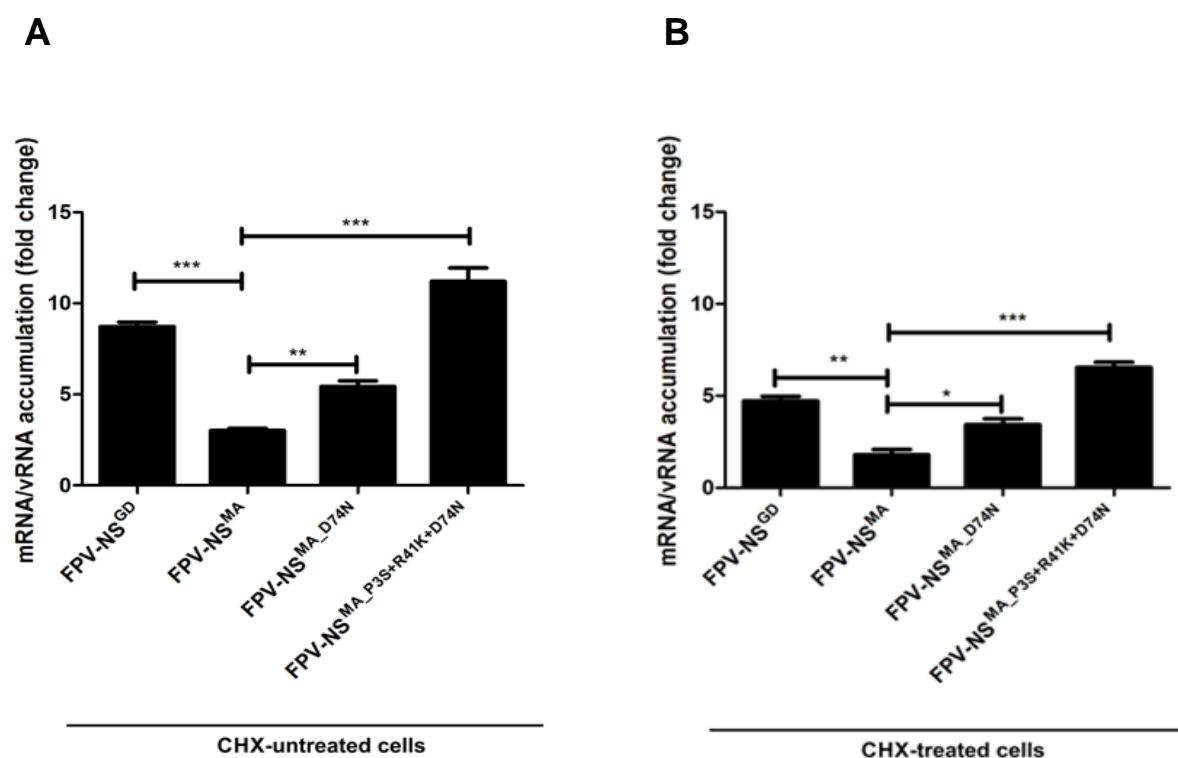
Fig. 3.14 Primary transcription activity of NS1 mutant influenza A viruses containing amino acids specific for mammalian adapted virus strains. A549 cells were infected with different viruses at MOI of 3 and incubated in the absence **(A)** or presence **(B)** of 100 µg/ml of CHX (right panel). At 4 h p.i., the accumulation levels of mRNA and vRNA were measured by qRT-PCR, and the amounts of these RNAs were normalized by that of cellular actin mRNA. The transcription activity is represented as a ratio of the amount of mRNA to that vRNA. Error bars represent standard deviation (n=3).

3.9 Substitutions D74N and P3S+R41K+D74N in NS1-MA result in a replication advantage at lower temperature

It has long been hypothesized that something as simple as the temperature at the site of replication could influence the host and tissue tropism of the virus [173-175]. Human-tropic influenza viruses are considered to replicate in the upper respiratory tract at 33–37°C, while AIV replicate in the gut of the birds at around 41°C [174]. The polymerase is an important determinant of influenza virus host range and pathogenicity [156,176,177] that is likely to be influenced by temperature. In our study, we could demonstrated that the substitution D74N and/or P3S+R41K+D74N in the NS1-MA protein contribute to enhanced polymerase activity, regulate viral genome synthesis, and thus increase the poor propagation of an avian virus in mammalian cell culture, thereby impeding the host restriction. To this point, I next asked, whether these substitutions would also result in a replication advantage at a

temperature comparable to the upper respiratory tract of mammals (e.g. humans). Since one of the substitution D74N is situated in the linker region (LR) of the NS1 protein, I reasoned that this substitution might influence in flexibility of the NS1 protein. Because of the inherent flexibility in the LR [178], a particular NS1 could acquire alternative conformational states allowing the RNA binding domain (RD) or the effector domain (ED) to engage in different quaternary interactions that participate in specific protein/protein or protein/RNA interactions. I therefore proposed that the ambient temperature might influence the flexibility of the NS1 protein. To this end, I applied temperature dependent *in silico* structure simulation (data provided by M. Lechner, Marburg) to investigate the flexibility of NS1 at 33°C and 41°C. The results are presented in Fig. 3.15. At 33°C, the D74N change in NS1-MA introduces significantly more flexibility compared to wild-type NS1-MA. Interestingly, this effect cannot be reproduced at 41°C. Here, the mutation does not apparently change the protein's flexibility, which remains similar to that of the wild-type NS1-MA. Notably, NS-GD is most flexible at 33°C as well as at 41°C.
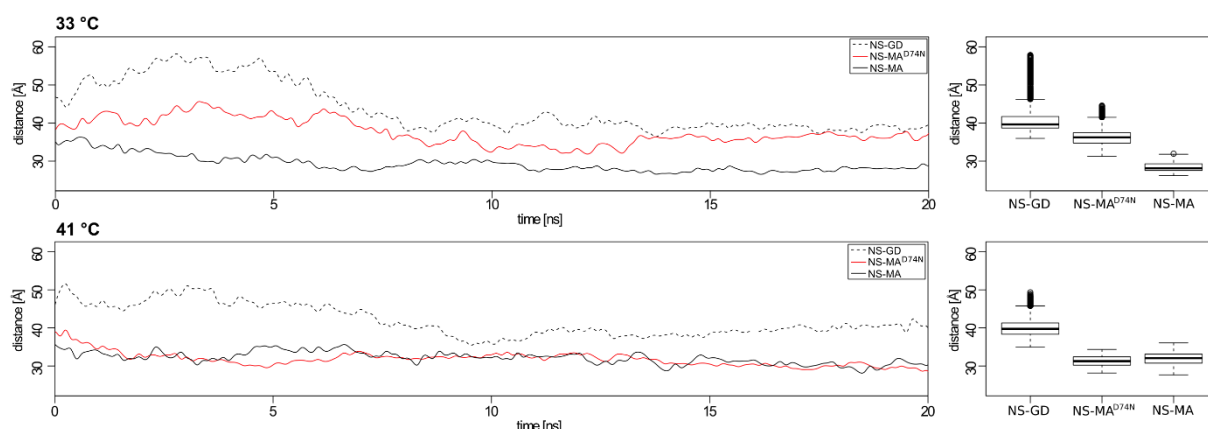
Fig. 3.15 Flexibility of the NS1 mutant protein. Distance of the geometric centers of both NS1 subunits connected by the linker (positions 5-70 and 106-225) over the course of 20 nanoseconds (ns) in a virtual molecular dynamics simulation using namd (http://www.ks.uiuc.edu/Research/namd/) at 33°C and 41°C. Boxplots summarize the distances of the last 12 ns (to mask border effects of the simulation in the first 8 ns).

Next I analyzed, whether the *in silico*-predicted increased flexibility given by D74N substitution would also affect viral replication at low (33°C) or elevated (41°C) temperatures *in vitro.* To study this in the context of a viral infection, A549 cells were infected with FPV-NS^{GD}, FPV-NS^{MA}, FPV-NS$^{MA\_D74N}$, and FPV-NS$^{MA\_P3S+R41K+D74N}$ viruses as indicated in Fig 3.16. Multiple-cycle growth curves show that FPV-NS^{GD},

FPV-NS$^{MA\_D74N}$, and FPV-NS$^{MA\_P3S+R41K+D74N}$ viruses replicate efficiently at 33°C, and 41°C, whereas, FPV-NS^{MA} was restricted at 33°C. However, at 41°C it replicated as efficiently as all the other variants. The comparable replication efficiency of the viruses tested at elevated temperature equivalent to the avian gut could be due to the fact that all viruses tested have an avian (FPV) background. Nevertheless, the data indicate that avian viruses with increased replication ability in mammals can arise in birds without any replication disadvantage in birds.
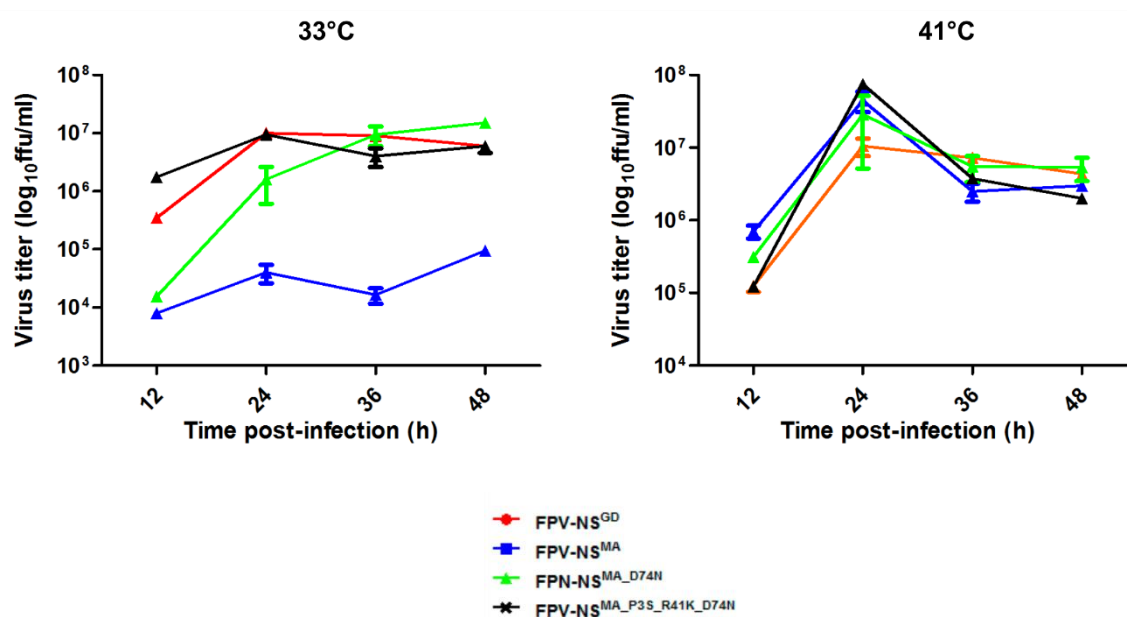
Fig. 3.16 Effect of temperature on virus replication. Comparison of the growth kinetic of NS1 mutant influenza A viruses containing amino acids specific to mammalian adapted virus strain by multi-cycle assay. A549 cells were infected at MOI of 0.001 and incubated at either 33°C or 41°C. Virus titers at indicated time points were determined by foci assay. Error bars represent standard deviation (n=3).

To further determine the influence of the incubation temperature on viral RNA synthesis in the context of an infection, cells were inoculated with the four different viruses (FPV-NS^{GD}, FPV-NS^{MA}, FPV-NS$^{MA\_D74N}$, and FPV-NS$^{MA\_P3S+R41K+D74N}$) and incubated at 33°C or 41°C. Lysates of infected cells were harvested every two hours until eight hours p.i., and total cellular RNA was isolated. Primer extension was performed for the simultaneous detection and quantification of v-, c- and mRNA from segment 5 (NP). The results are presented in Fig. 3.17. Compared to FPV-NS^{GD} infected cells, the vRNA accumulation from FPV-NS^{MA} infected cells showed similar kinetics at 41°C, but two to threefold decreased accumulation rates at 33°C.

However, this reduction was partially rescued in FPV-NS$^{MA\_D74N}$ and fully compensated in FPV-NS$^{MA\_P3S+R41K+D74N}$ infected cells. To analyze whether the reduction of vRNA obtained by FPV-NS^{MA} was a consequence of a decreased cRNA production, the accumulation of NP cRNA was also determined at both temperatures. The result is presented in Fig. 3.17. Here, I could not observe a temperature-dependent effect on the cRNA accumulation of the different viruses. These results indicated that the aa at position S3, K41 and N74 in the NS1-MA protein might affect the process of vRNA generation rather than cRNA production and demonstrate that the functional disadvantage of the NS1-MA at lowered temperature can partially be rescued by the D74N substitution and fully compensated by the triple change (P3S+R41K+D74N), suggesting that the aa S3+K41+N74 in the NS1-MA contribute to the temperature-sensitive phenotype observed for FPV-NS^{MA}.

To elucidate whether the reduction in vRNA accumulation of FPV-NS^{MA} at the 33°C would be reflected in viral transcription, the accumulation of the various mRNAs was analyzed. The results obtained for NP mRNA are presented in Fig 3.17. Similar to the effect on vRNA accumulation, NP mRNA accumulation was significantly reduced at 33°C in FPV-NS^{MA} infected cells, but was comparable to the amount of the other mRNAs at 41°C. Again, this difference in the levels of the specific mRNAs was equilibrated in FPV-NS$^{MA\_D74N}$ and FPV-NS$^{MA\_P3S+R41K+D74N}$ infected cells. These results are fully compatible to the growth kinetic of the viruses-infected cells. In summary, these data support the concept that the substitutions in NS1-MA significantly contribute to overcome the notable physiological difference between avian and mammalian host systems.
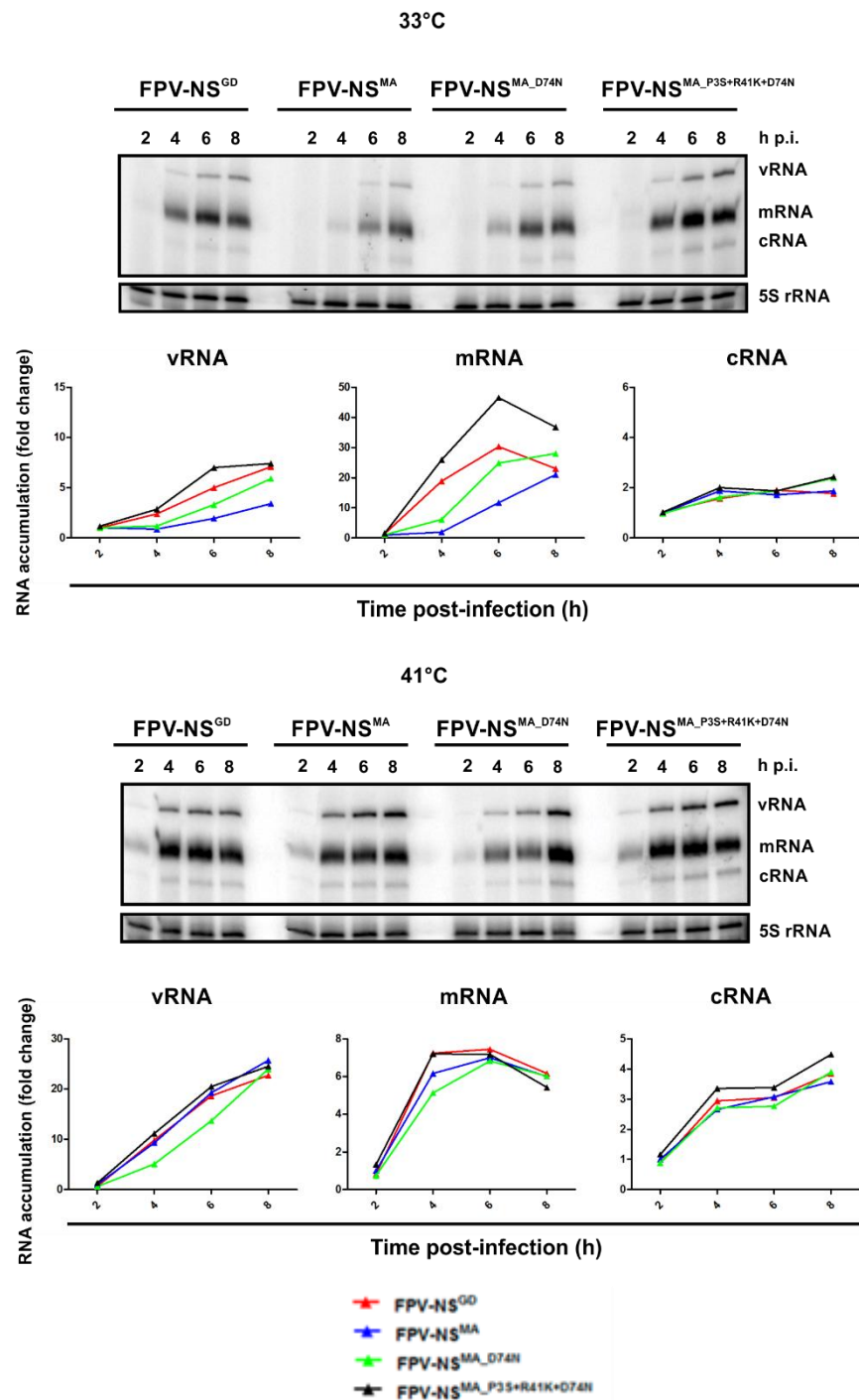
Fig. 3.17 Effect of temperature on viral RNA synthesis. A549 cells were infected at MOI of 3 and incubated at either 33°C or 41°C. After the indicated time points post infection, cells were lysed and RNAs accumulation levels were determined by primer extension analysis using primer specific for segment 5 (NP). The accumulation levels of viral mRNA and vRNA were measured by primer extension, and the amount of these RNAs were normalized by that of cellular actin mRNA. Increase in the levels of vRNA, cRNA and mRNA at 4, 6, 8 h p.i. of each viruses were set in relation to the strain-specific RNA levels at 2 h p.i. This experiment is represented one out of at least three independent experiments.

3.10 Substitutions P3S+R41K+D74N in the NS1-MA contributed to pathogenic in mice

In cell culture I have identified adaptive changes in the NS1, which contribute to the ability of avian viruses to overcome host range restrictions and to replicate efficiently in mammalian cells. To evaluate the effect of the adaptive changes P3S, R41K and D74N in the NS1 of avian virus on the virulence and replication in a mammalian model, I infected C57BL/6J mice with $2x10^4$ PFU of FPV-NS^{GD}, FPV-NS^{MA}, FPV-NS$^{MA\_D74N}$ and FPV-NS$^{MA\_P3S+R41K+D74N}$ by intranasal infection. It was previously shown that FPV wild-type is not pathogenic for mice [179]. I then monitored body weight and survival rate. In my experiments, mice either succumbed to the infection or were euthanized when they had lost more than 30% of their initial body weight. FPV-NS^{GD} and FPV-NS^{MA} viruses showed similar levels of virulence in mice (Fig. 3.18). Mice that were infected with these two viruses showed a slight loss of body weight (10-15%) up to day 5 p.i.. First mice started to die at day 9 p.i.. Surprisingly, no major differences in overall mortality caused by the two viruses were observed. In contrast, mice infected with FPV-NS$^{MA\_P3S+R41K+D74N}$ succumbed to infection even more rapidly, and there was a dramatically loss of body weight up to 17% at day 2 p.i. and up to 30% at day 3 and no mouse survived beyond day 5 p.i.. In contrast, only one mouse infected with FPV-NS$^{MA\_D74N}$ succumbed to the infection (Fig. 3.18B). These results strongly suggest that the adaptive substitutions P3S+R41K+D74N in the NS1-MA protein resulted in severe pathogenicity in mice. However, the single change D74N (FPV-NS$^{MA\_D74N}$) had no appreciable effect on the virulence of FPV-NS^{MA}, but in contrast to the *in vitro* experiment did not show strong pathogenicity for mice.
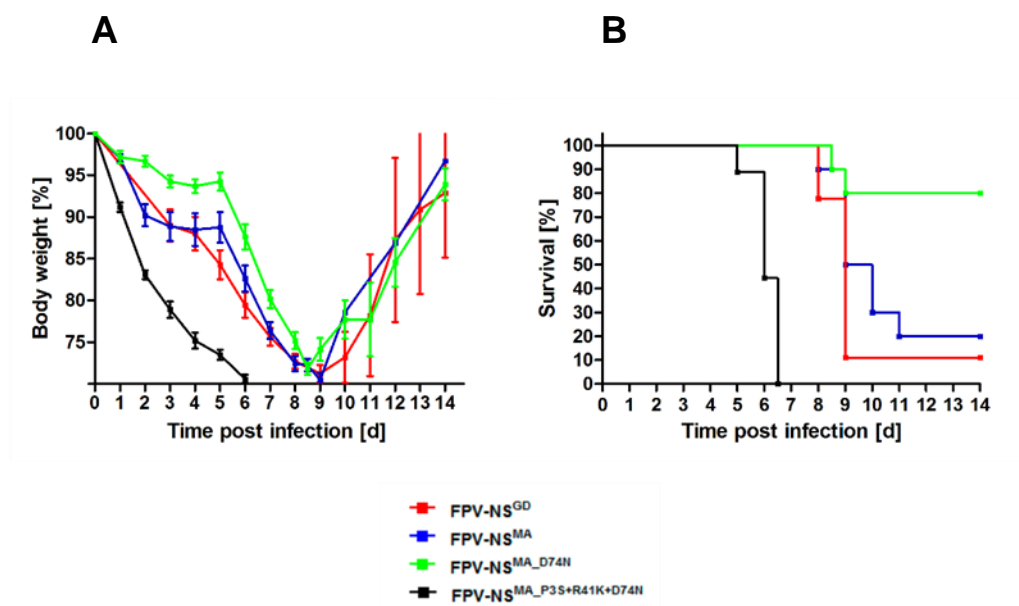
Fig. 3.18 Pathogenicity of NS1 mutant viruses in mice. Female mice (10-12 weeks of age) C57BL/6J mice were inoculated intranasal with the recombinant FPV-NS variant viruses. The percentages of surviving mice and weight loss during the course of the experiment are given. **(A)** The body weights of infected mice were recorded up to 14 days p.i.. Error bars indicate standard deviations. Mice had to be euthanized when they lost more than 30% of their initial body weight **(B)**. Morbidity and mortality were analyzed for mice intranasal infected with 2×10^4 PFU of the virus.

3.11 Prevalence of D74N and/or P3S+R41K+D74N in the NS1 of IAV

To assess the prevalence of the aa S3, K41 and N74 in the NS1 protein of IAV, I determined the frequency of these residues from NS sequences (31,237 sequences) that were obtained from the NCBI's Influenza Virus Resource database [180]. I found that the pathogenicity marker, the aa N74 and the combination S3+K41+N74 represents only 0.1-2% of the available human-, avian-, and other-isolates except for swine viruses where it is represented around 10% (Fig. 3.19). Although the pool of viruses encoding the N74 and/or S3+K41+N74 in the NS1 gene was small, a pattern emerged that associated this substitutions with adaptation to host-switching (Table 3.1). P3S+R41K+D74N was found in swine isolates from 1976-1979 of H1N1 virus that switched from avian to swine hosts (Table 3.1) P3S+R41K+D74N was also independently observed in two case of the 1997 H5N1 virus (A/Hong Kong/481/97-H5N1 and A/Hong Kong/437-6/1997-H5N1) that switched from avian to human host, in one case of the 2013 H7N9 virus A/Fujian/1/2013 (H7N9) that also switched from avian to human host and was also found in the pandemic 2009 H1N1 virus that

switched from swine to human host (Table 3.1). Interestingly, the aa 3S+41K are already highly conserved in human, avian, swine, and other IAV (Fig. 3.19) resulting in a significant percentage of around 94-96% of all virus isolates (Fig. 3.19). I therefore asked next what function (s) are affected by Asparagine (N) at position 74 in an NS1, which already possesses S3+K41.
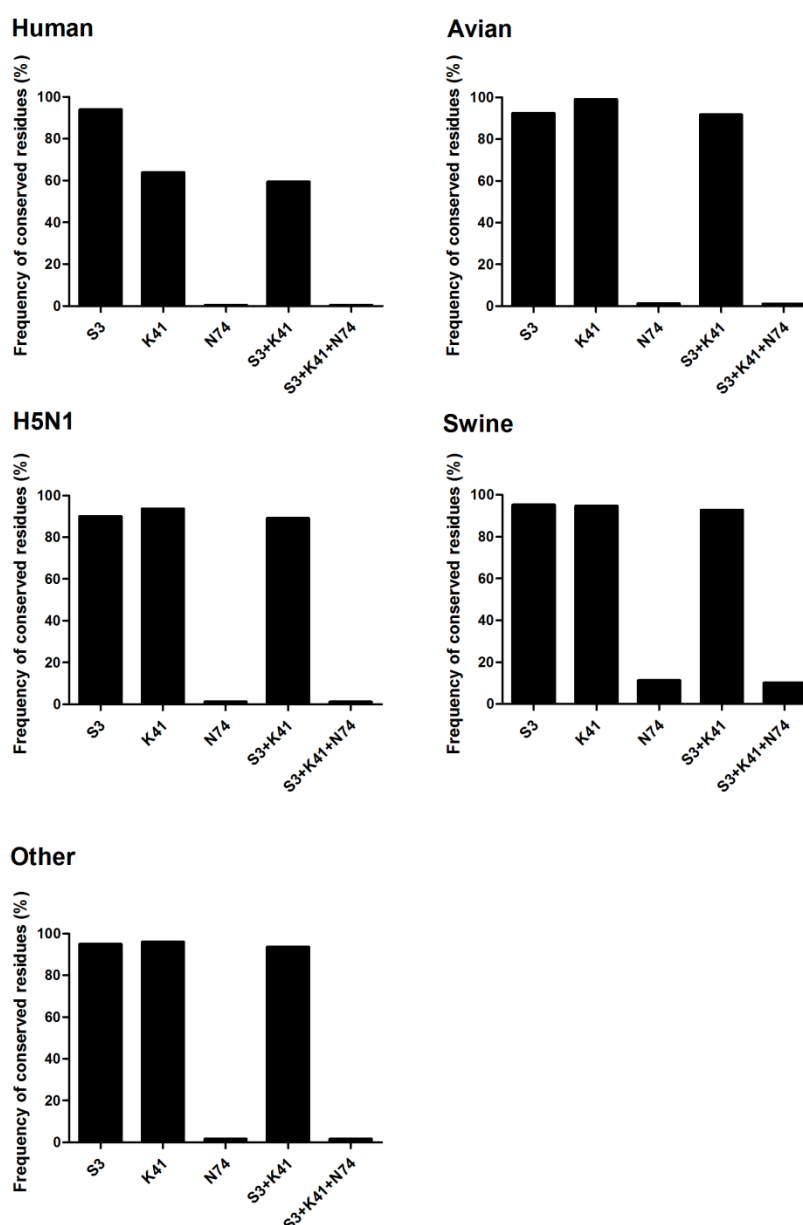
Fig. 3.19 Percentage of viruses encoding NS1 protein with adaptive residues (S, K, N) at aa position 3, 41 and 74. Amino acid sequences of the NS1 proteins (Human: 11,152, Avian: 10,678, H5N1: 2,715, Swine: 3,085, and other: 851 sequences) of influenza A viruses obtained from the NCBI's Influenza Virus Resource database were analyzed (accessed: 20 October 2014). The percentages of isolated virus of human, avian, swine and other origin containing the indicated aa S3, K41, N74 alone or in combination, S3+K41 and S3+K41+N74 in their NS1 are shown.

Table 3.1 List of represent virus containing the 3S+41K+74N in NS1 protein

Accession number	Name	subtype	Origin	Host	Amino acids
ACZ47203	A/Hong Kong/437-6/1997	H5N1	Avian	Human	S3+K41+N74
AF084285	A/Hong Kong/482/97	H5N1	Avian	Human	S3+K41+N74
AGK82162	A/Fujian/1/2013	H7N9	Avian	Human	S3+K41+N74
AEL89636	A/Bangkok/INS481/2010	H1N1	Avian	Human	S3+K41+N74
ACZ96032	A/Texas/45104048/2009	H1N1	Swine	Human	S3+K41+N74
ADG42288	A/Hvidovre/INS141/2009	H1N1	Swine	Human	S3+K41+N74
ACY30105	A/Niigata/749/2009	H1N1	Swine	Human	S3+K41+N74
ADM33114	A/Lagos/WRAIR1984T/2009	H1N1	Swine	Human	S3+K41+N74
ADM86424	A/Copenhagen/INS434/2009	H1N1	Swine	Human	S3+K41+N74
ADM33094	A/Lagos/WRAIR1982N/2009	H1N1	Swine	Human	S3+K41+N74
ABQ45419	A/swine/Tennessee/3/1976	H1N1	Avian	Swine	S3+K41+N74
ABQ45430	A/swine/Tennessee/7/1976	H1N1	Avian	Swine	S3+K41+N74
ABQ45441	A/swine/Tennessee/15/1976	H1N1	Avian	Swine	S3+K41+N74
ABQ45452	A/swine/Tennessee/17/1976	H1N1	Avian	Swine	S3+K41+N74
ABQ45463	A/swine/Iowa/1/1976	H1N1	Avian	Swine	S3+K41+N74
ABQ45538	A/swine/Tennessee/19/1976	H1N1	Avian	Swine	S3+K41+N74
ABR15824	A/swine/Iowa/4/1976	H1N1	Avian	Swine	S3+K41+N74
ABD95717	A/swine/Tennessee/25/1977	H1N1	Avian	Swine	S3+K41+N74
ABR15835	A/swine/Tennessee/19/1977	H1N1	Avian	Swine	S3+K41+N74
ABR15846	A/swine/Tennessee/21/1977	H1N1	Avian	Swine	S3+K41+N74
ABR15857	A/swine/Tennessee/31/1977	H1N1	Avian	Swine	S3+K41+N74
ABR28641	A/swine/Minnesota/5892-7/1979	H1N1	Avian	Swine	S3+K41+N74
CY037902	A/Swine/Belgium/WVL1/1979	H1N1	Avian	Swine	S3+K41+N74

3.12 Asparagine at position 74 of the NS1 enhances viral RNA synthesis also in the FPV wild type

I could show that either the single D74N or the triple P3S+R41K+D74N substitution in the NS1-MA protein, placed in the FPV background, enhanced viral genome replication and transcription in mammalian cells. To now determine whether this effect would only occur in this specific genetic constellation or whether this would also apply for NS1 proteins belonging to allele A and to a wild type avian IAV, I changed D74 to N in the NS1 protein of FPV-WT, which already carries S and K at position 3 and 41. I hypothesized that this virus would show a similar phenotype as

FPV-NS$^{MA\_P3S+R41K+D74N}$. Following my hypothesis, I found that the FPV-NS$^{WT\_D74N}$ was able to replicate in A549 to higher (1 log) titre than FPV-NS^{WT}, whereas similar replication kinetics of both, FPV-NS^{WT} and FPV-NS$^{WT\_D74N}$ were observed after infection of QT6 cells (Fig. 3.20A). In agreement with my previous results from the primer extension assay for FPV-NS$^{MA\_P3S+R41K+D74N}$, infection of A549 cells with FPV-NS$^{WT\_D74N}$ resulted in significantly increased transcript levels of viral mRNA (Fig. 3.20C) and thus in higher accumulation of viral protein (Fig. 3.20B), while both viruses showed similar protein production in QT6 cells (Fig. 3.20B). I also confirmed that this single adaptive mutation has the potential to contribute significantly in overcoming the temperature restriction that avian viruses are faced in the upper respiratory tract of humans, leading to strongly increased virus titers at 33°C (Fig 3.21A). In agreement with primer extension result (Fig. 3.20C), A549 infected with FPV-NS$^{WT\_D74N}$ at 33°C resulted in increased transcription levels of mainly vRNA and mRNA compared to cells infected with FPV-NS^{WT}. However, similar differences in transcript levels were observed after infection at 41°C (Fig. 3.21B).
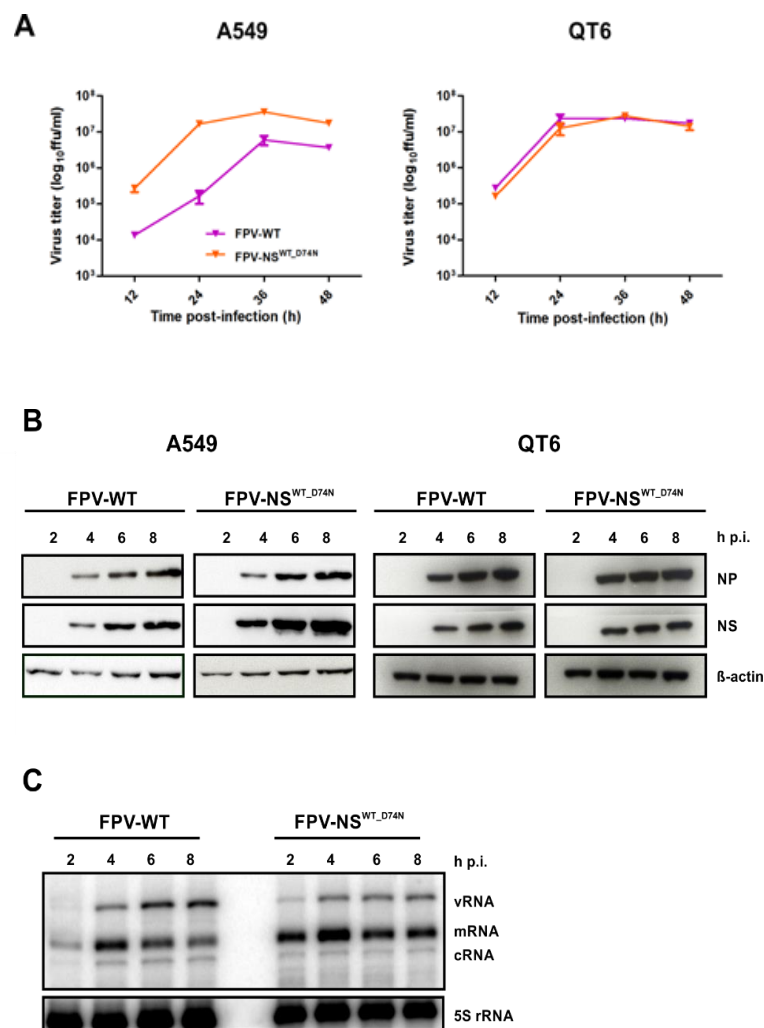
Fig. 3.20 General effect of amino acids in the NS1 for the mammalian adaptation of avian virus strain. (A) Comparison of the growth kinetic of avian FPV wild-type and FPV NS1 mutant containing amino acids specific to mammalian adapted virus strain (FPV-NS$^{WT\_D74N}$) on A549 and QT6 cells by multi-cycle assay. Error bars represent standard deviation (n=3). **(B)** A549 and QT6 cells were infected with FPV wild-type or FPV-NS^{WT} at MOI of 3. Cells were lysed at the indicated time points, and the lysates were analyzed for the viral proteins NS1 and NP by immunoblotting under identical conditions. Cellular actin was detected as a loading control. A549 cells were infected with FPV wild-type or FPV-NS$^{WT\_D74N}$ at MOI of 3 and incubated at 37°C. This experiment is represent one out of at least three independent experiment. **(C)** A549 cells were infected with FPV wild-type or FPV-NS^{WT} at MOI of 3. After the indicated time points post infection, cell were lysed and RNAs accumulation levels were determined by primer extension analysis using primer specific for segment 6. The accumulation levels of viral mRNA and vRNA were measured by primer extension. This experiment is represent one out of at least three independent experiments.

Finally, the pathogenic potential of the adaptive changes P3S+R41K+D74N for mice was further demonstrated by mice infection with FPV wild-type and FPV-NS$^{WT\_D74N}$. FPV wild-type is known to be apathogenic for mice [179], but already carries S3 and K41 presented in its NS1 protein. By introduction of D74N into NS1 of FPV wild-type. I mimicked a FPV-NS$^{MA\_P3S+41K+74N}$ phenotype. Following my hypothesis, mice infected with FPV-NS$^{WT\_D74N}$ showed a dramatic decrease in body weight of up to 30% at day 8.5 p.i. and beyond day 9 p.i. only one mouse out of ten survived infection, while FPV-NSWT only caused a slight loss of body weight up to 20% and mice that recovered (9/10) regained 100% (Fig. 3.22). These results strongly confirmed the effect on pathogenicity of the adaptive substitutions P3S+R41K+D74N in mice.

A
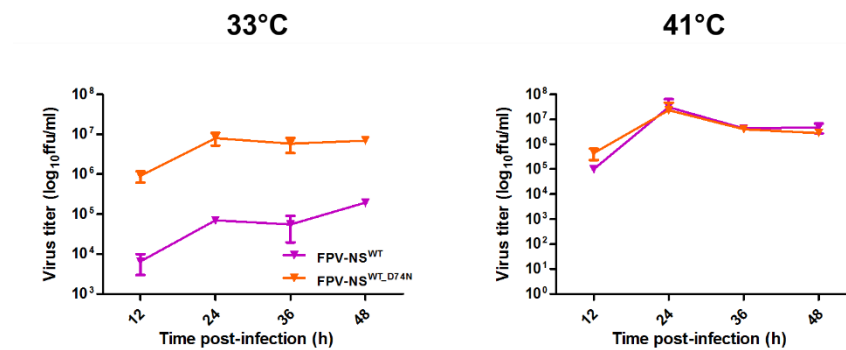
B
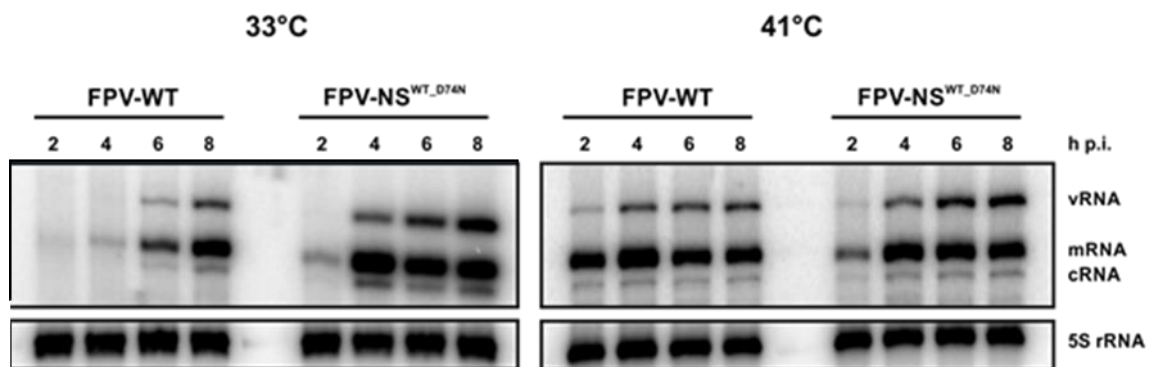
Fig. 3.21 General effect of amino acids in the NS1 for the mammalian adaptation of avian virus strain at different temperatures. (A) Comparison of the growth kinetic of avian FPV wild-type and FPV NS1 mutant containing amino acids specific to mammalian adapted virus strain (FPV-NS$^{WT\_D74N}$) on A549 and QT6 cells by multi-cycle assay at 33°C and 41°C. Error bars represent standard deviation (n=3). **(B)** A549 cells were infected with FPV wild-type or FPV-NS$^{WT\_D74N}$ at MOI of 3 and incubated at 33°C or 41°C. After the indicated time points post infection, cells were lysed and RNAs accumulation levels were determined by primer extension analysis using primer specific for segment 6. The accumulation levels of viral mRNA and vRNA were measured by primer extension. This experiment is represent one out of at least three independent experiments.

A

B
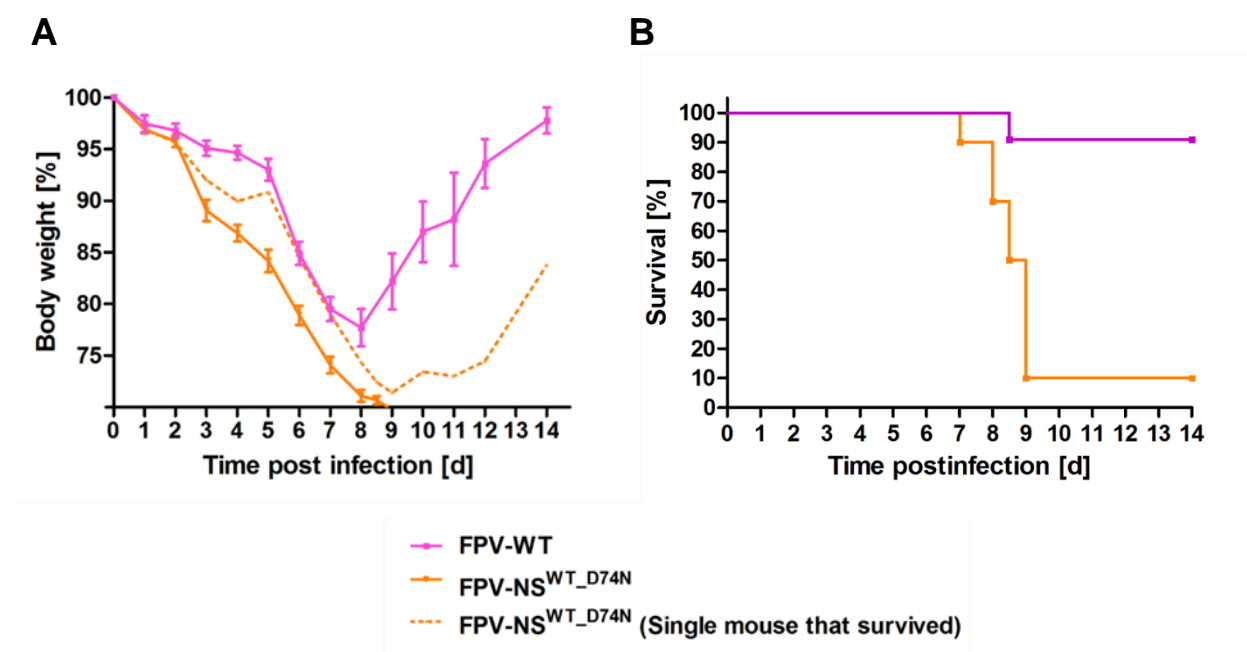
Fig. 3.22 Pathogenicity of FPV-NS1 mutant viruses in mice. Female C57BL/6J mice (10-12 weeks of age) (n=10) were inoculated intranasal with the recombinant FPV-NS variant viruses. The percentages of surviving mice and weight loss during the course of the experiment are given. **(A)** The body weights of infected mice were recorded up to 14 days p.i.. Error bars indicate standard deviations. Mice had to be euthanized when they lost more than 30% of their initial body weight **(B)**. Morbidity and mortality were analyzed for mice intranasal infected with 2×10^4 PFU of the virus.

3.13 Asparagine at position 74 of the NS1 enhances viral replication also in the broad spectrum of influenza virus

In an alternative attempt to confirm my finding that the collectively residues S3, K41 and N74 in the NS1 significantly contribute to the adaption of avian IAV towards mammalian cells, I introduced aa 74N into the NS1 protein (carrying S3+K41) of another avian IAV, which basic replication in mammalian cells is impaired. For this I selected a pair of viruses SC35 and SC35M.

SC35 was originally derived from A/Seal/Massachusetts/1/80 (H7N7) by serial passages in chicken embryo cells, thereby acquiring a multi-basic cleavage site in its Haemagglutinin (HA) [181] becoming 100% lethal for chickens, but being low-pathogenic for mice. Passaging SC35 in mouse lung, resulted in the mouse-adapted variant SC35M [163]. In contrast to SC35, SC35M is highly pathogenic for both mice and chickens. Both viruses differ mainly by mutations in their polymerase proteins

(PB2, PB1, and PA) and in the nucleoprotein (NP). SC35M has a considerably higher polymerase activity in mammalian cells than SC35, which correlates with increased virulence in mice. Similar polymerase mutations were found in unrelated strains, especially H5N1 HPAIV and human isolates [92].

I determined the viral genome replication and transcription kinetic by primer extension. For this, A549 cells were infected with the mutant SC35$^{NS\_D74N}$ (NS allele A) and compared it to SC35^{WT} and SC35M. The replication of SC35$^{NS\_D74N}$ resulted in virus titers that were higher than those of SC35^{WT}, but lower than those of SC35M for entire time course of infection (Fig. 3.23A). Consistently, determination of viral RNA species accumulation by primer extension (Fig. 3.23B) showed a strong increase for all viral RNA species in SC35$^{NS\_D74N}$ compared to SC35^{WT} infected A549 cells. Again, the values for SC35M remained higher, indicating an optimized adaptation. Nevertheless, this result demonstrates that one single D74N substitution in NS1 protein can strongly alter the viral genome replication and transcription, thus contributing to improved virus replication in a mammalian host.

Moreover, the introduction of this single mutation N74 into the NS1 of the 2009 pandemic influenza virus A/Gießen/6/2009 (S-OIV-H1N1) and a A/Thailand/1(KAN-1/2004 (H5N1) HPAIV both already possessing S3+K41 demonstrated that now these mutant viruses show significantly increased replication in human A549 cells compared to wild-type viruses (Fig. 3.24). This finding suggest that the acquisition of N74 for the AIV that already possess S3+K41 in their NS1, may create viruses with improved replication ability in mammalians, including humans.
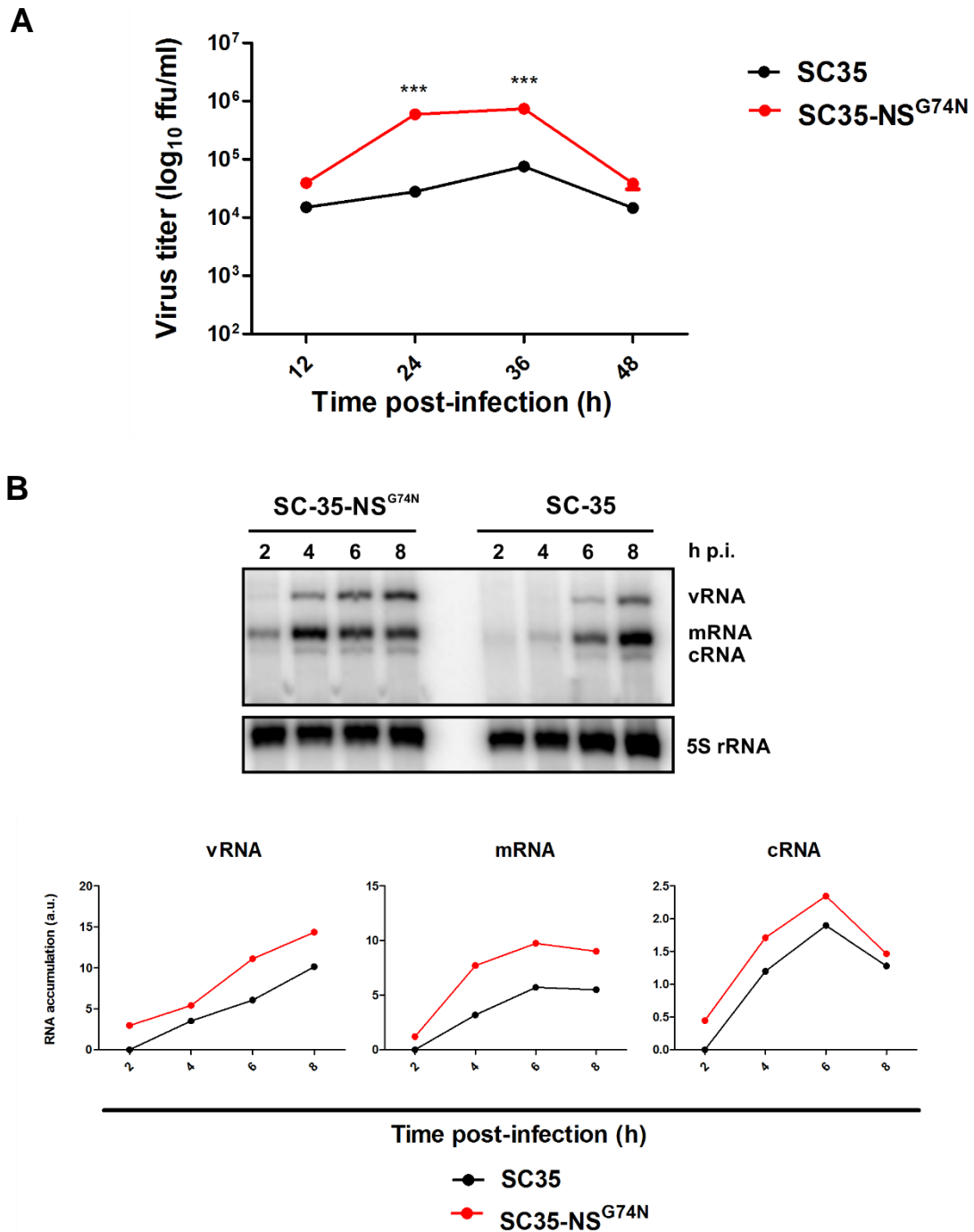
Fig. 3.23 Replication kinetics and viral RNA synthesis of SC35 and SC35-NS^{G74N} on A549 cells. (A) Cells were infected with viruses at MOI of 0.001. Supernatant of inoculated cells were harvested at 12 h interval until 48 h post infection. The virus titrations were determined by foci assay on MDCK cells. **(B)** Cells were infected with viruses at MOI of 2 and incubated for the indicated time post infection. The accumulation levels of viral mRNA and vRNA were measured by primer extension, and the amount of these RNAs were normalized by that of cellular actin mRNA. Increase in the levels of vRNA, cRNA and mRNA at 4, 6, 8 h p.i. of each viruses were set in relative to the strain-specific RNA levels at 2 h p.i. This experiment is represent one out of at least three independent experiments.

A

B
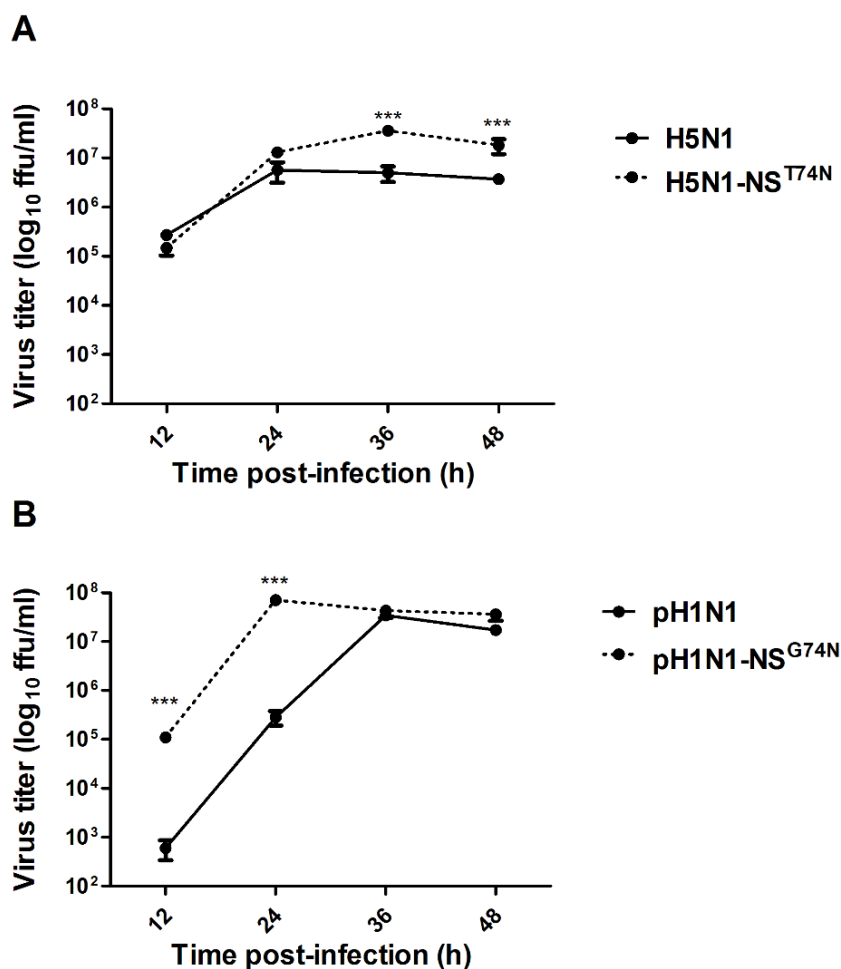
Fig. 3.24 Replication kinetic of (A) A/Thailand/1(KAN-1/2004) (H5N1) and (B) A/Gießen/6/2009 (S-OIV-H1N1) harboring specific amino acid N74 in their NS1 segment compared to its wild-type viruses on A549 cells. Cells were infected with viruses at MOI of 0.001. Supernatant of inoculated cells were harvested at 12 h interval until 48 h post infection. The virus titrations were determined by foci assay on MDCK cells. Error bars represent standard deviation (n=3).

Cellular transcription profile response to infection of different NS Gene reassortant avian influenza viruses in human host

To optimize virus production, virus is expected to direct cellular machinery for its replication and interfere with cellular pathways that inhibit virus replication. Most viruses have evolved countermeasures to limit or delay the cellular innate immunity by blocking the activation or signaling of pattern recognition receptors (PRRs), inhibiting interferon (IFN) signaling from the IFN receptor or directly inhibiting the activity of one or several Interferon-stimulated genes (ISGs) (reviewed in [182]). In

addition, many viruses down-regulate transcription and/or translation of cellular genes and hence indirectly inhibit the induction of IFNs and ISGs. In the case of influenza A viruses, the non-structural NS1 protein is a major molecular determinant of virus virulence and contributes significantly in disease progression by modulating a number of virus and host cell processes [19, 183, 184]. NS1 is highly multifunctional, NS1 can bind many proteins and RNAs, and although it is non-essential for virus replication, it has roles in viral protein synthesis, viral RNA replication, virion production and can modulate cellular post-transcriptional RNA processing and transport [56, 58, 118, 185]. The anti-IFN action of NS1 is exerted through a combination of several possible NS1-host cell interactions, such as: (i) down-regulation of new cellular transcription elongation and post-transcriptional RNA processing after infection [186, 187], (ii) inhibition of RIG-I activation [188-190], (iii) interference with the IFN signaling [191, 192] and (iv) direct inhibition of specific ISGs, like PKR and RNAse L [142, 143, 193].

Another important function of NS1 protein is to regulate host apoptotic mechanism. Apoptosis was initially thought to be a host cellular mechanism to restrict virus replication however, there are evidences now that it can be triggered by viral factors and can be used by the virus for its own benefit [135, 194]. Both induction as well as suppression of apoptosis has been shown to be associated with NS1 protein [138, 140, 195]. Some studies have shown that NS1 protein specifically derived from H5 subtypes can induce apoptosis in human cells [138, 140, 196-198] however contrasting to that, other studies have shown suppression of apoptotic events by NS1 protein specifically derived from H1 subtypes in mammalian hosts [140, 195]. Clearly, these observations were dependent on virus strain and cellular host system used for the study.

In this report, I compared the ability of NS1 proteins of two distinctly different subtypes NS-GD (H5N1) and NS-MA (H7N3) in genetic backbone of avian influenza viruses FPV (H7N1) to induce host cellular responses. The recombinant virus FPV-NS^{GD} shows increased replication, whereas the FPV-NS^{MA} replication ability is impaired in mammalian cell [160, 179]. However, the global effects of viral infection on host cell gene expression profile are largely unknown. Indeed, the understanding of host protection at the organism level must take into account factors that are

beyond cell-intrinsic viral control. A comprehensive analysis of the global host response is essential for the development of a complete understanding of the factors following infection that might be involved in the adaptation of avian influenza virus to the mammalian (human) cell. Microarray analysis, are well suited for this purpose in order to have an insight into a role of the NS1 protein in modulating host cellular environment.

3.14 The global transcriptomic response to influenza viruses infected A549 cells

To assess the whole transcriptomic cellular response to IAV infection, I used hierarchical clustering (Fig. 3.25A) to visualize "Euclidian" distances between each transcriptomic profile of A549 cells infected with FPV-NS^{GD}, FPV-NS^{MA}, FPV-NS$^{MA\_D74N}$ and FPV-NS$^{MA\_P3S+R41K+D74N}$. This analysis shows that FPV-NS$^{MA\_P3S+R41K+D74N}$ was mostly closer to FPV-NS^{GD} virus strain than FPV-NS$^{MA\_D74N}$. The FPV-NS^{MA} was the most distinct. Of note, the response to FPV-NS^{MA} was different from mock infected samples. To study the specificity in the host response and to detect significant changes in the transcription of the cells infected with the four different of IAV, I identified the differentially expression (DE) between IAV-infected samples and mock-infected samples at 6 h p.i. using the following criteria: a q value of <0.01, as determined by Limma's empirical Bayes moderated t-test, and a $\log_{1.5}$ fold change ($\log_{1.5}$ FC) (Fig. 3.25B, 3.25C). Consistent with transcriptomic distance analysis, IAVs induced transcriptomic change at 6 h p.i.. The cellular response to avian FPV-NS^{MA} infection was significant robust, with 62 DE genes, while there were only 39, 47, and 45 DE genes after infection of FPV-NS^{GD}, FPV-NS$^{MA\_D74N}$ and FPV-NS$^{MA\_P3S+R41K+D74N}$, respectively. Altogether, these results show that the host response to FPV-NS$^{MA\_D74N}$ and FPV-NS$^{MA\_P3S+R41K+D74N}$ which harbour the specific amino acids D74N alone (FPV-NS$^{MA\_D74N}$) and/or combined P3S+R41K+D74N (FPV-NS$^{MA\_P3S+R41K+D74N}$) in the NS1-MA segment render the FPV-NS^{MA} virus affected globally gene expression more similar to that of the mammalian adapted reassortant FPV-NS^{GD}, which is also reflected in the viral properties as mention in the previous results.

3.15 Functional characterization of host responses specific to FPV-NS^{GD}, FPV-NS^{MA}, FPV-NS$^{MA\_D74N}$ and FPV-NS$^{MA\_P3S+R41K+D74N}$ viruses

In the further study of the specificities in the host response to each of the four IAV using the following criteria: a *q* value of <0.01, as determined by Limma's empirical Bayes moderated t-test, and a log$_2$ fold change (log$_{1.5}$ FC) (Fig. 3.25C). I found that the FPV-NS^{MA} infected cells show highest number up-regulated genes; 50 genes were up-regulated whereas FPV-NS^{GD}, FPV-NS$^{MA\_D74N}$ and FPV-NS$^{MA\_P3S+R41K+D74N}$ up-regulated 31, 35 and 38, respectively (Fig. 3.25C). Interestingly, the 31 common genes among the virus infected cells show that the majority of the up-regulated genes upon virus infection are ISG genes. The ISG RNA expression patterns show similarity, however contrasts in the levels of up-regulation (Table 3.2). For four recombinant IAV at the log$_{1.5}$ FC cut-off selected genes belong to early innate immune response pathways. A complete list of genes is provided in Table 3.2. For all four recombinant IAVs the largest category of up-regulated genes was the ISGs (e.g. IFIT2, IFI44L, IFIT3, OAS2, OASL, MX1, RSAD2). Other genes up-regulated by all four isolated included interferon-induced chemokines (e.g., CCL5), type III-IFN (e.g., IL28A, IL28B and IL29), PRRs (e.g., DDX58, IFIH1, IRF7, IRF3) and other apoptosis signaling (e.g. BATF2). Surprisingly, when a log$_2$ FC cut-off with a significance of p<0.01 was applied there was unique to FPV-NS^{MA} infected cells (Table 3.27A, Fig. 3.26A) 12 genes which are not up-regulate in FPV-NS^{GD}, FPV-NS$^{MA\_D74N}$ and FPV-NS$^{MA\_P3S+R41K+D74N}$ infected cells. Also there are three genes up-regulate in FPV-NS$^{MA\_D74N}$ but not in NS$^{MA\_P3S+R41K+D74N}$ (Table 3.3, Fig. 3.26B). Altogether the results indicate that FPV-NS^{MA} carrying amino acid change D74N and combined P3S+R41K+D74N in the NS1-MA segment affected the expression of lower number of genes than in FPV-NS^{MA} infected cells. Interestingly, all genes that were up-regulate to FPV-NS^{MA} infected cells are involved in interferon-stimulated genes (e.g. poly(ADP-Ribose) polymerases; PARP9, PARP10, OAS1, IDO), involved in antiviral activities (e.g.TRIM14, TRIM21, ZC3HAV1) and in the innate immune response (IER5L). However, the fact that these genes were not up-regulate in FPV-NS$^{MA\_D74N}$ and FPV-NS$^{MA\_P3S+R41K+D74N}$ infection, indicates that the amino acid changes D74N and combined P3S+R41K+D74N in NS1-MA are prevent interferon-stimulated activity, antiviral activity and also innate immune responses of the cells against these viruses.

Table 3.2 Notable common genes up-regulated and down-regulated in A549 cells infected with different recombinant FPV viruses at 6 h p.i.

Gene Symbol	FPV-NS^{GD}	FPV-NS^{MA}	FPV-NS^{MA_D74N}	FPV-NS^{MA_P3S+R41K+D74N}
IFIT1	8.5	9.7	8.6	8.8
IFIT3	8.2	9.5	8.4	8.5
OASL	8.1	9.3	8.2	8.4
IFIT2	7.7	9.0	7.9	8.0
MX1	7.6	8.7	7.7	7.9
PRIC285	7.2	8.4	7.4	7.5
BATF2	7.2	8.6	7.5	7.5
CCL5	6.2	8.6	7.5	6.5
IL28A	7.0	8.5	7.4	7.4
IFI6	6.6	7.8	6.9	6.7
IFITM1	6.5	7.8	6.8	6.7
IRF7	6.5	7.6	6.7	6.8
IFI44	6.4	7.4	6.1	6.5
IFIH1	5.4	7.1	5.5	5.4
RSAD2	5.2	7.3	6.1	4.4
OAS2	4.7	5.1	5.0	4.7
TNFSF10	4.7	6.4	5.4	4.4
DDX58	4.6	6.4	5.4	5.1
ISG15	4.6	5.6	4.8	4.9
IRF1	4.2	6.4	5.1	3.4
IFIT5	4.2	5.7	4.7	4.5
SAMD9L	4.1	5.1	4.5	3.9
IL28B	4.0	6.0	5.3	3.9
CMPK2	3.9	4.9	4.1	3.4
IL29	3.8	5.9	4.5	3.2
MYH9	-1.8	-1.6	-1.5	-1.7
HERC5	2.8	4.9	3.8	2.8
IRF9	2.6	3.2	2.7	2.5
REC8	2.4	3.6	3.3	3.4
LMO2	2.4	3.9	2.9	2.2
IFI27	2.3	4.3	3.0	3.3
SPTAN1	-1.8	-1.9	-1.7	-1.8
FLNA	-1.3	-1.3	-1.2	-1.4
PLEKHA4	1.8	3.4	2.6	2.5
FLNB	-1.2	-1.3	-1.3	-1.3

Table 3.3 List of up-regulated genes in unique response to FPV-NS^{MA} infection

Gene	Gene description	Log$_{1.5}$ FC
TRIM14	tripartite motif containing 14	1.5
ZC3HAV1	zinc finger CCCH-type, antiviral 1	1.5
FBXW10	F-box and WD repeat domain containing 10	1.6
IER5L	immediate early response 5-like	1.7
MME	membrane metallo-endopeptidase	2.6
DTX3L	deltex 3-like (Drosophila)	2.3
SLC6A13	solute carrier family 6 (neurotransmitter transporter, GABA), member 13	2.2
PARP9	poly (ADP-ribose) polymerase family, member 9	2.9
IDO1	indoleamine 2,3-dioxygenase 1	3
UBE2L6	ubiquitin-conjugating enzyme E2L 6	1.6
OAS1	2'-5'-oligoadenylate synthetase 1, 40/46kDa	1.3
PCF11	cleavage and polyadenylation factor subunit, homolog (S. cerevisiae)	1.5

A

B

C
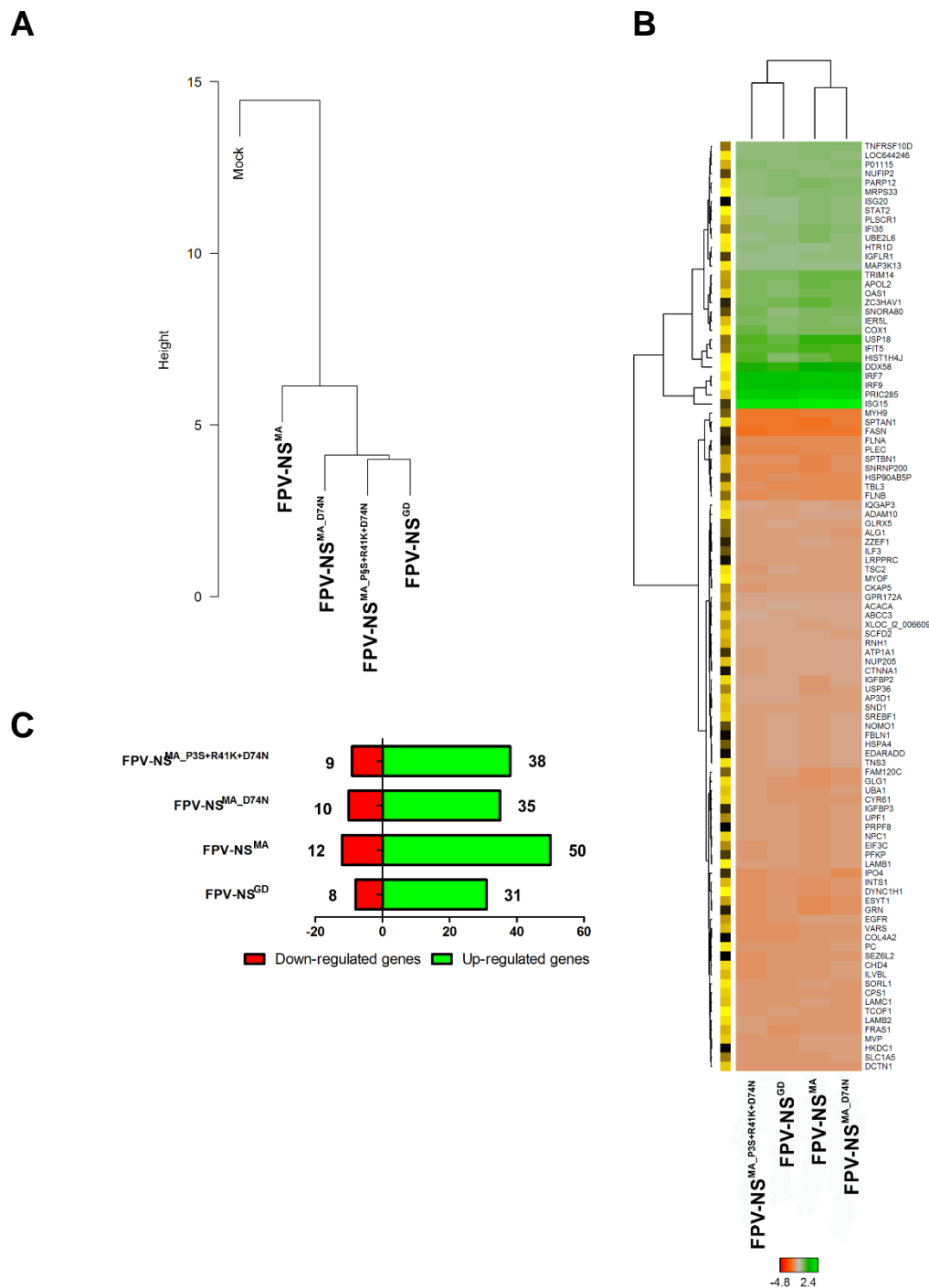
Fig. 3.25 Number of up-regulated and down-regulated differentially expressed (DE) gene after infection with reassortant viruses compared to time matched mock infection. **(A)** Hierarchical clustering by average linkage of reassortant viruses- and mock-infected samples at 6 h p.i. based on their gene expression profiles. Distances were calculated using Peason correlation distance. **(B)** Heat map showing microarray gene profiles of reassortant viruses infected A549 cells at 6 h p.i.. Expression of genes with p-value <0.01 and fold change ≥ 1.5. For each viral condition, DE genes were classified as up- or down-regulated across infection. Genes were clustered in 25 clusters by a constant height cut of the hierarchical clustering dendrogram of Euclidean distance of DE profiles. **(C)** Genes up-regulation and down-regulation in A549 cells infected with recombinant FPV viruses at 6 h p.i.: Criteria used for differential expression analysis are a q value of < 0.01 as determined by student t-test and ($\log_{1.5}$ FC).

Table 3.4 List of differentially up-regulated genes between FPV-NS$^{MA\_D74N}$ and FPV-NS$^{MA\_P3S+R41K+D74N}$ in infected cells

Gene	Gene description	Log$_{1.5}$ FC
APOL2	apolipoprotein L, 2	2.3
PARP10	poly (ADP-ribose) polymerase family, member 10	3.6
TRIM21	tripartite motif containing 21	3.2
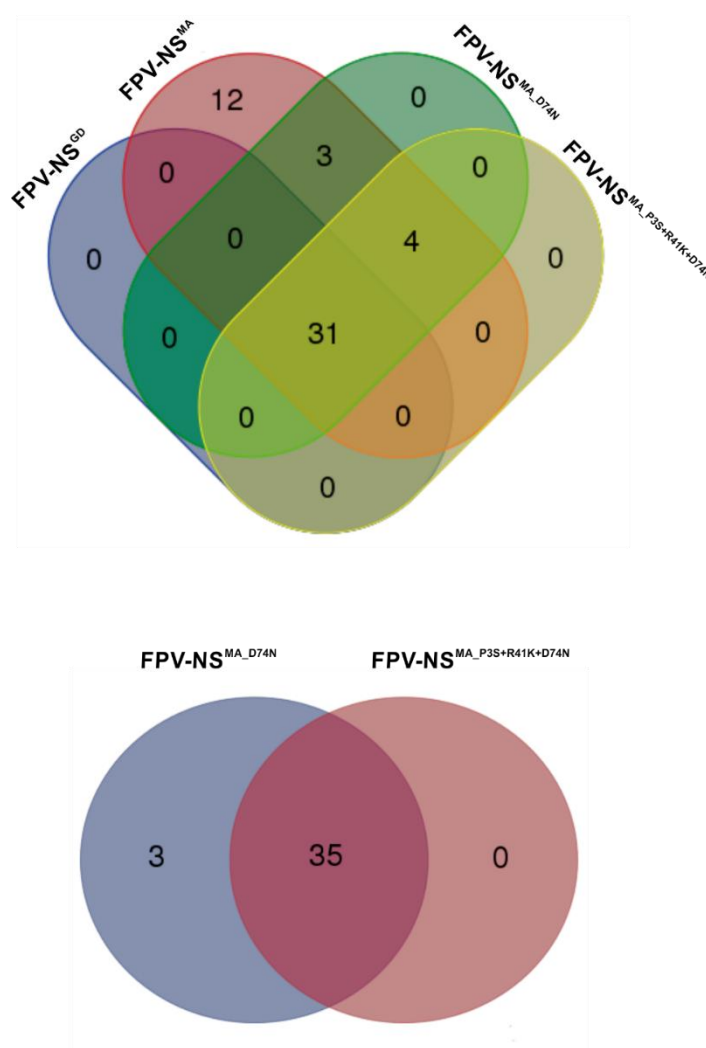
Fig. 3.26 Global analysis of DE genes distinguishing IAV infected A549 cells relative to mock. Venn diagram representing the agreement between the lists of DE genes by microarray of IAV viruses relative to mock infection at 6 h p.i..

3.16 Pathway enrichment analysis

I further conducted pathway analyses using the Ingenuity Pathway Analysis (IPA) to identify the intracellular signaling pathways that were most significantly represented in FPV-NS^{GD}, FPV-NS^{MA}, FPV-NS$^{MA\_D74N}$ and FPV-NS$^{MA\_P3S+R41K+D74N}$ infected cells using Fisher's Exact Test (Table 3.6). The five ranking pathways for all four viruses were the same; IFN signaling, chemokine signaling, role of PRRs in recognition virus, communication between immune cells and apoptosis signaling. Interestingly, the role of five pathways were shared but greatest for FPV-NS^{MA}. This suggests an importance of the IFN signaling and apoptosis for FPV-NS^{MA}, while an importance of apoptosis also suggested for FPV-NS$^{MA\_P3S+R41K+D74N}$. A role of PRRs in recognition virus and communication between immune cells is suggested for all viruses. Interestingly, FPV-NS$^{MA\_P3S+R41K+D74N}$ stronger affects the apoptosis pathway than FPV-NS$^{MA\_D74N}$, suggesting that apoptosis might have an important but different role between FPV-NS$^{MA\_P3S+R41K+D74N}$ and FPV-NS$^{MA\_D74N}$ infected cells. Combined with the individual gene analysis, the pathway analysis underscores important similarities but also gene specific differences.

Table 3.5 Top five significant canonical pathways affected in IAV-infected A549 cells at 6 h p.i. relative to mock

Pathway	FPV-NS^{GD}	FPV-NS^{MA}	FPV-NS$^{MA\_M74}$	FPV-NS$^{MA\_P3S+R41K+D74N}$
IFN signaling	6.50E-07	6.50E-12	6.50E-09	6.50E-08
Chemokine signaling	3.70E-06	7.70E-10	1.20E-08	5.50E-06
Role of PRRs in recognition virus	7.50E-06	5.40E-06	5.70E-05	8.30E-05
Communication between immune cells	3.07E-05	4.70E-06	6.51E-05	4.12E-05
Apoptosis signaling	7.14E-04	5.17E-08	5.35E-05	5.17E-08

For each canonical pathway we report the p-value of Fisher's exact test to measure significance in the pathway

3.17 Reassortant IAV infected A549 cells affects IFN-beta levels

The difference in the up-regulation of genes, which are mostly interferon-stimulated genes (Table 3.2, 3.3) prompted me to ask whether differences occur in the amount of interferon secreted from infected A549. IFN-beta levels were measured by ELISA in A549 cells infected with recombinant viruses at an MOI of 0.01 at various time points (24 h, 36 h and 48 h p.i.). I found that FPV-NS^{MA} induced the highest IFN-beta response at all-time points compared to the other three viruses, followed by FPV-NS$^{MA\_D74N}$ at 24 and 36 h p.i. (Fig. 3.27). This result is well in agreement with the result that the highest number and greatest degree of expressed interferon-stimulated gens are found in FPV-NS^{MA} infected A549 cells (Table 3.2, 3.3, Fig. 3.25) great interferon secretion. When these results are compared to the titres of the various viruses (Fig. 3.3) it can be concluded that in general the more IFN-beta is induced, the lower the virus titre is.
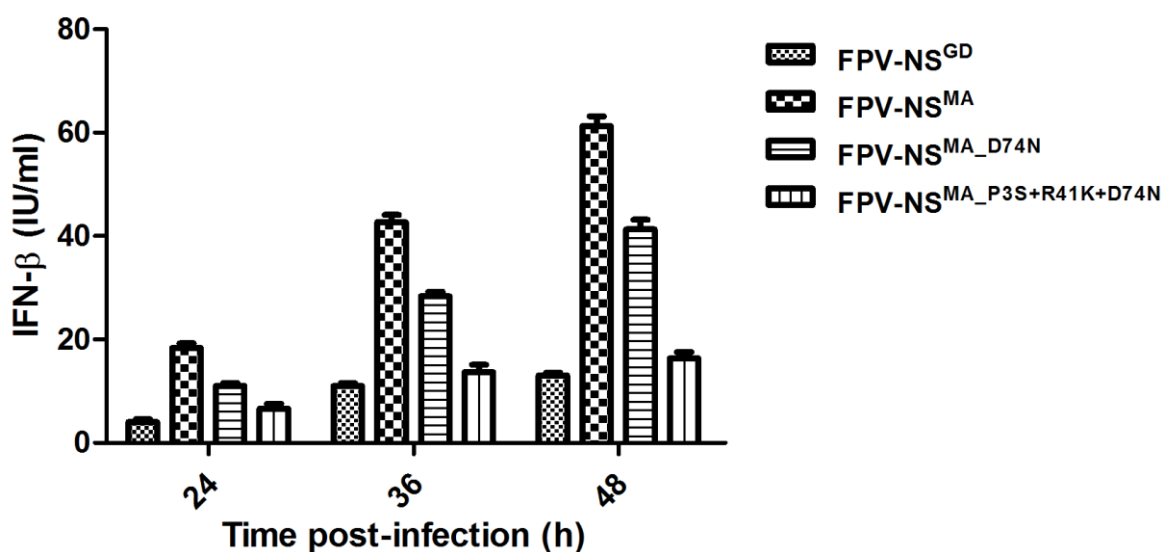
Fig. 3.27 Recombinant viruses induce different levels of IFN-beta. A549 cells were infected with the recombinant viruses at an MOI of 0.01. Supernatants were harvested at 24, 36 and 48 h p.i. and measurements were taken using an IFN-beta ELISA Kit. Results represent the average of three independent experiments.

3.18 Recombinant viruses induce different levels of apoptosis

During the course of my experiments I observed that the FPV-NS^{MA} and FPV-NS$^{MA\_P3S+R41K+D74N}$ viruses appeared to cause cell death in a different way than the

FPV-NS$^{MA\_D74N}$, and FPV-NS^{GD} viruses in A549 cells. Cells infected with FPV-NS^{MA} and FPV-NS$^{MA\_P3S+R41K+D74N}$ rounded-up but did not detach from the dishes, while infection with the other two viruses resulted in the cells becoming detached. I hypothesized that the FPV-NS^{MA} and FPV-NS$^{MA\_P3S+R41K+D74N}$ viruses were inducing a different level of apoptosis compared to the other viruses. This would be in well agreement with the microarray results, FPV-NS^{MA} and FPV-NS$^{MA\_P3S+R41K+D74N}$ prominent apoptosis signaling than FPV-NS^{GD} and FPV-NS$^{MA\_D74N}$ in infected A549 cells (Table 3.3). In order to determine the extent of apoptosis induced in cells infected with the different viruses. A casespase-3 activity was analyzed as a marker for cellular apoptosis and an additional alternative assay (Tunel assay) was used in which A549 cells were infected and examined by FACs analysis. I observed that the FPV-NS^{MA} and FPV-NS$^{MA\_P3S+R41K+D74N}$ viruses induced the highest casespase-3 activity as well as highest DNA-fragmentation shown by Tunel assay, followed by FPV-NS$^{MA\_D74N}$ and FPV-NS^{GD} (Fig. 3.28). Reassortant viruses containing different NS segments therefore differ in their abilities to induce cell death. When the extent of apoptosis is compared to the infectious titres of the various viruses no correlation between levels of apoptosis and virus titres.
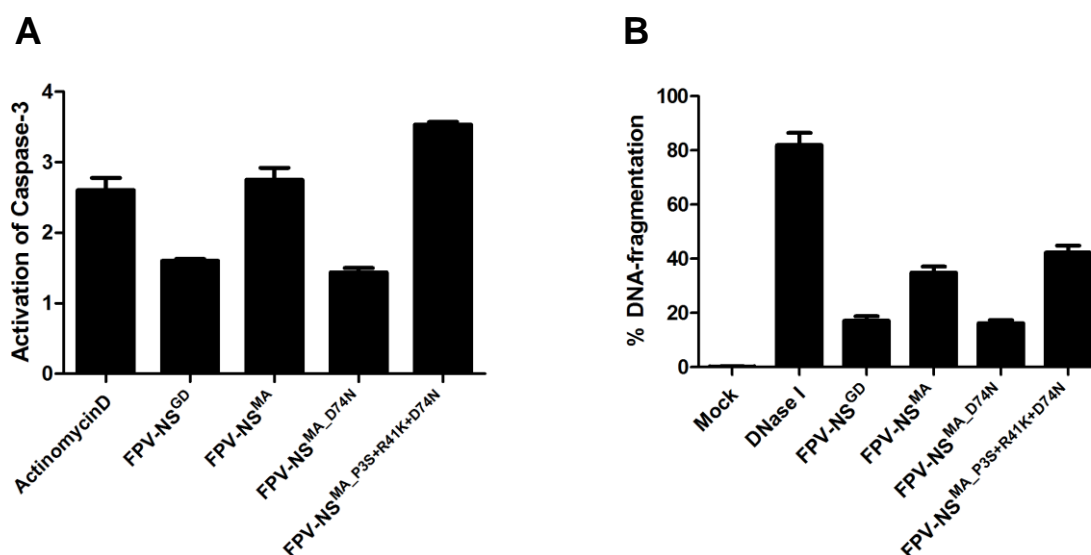
Fig. 3.28 Levels of apoptosis induced by the recombinant viruses. (A) Caspase-3 activity, A549 cells were infected with recombinant viruses at an MOI of 1 and at 10 h p.i. the cells were lysed and being processed using Caspase-3 assay Kit (colorimetric, Abcam) according to the manufacturer's instructions. **(B)** Detect fragmented DNA by Tunnel assay, A549 cells were infected with recombinant viruses at an MOI of 1 and at 10 h p.i. the cells were harvested and being processed using the In-Situ Cell Death Detection Kit (Roche). The specimens were then examined by FACs analysis. Results represent the average of three independent experiments.

Chapter 4

Discussion

In my thesis work I have demonstrate that the specific aa changes D74N and/or P3S+R41K+D74N in the NS1 protein are sufficient for mammalian adaption of AIV. I provide a detailed characterization of the phenotypic changes caused by these residues and I found the importance of these specific residues for strongly enhanced mRNA production as well as viral protein production in mammalian cells. At the same time these adaptive changes are not disadvantageous in avian cells. My study also suggest that the D74N and/or P3S+R41K+D74N substitutions are involved in the temperature adaptation of the AIV polymerase from birds to mammals, as the adaptive changes enhanced the production of viral RNAs synthesis at temperatures representative for the human upper respiratory tract (33-37°C), whereas no affect occurred at avian temperature (41°C). Furthermore, these substitutions enable a strictly avian influenza virus to replicate in mice and cause disease. Together, the adaptive mutations D74N and/or P3S+R41K+D74N in NS1 protein allow AIV to establish successful infections in mammalian cells.

4.1 The effect of different NS segments on the replication of a recombinant HPAIV FPV is independent of the NS allele, the virus subtype and the year of the virus isolation, but depends on host factors and the genetic background

It was previously shown that replacement of the NS segment of the avian influenza virus A/FPV/Rostock/34 (H7N1, FPV) by NS segments from the avian strains A/Goose/Guangdong/1/1996 (GD, H5N1) and A/Mallard/NL/12/2000 (MA, H7N3) resulted in changes of the viral replication characteristics in mammalian cell culture. In my work I show that the replication differences of the reassortant viruses in mammalian and avian cells based on the specific NS segments should depend on specific host factors. In avian cells, FPV-NS^{GD} and FPV-NS^{MA} had similar titers, whereas in mammalian cells FPV-NS^{GD} replicated to titers almost 2 logs higher than that of FPV-NS^{MA} (Fig. 3.3 and Fig. 3.4). The NS segments of GD and MA originated from avian viruses, and therefore it is plausible to speculate that in the genetic background of the avian FPV they should not confer a replication disadvantage in avian cells. In this context, it should be noted that in a previous study, the NS

segment of the 1918 IAV (H1N1) was set in the genetic background of A/WSN/33 (H1N1). The virus replicated well in tissue culture (MDCK cells), but was attenuated in mice compared to the A/WSN/33 wild type [199]. It was suggested that the attenuation in mice may be related to the human origin of the 1918 NS1 gene and that interaction of the NS1 protein with host-cell factors might play a significant role in viral pathogenesis. Taken together, for the effects exerted by the NS segment exchange, it seems to be relevant from which host the donor strain was isolated and in which host the recipient is tested.

In an overall comparison of the different NS proteins, I found that the NS1-GD protein sequence is similar to that of NS1-MA, differing by only eight amino acids (see Fig.3.1A). Using site direct mutagenesis and reverse genetic, I was able to identify of key NS1 residues responsible for the adaptation and the virulence in a mammalian host namely, S3, K41 and N74. Here I show that avian FPV virus harboring the single mutation N74 alone or combined S3+K41+N74 in the NS1 increased viral replication in mammalian A549 cells indicating that the mutations demonstrated adaptive properties. Increased replicative fitness in mammalian cells was seen at the levels or rate of virus propagation as well as viral gene expression (at both the mRNA and/or protein level) (see Fig. 3.3, 3.9).

4.2 NS1 localization and expression level are not correlated to the alteration of viral propagation

In order to investigate whether the effect of NS mutants on the propagation of the recombinant viruses was caused by differences in the NS1 protein expression levels, the individual expression rate was investigated (Fig. 3.8). I found that early in infection the FPV-NS[GD] virus had higher levels of NS1 protein expression than the other viruses, however by later time points there were no significant differences. The different properties of the recombinant viruses could therefore not be explained by different NS1 expression levels. In theory, newly synthesized NS1 is present in the cytoplasm, where it may be involved in inhibiting the type 1 interferon expression by binding to dsRNA or pppRNA, or inducing a pro-apoptotic or anti-apoptotic pathway. After synthesis, the protein is also transported into the nucleus where it interferes with the processing and export of cellular mRNAs [105,114,125,200,201]. Later,

some of the NS1 will be re-exported into the cytoplasm, where it may play a role in the regulation of the host anti-viral response. The NS1 protein has many diverse roles in both the cytoplasm and nucleus of infected cells, and therefore at this stage I cannot exclude the possibility that the different localizations of the NS1 proteins studied may play a role in the downstream effects observed.

Another report showed that all NS1 is located in the nucleus of cells transfected with plasmids expressing NS1 protein. It was suggested that the NES of the NS1 was specifically inhibited by the adjacent aa sequence in the effecter domain [109]. In contrast, in IV-infected cells the NES of the NS1 protein molecules was unmasked, and a substantial amount of the NS1 protein is exported in the cytoplasm. Since this unmasking only happened in infected cells but not in uninfected cells, it was concluded in the report that it is more likely that this unmasking resulted from specific interaction between another virus-specific protein or host factors induced/altered by infection and the NS1 protein. Here, in A549 infected cells, NS1-GD, NS1-MA-D74N and NS1-MA-P3S+R41K+D74N showed the tendency that an increased proportion of the NS1 protein resides in the cytoplasm. I assume that the four different NS1 may have extended functions in the cytoplasm, which may lead to stronger limitation of host antiviral response, including IFN response and apoptosis in the cytoplasm. NS1 contains two nuclear localization signals and one nuclear export signal responsible for their transport between nucleus and cytoplasm. Therefore NS1 can be present in the nucleus or the cytoplasm or both [119,166,200-203]. The aa sequence comparison between my four NS1 (Fig 3.1A) showed that the NLS1 (34aa-39aa) and NLS2 (216aa-220aa) are identical between the four NS1. Maybe this is the reason for the similar localization of the four NS1.

NS1 accumulation in the nucleus has been reported to help the replication of IV [204]. Here, although NS1-GD, NS1-MA, NS1-MA-D74N, and NS1-MA-P3S+R41K+D74N had the same NS1 localization patterns, they produced different virus titer. The results showed that there was no correlation between intra cellular NS1 localization and virus titres, which means they may have different functions even they are all localized in nucleus or cytoplasm.

4.3 NS exchange also changes the RNP export patterns and this is correlated to the virus titer

The influenza virus genome is transcribed and replicated in the nucleus, where its eight segments of negative-sense RNA are encapsidated into ribonucleoproteins (RNPs) by the viral nucleoprotein [21]. Newly assembled RNPs are subsequently exported to the cytoplasm to be packaged into virus particles. Nuclear export of RNPs results from their sequential binding by the viral M1 and NS2/NEP proteins, followed by recognition of a nuclear export signal in NEP by the cellular nuclear export receptor CRM1 [205]. Accordingly, inactivation of CRM1 in infected fibroblasts by the toxin leptomycin B (LMB) causes nuclear retention of RNPs and also causes them to redistribute to the nuclear periphery [206, 207]. Here, I show that, in A549 infected cells, RNP localization of the FPV-NS^{GD} viruses had a mostly cytoplasmic distribution, while FPV-NS^{MA} showed a more nuclear RNP localization. This suggests that transport of the viral genome out of the nucleus was reduced for these viruses (Fig. 3.7). However, FPV-NS$^{MA\_D74N}$ and FPV-NS$^{MA\_P3S+R41K+D74N}$ had a cytoplasmic distribution similar to FPV-NS^{GD}. This suggests this substitutions on the NS1-MA had an impact to RNP localization. The more rapid RNP export was found to correlate with higher virus titers, an explanation for this could be that less efficient RNP export should lead to lower infectious titres by limiting RNPs available for packaging [208]. It has recently been proposed that NS2 plays a major role in the transport of vRNPs out of the nucleus [209]. Although NS2 does not interact directly with RNPs, it binds to M1 associated with vRNPs [210]. Furthermore, NS2 contains a functional nuclear export signal (NES) and interacts with components of the nuclear pore complex (NPC) in a yeast two-hybrid system [209]. Accordingly, it has been suggested that NS2 acts as an adapter molecule that links M1-RNP complexes with the NPC, thus mediating their NS2 can mediate RNP export by interaction with M1 protein. The aa comparison of NS2/NEP [160] shows that there are only two aa differences between the GD and MA NS2/NEP protein sequences. Therefore, if NS2/NEP confers the demonstrated difference in RNP export, it should be based on this two aa difference, otherwise the RNP export of FPV-NS-GD should be similar to FPV-NS-MA, however, here data showed RNP export of FPV-NS$^{MA\_D74N}$ and FPV-NS$^{MA\_P3S+R41K+D74N}$ is stronger than FPV-NS^{MA} without any changes in the NS2/NEP. I therefore unlikely

that NS2/NEP is responsible for the observed differences. Further experiments need to be performed to investigate this.

4.4 Substitutions D74N and P3S+R41K+D74N in NS1-MA enhance viral polymerase activity and thus enhance viral RNA synthesis

My results suggest that the major impairment of the polymerase of avian FPV-NS^{MA} in mammalian cells is due to deficient viral genome replication and transcription, which seems to be affected by the NS1. I observed that the reassortment of the FPV-NS^{GD} and FPV-NS^{MA} differently affected both, replication and transcription and thereby the accumulation of viral genomes in the infected cells (See Fig. 3.11 and 3.13). FPV-NS^{MA} displayed a lower accumulation as well as a delayed peak of viral mRNA accumulation compared to FPV-NS^{GD} (See Fig. 3.13), suggesting that NS segments can influence the time course of RNA synthesis with is in line to previously study that the NS1 protein has been shown previously implicated in the regulation of viral RNA synthesis [56, 104, 160, 168, 211], possibly through interaction with the viral RNP complex. In addition, NS1 protein also exhibits binding to influenza virus RNA [113]. NS1 can be co-immunoprecipitated with the polymerase proteins and NP from infected cell lysates [117]. In addition, NS1 interacts with CPSF30, a host RNA polymerase II (Pol II)-associated factor involved in the 3′-end processing of host mRNAs, in a macromolecular complex also containing viral polymerase and NP [161]. I found that the polymerase activity of FPV virus could be increased to a very large extent by substituting of NS1-MA segment with NS1-MA segments harboring D74N and/or P3S+R41K+D74N. I found that avian FPV-NS^{MA} confers an impaired rate of overall RNA synthesis in human cells most likely due to the low transcriptional activity of the RdRp and, consequently, the low protein levels expressed in cultured cells. FPV-NS$^{MA\_D74N}$ and FPV-NS$^{MA\_P3S+R41K+D74N}$ were found to increase viral polymerase activity in mammalian 293T cell as well as an increase viral mRNA synthesis in infected A549 cells, which correlates with increased viral protein synthesis compared to FPV-NS^{MA} (See Fig. 3.9, 3.13). This indicates that the substitutions D74N and/or P3S+R41K+D74N in NS1-MA protein affect a functional interaction between the NS1 and polymerase activity due to direct or indirect interactions of the NS1 with viral polymerase components. This hypothesis is in line with numerous studies that have linked NS1 action with the ability of influenza virus

to synthesize viral RNA or associate with components of the polymerase complex [117, 159]. In addition to increased yields of viral mRNA and protein, I observed a differential regulation of NP and NS1 protein synthesis relative to FPV-NS^{MA} infected cells. NS1-MA mutants D74N and/or P3S+R41K+D74N induced higher levels of NP and NS1 protein relative to FPV-NS^{MA} infected cells. This is also demonstrated at the level of mRNA synthesis and probably efficiency in mRNA translation. Interestingly, other reports have shown that the N-terminal half of the NS1 protein is sufficient for nuclear retention of poly (A)-containing RNA and enhancement of viral mRNA translation [57]. And given the location of the substitution D74N and/or P3S+R41K+D74N within binding domains for cellular factors involved in translation (PABPI), I cannot rule out the possibility that enhanced interaction with this factor may also contribute to increase levels of virus protein synthesis.

4.5 Substitutions D74N and P3S+R41K+D74N in NS1-MA result in a replication advantage at lower temperature

This study examined the enhancing polymerase activity of the NS1 segment of avian virus. Interestingly, FPV-NS^{GD}, FPV-NS$^{MA\_D74N}$ and FPV-NS$^{MA\_P3S+R41K+D74N}$ were well adapted to 33°C (See Fig. 3.16A), which is closer to the temperature of human upper airway, but the activity of FPV-NS^{MA} was much lower at this temperature. This observation is in line with the fact that the avian FPV-NS^{MA} viruses have limited replication in A549 human cells as well as human upper airway, and thus they have a lower efficiency in transmission from human to human.

I found that the polymerase activity of FPV-NS^{MA} could be increased to a very large extent by substituting the NS1-MA protein with a D74N and/or P3S+R41K+D74N which are corresponding to FPV-NS^{GD}, and this effect was more pronounced at 33°C (See Fig. 3.16). This is an important concern as such reassortants may be able to adapt to the human upper airway and might show an increased human to human transmission efficiency. By contrast, at avian gut temperature (41°C), the polymerase activity of all viruses are similar. These results clearly demonstrated that optimal polymerase activity, due to a better compatibility, is probably required for efficient viral replication in given host [212]. Although the underlying mechanism of temperature dependency of the polymerase activity is not clear, NS1-MA harbouring

D74N and/or P3S+R41K+D74N substitutions are likely to be important for host range restriction. The differential quantitative analysis of different viral RNA species (See Fig. 3.16B) revealed that substitutions D74N and/or P3S+R41K+D74N on the NS1-MA enhanced both the transcription and replication activity of the viral polymerase. However, notable differences in the profile of transcriptive (mRNA) and replicative (vRNA and cRNA) intermediates were observed between 33°C and 37°C. Similar to an earlier study showing that mutant influenza viruses encoding C-terminally deleted NS1 are thermosensitive and are defective in virus RNA replication and translation of late virus mRNAs at 33°C [56]. My results show that at 41°C, all three substitutions only resulted in the elevation of vRNA level but not mRNA and cRNA levels, suggesting that these substitutions may only enhance the polymerase activity of cRNA-dependent vRNA synthesis but not the activity of vRNA-dependent mRNA and cRNA synthesis. In contrast, at 33°C, the effect on transcription was stronger than on replication. Of note, the substitution D74N in the NS1-MA showed a dramatically increase in the mRNA level at 33°C, whereas the increase in levels of cRNA and vRNA was less pronounced. Interestingly, P3S+R41K+D74N substitution on the NS1-MA showed a dramatically increase in all RNA species level at 33°C.

4.6 What function(s) are affected by the substitutions at position 3, 41, and 74 of NS1-MA?

An X-ray crystallographic model shows that the residue at position K41 is located within the second-helix spanning amino acids 30 to 50 of the RNA-binding domain (RBD) of the NS1 protein [112]. The basic amino acid K41, in this same region has previously been reported to be important for inhibiting host IFN induction and virulence of influenza A viruses in mice [213]. K41 is also reported to be a part of NLS1 [110], and comprises an ISG15 acceptor site, which is also involved in IFN production [214]. A recent study reported that the NS1 protein interacts specifically with NP and not with the polymerase subunits and amino acid K41 is part of a binding site directly involved in the NP interaction. This might be a reason for changing in the polymerase activity [159]. Moreover, the N-terminal domain of NS1 can bind to the host DDX21 RNA helicase. This leads to free PB1, thus inducing higher viral RNA and viral protein synthesis [215]. The amino acid N74 is located in a linker region (LR) of NS1 and is implicated in replication, pathogenesis, and host

range [157, 216-218] probably due to the result of the altered structural flexibility that may exists among NS1s due to sequence variations, particularly in the regions close to the LR. No biological function is available for residue S3 of NS1. However, it is located in the RBD, and it is tempting to speculate that it might influence RNA binding of NS1. Taken together, the exact answer to the above question and the exact mechanism by which the aa at position 3, 41 and 74 of NS1 affect the adaptation of AIV to mammalian hosts currently remains elusive. Interestingly, I found that a high percentage of influenza viruses encode S3+K41 in the NS1 in nature, resulting in a significant percentage around 94-96% (See Fig. 3.19), which were associated with increased polymerase activity and virulence in this study. My data represented the fact that just only single mutation (D74N) occur in such virus which already possessing 3S+41K in NS1 protein can affect the adaptation of avian influenza viruses to mammalian hosts (See Fig. 3.20 and Fig. 3.23). Moreover, introduced these single mutation N74 into NS1 of pandemic influenza virus (SOIV-H1N1) and H5N1 (A/Thailand/1(KAN-1)/2004), with already possess NS1-S3+K41 and respect to high replication in human. We found that these mutant viruses highly replicate in human A549 cells compared to wild-type viruses (See Fig. 3.24). This findings suggest that acquisition of NS1-N74 for the viruses that already possess NS1-S3+ K41, may create viruses with high replicative ability in mammalian, including humans.

4.7 Pathogenicity of NS1 mutant viruses in mice

In contrast to cell culture, the reassortant FPV-NS^{GD} and FPV-NS^{MA} viruses show similar levels of virulence in mice, with only minor differences. The FPV-NS^{GD} virus was slightly more virulent than the FPV-NS^{MA}, as judged by faster weight loss and shorter average survival time. However, I demonstrate that S3, K41 and N74 (FPV-NS$^{MA\_P3S+R41K+D74N}$) act together to affect FPV-NS^{MA} virus virulence. Specifically, I found that the overall effect on the virulence on mice of the three combined mutations is greater than that of FPV-NS^{MA} and even greater than that of FPV-NS^{GD}. As demonstrate by body weight and survival rate (See Fig. 3.18A and 3.18B), FPV-NS$^{MA\_P3S+R41K+D74N}$ infected mice show faster weight loss (weight loss up to 20% at 2 day post infection) and shorter time until the mice died (all mice succumbed to dead at 5 day post infection) compared to FPV-NS^{GD} and FPV-NS^{MA} mice infected that succumbed to death at 8 day post infection. My findings emphasize that multiple

genetic constellations exist (such as NS1-N74 and NS1-S3+K41) that may render the virus highly virulent as demonstrate in mice infected with FPV-NS$^{WT\_D74N}$ (already possessing NS1-S3+K41) showing high pathogenicity in mice in contrast to wild type FPV, which is apathogenic for mice (See Fig. 3.22A and 3.22B). Furthermore, these substitutions not only render avian viruses highly virulent in mammalians but also render human virus more virulent in mammalian cells as demonstrated in the case of SOIV-H1N1 (A/Gießen/6/2009) and H5N1 (A/Thailand/1(KAN-1)/2004) (See Fig. 3.24). Moreover, functional interactions among genetic constellations as described here add significantly to the potential to predict virulence-enhancing mutations. All viruses that I studied here, possessed S3+K41 in the NS1 segment, A/FPV/Rostock/1934 (H7N1) isolated in 1934, A/Thailand/1(KAN-1)/2004 (H5N1) isolated in 2004 and A/Gießen/6/2009 (H1N1) isolated in 2009, are genetically not closely related as shown by phylogenetic tree analysis (data not shown) yet, the introduction of the N74 into their NS1 protein made them highly pathogenic. Therefor my findings indicate that these amino acids in the NS1 are likely to have a broad effect on viral replication and virulence.

4.8 Type I IFN response is enhanced in response to FPV-NS^{MA} infection

Pathogenesis of influenza A viruses is a multigenic trait, which involves the interaction of different viral proteins in host cells. NS1 works as a primary host defending factor by inhibiting IFN induction, which is considered as the most powerful innate defenses to limit viral replication [19, 219]. Many reports are available to demonstrate how NS1 works in host cells to limit the production of IFN. NS1 inhibition of antiviral responses is strain-specific and it is likely that certain viruses have evolved distinct mechanisms to counter host defences [121, 122].

In this study, I found that 31 of the common genes that were up-regulated in all viruses infected cells are IFN-stimulated genes and these were expressed to the highest degree in response to FPV-NS^{MA} infection (Table 3.2, Fig. 3.25). However, when D74N (FPV-NS$^{MA\_D74N}$) or P3S+R41K+D74N (FPV-NS$^{MA\_P3S+R41K+D74N}$) were introduced into NS1-MA segment they resulted in a lower number of IFN-related gens as well as lower degree of gene expression. For instance, the gene expression data indicates an increased expression of IL29 at 6 h following infection with all

viruses, but with the highest expression induced by FPV-NS^{MA} infection. IL29 was recently recognized as a type III IFN, which signals through a similar JAK-STAT pathway as type I IFNs [220]. Type I and III IFN bind to the IFNAR1/IFNAR2 and IL10R2/IFNλR1 receptors respectively. Upon binding of IFNs, the corresponding receptor subunits dimerize to form the receptor complex and activate JAK-STAT signaling, which then results in downstream induction of a range of genes through ISGF3, a trimeric transcription factor complex of signal transducer and activator of transcription 1 and 2 (STAT1 and STAT2) and IRF9. Downstream genes regulated by ISGF3 include viral sensors, antiviral effector molecules, inhibitors of IFN signaling and viral sensing, and a range of other IFN-stimulated genes (ISGs).

Amongst the IFN-stimulated genes, I found both positive and negative effectors. A number of genes implicated in the antiviral response are up-regulated, many to a much higher degree in FPV-NS^{MA} infection. For instance the 2′-5′-oligoadenylate synthetases OASL, OAS2, as well as OAS1 were only expressed after FPV-NS^{MA} infection, but not other virus infection. OAS is activated by dsRNA, a putative by-product of viral replication, and polymerizes ATP into 29-59 oligoadenylate chains. These chains cause dimerization and activation of the latent RNase, RNase L, which inhibits virus replication by degradation of RNA [221]. Data indicate that a predominant function of the NS1 RNA-binding domain is to out-compete OAS for interaction with dsRNA, thereby inhibiting this host antiviral strategy [143]. Given the role of RNase L in augmenting the production of IFN-β [221], it is possible that NS1-mediated OAS inactivation also contributes to suppression of IFN-β synthesis [203, 213].

Several guanylate binding proteins, myxovirus resistance protein 1 (MX1), radical S-adenosyl methionine domain containing protein 2 (RSAD2), pentraxin related protein PTX3, IFN-induced protein with tetratricopeptide repeats 1 (IFIT1) were up-regulated to the highest degree in FPV-NS^{MA} infected cells and Zinc finger CCCH-type antiviral protein 1 (ZC3HAV1) was only expressed in FPV-NS^{MA} infection. However, as above all these genes were down regulated when the substitutions D74N or P3S+R41K+D74N were introduced into the NS1-MA. This result strongly supports the idea that this substitutions regulate the IFN pathway.

4.9 Activation of the poly(ADP-ribose) polymerase IFN response in FPV-NS^{MA} infected cells

In parallel with the type I IFN-mediated activation of the JAK-STAT pathway, FPV-NS^{MA} also causes the poly(ADP-ribose) polymerase, PARP9 and PARP9 genes (Table 3.3), which have been identified as potent inhibitors of replication of a variety of alphaviruses and other RNA viruses [222], suggesting a broad-spectrum antiviral function via interference with common cellular processes is involved in virus replication. PARP9, PARP10 were found to be very potent regulators of cellular translation [223]. Their effect on translation was shown to be stronger than that described for a well-characterized ISG, the double-stranded RNA (dsRNA)-activated protein kinase PKR. PKR was one of the first antiviral proteins described. It interacts with virus-specific dsRNA, and this in turn leads to autophosphorylation and dimerization of PKR, making it capable of phosphorylating the α-subunit of eukaryotic initiation factor 2 (eIF-2α) and thus inducing translation inhibition. Furthermore, the inhibitory functions of PARP9 and PARP10 are determined by more than a single mechanism, and one of them is based on the ability of these proteins to regulate cellular translation. Interference with the cellular translational machinery depends on the integrity of both the amino-terminal domain, containing a number of putative RNA-binding motifs, and the catalytic function of the carboxy-terminal PARP domain. The PARP-induced changes in translation efficiency appear to have a more potent effect on the synthesis of virus-specific proteins than on that of cellular proteins, thus making PARP-specific translational down-regulation an important contributor to the overall development of the antiviral response [222]. Therefore this mechanism could be one of the reasons that restrict FPV-NS^{MA} replication in mammalian cells, which is not the case in FPV-NS^{GD}, FPV-NS$^{MA\_D74N}$ and FPV-NS$^{MA\_P3S+R41K+D74N}$ infected cells.

4.10 Apoptosis

From the microarray data in the present study, I have used the Ingenuity Pathway Analysis (IPA) (QIAGEN) to identify the intracellular signaling pathways that were most significantly represented in FPV-NS^{GD}, FPV-NS^{MA}, FPV-NS$^{MA\_D74N}$ and FPV-NS$^{MA\_P3S+R41K+D74N}$ infected cells using, Fisher's Exact Test (Table 3.6). Apoptosis signaling was a suggested response to FPV-NS^{MA} and FPV-NS$^{MA\_P3S+R41K+D74N}$ infection. Microarray data is in well agreement with the caspase-3 activity and DNA

degradation (Tunel assay) (Fig. 3.29) of FPV-NS^{MA} and FPV-NS$^{MA\_P3S+R41K+D74N}$ infected cells. When the extent of apoptosis is compared to the infectious titres of the various viruses it can be concluded that there is no correlation between degree of apoptosis and virus titres.

The role of apoptosis in viral replication may vary with different viruses. For example, in certain acute viral infections, lytic viruses can utilize host apoptotic cascades to aid in cell lysis and virus dissemination [224]. In such cases, the infected cell releases the infectious viral particles as well as the immature unpacked viral material including dsRNA to the micro-environment. The dsRNA can trigger innate sensing receptors of neighbouring cells and trigger apoptosis in these cells which otherwise may have hosted additional cycles of virus replication. This is an example of the host initiating "altruistic" apoptosis in bystander cells which can lead to limiting viral spread [225]. Taken together, further investigation of the pathogenic significance of the early expression factors involved in apoptosis signaling in response to FPV-NS^{MA} and FPV-NS$^{MA\_P3S+R41K+D74N}$ infection observed in my microarray data is necessary. The role of apoptosis, as well as whether apoptosis or delayed apoptosis contributes to FPV-NS^{MA} and FPV-NS$^{MA\_P3S+R41K+D74N}$ pathogenesis through its positive or negative effects on viral replication, remain to be determined. Nevertheless, I have shown that compared with FPV-NS^{GD} and FPV-NS$^{MA\_D74N}$ viruses, FPV-NS^{MA} and FPV-NS$^{MA\_P3S+R41K+D74N}$ infected A549 cells were found to have highest production of apoptosis related factor.

Chapter 5

Conclusions

Zoonotic transmissions of avian influenza viruses pose a constant threat to the human population and can cause severe pandemics associated with high fatality. Due to effective species barriers, avian influenza virus can establish a new lineage in humans only in rare cases. To overcome these species barriers avian influenza virus require adaptive mutations in order to achieve high-level replication in the new host. Here, I demonstrate that three amino acid substitutions P3S+R41K+D74N in the viral NS1 protein prove to be sufficient for a strictly avian influenza virus to achieve high-level replication in human cell culture and mice. I demonstrate that these adaptive substitutions enhanced viral genome replication and transcription, thus contributing to the overall viral protein production. This observation raises the possibility that as yet unknown molecular features in NS1 could affect the level of polymerase activity. Furthermore, the viral polymerase activity is increased at the temperature of the human upper respiratory tract. Remarkably, these substitutions do not impair replication in avian cells, indicating that such viruses with enhanced replication efficiency in mammalian host could be generated in avian hosts. Thus, monitoring for these amino acids in avian influenza viruses is important to assess their potential zoonotic risk.

The frequency of the amino acids N74 alone or in combination with S3+K41 in the NS1 protein sequence was found to be only 0.1-2% available in IAV. Interestingly, the aa S3+K41 are already highly conserved in human, avian, swine, and other IAV with 94-96% of all virus isolates. My data present here shows that such viruses already possess S3+K41 in the NS1 protein, just one further single substitution (N74) must occur to gain the combination S3+K41+N74 that could greatly affect the adaptive ability of AIV to mammalian hosts. The acquisition of N74 for AIV that already possess S3+K41 in their NS1, may create viruses with improved replication ability in mammalians, including humans.

My results demonstrate gene expression analysis of A549 cells infected with comparable virus doses of the FPV-NS^{GD}, FPV-NS^{MA}, FPV-NS$^{MA\_D74N}$ and FPV-

NS$^{MA\_P3S+R41K+D74N}$ viruses, reveals differences at the quantitative rather than at the qualitative protein levels. An up-regulation of pathway ligands rather than signaling intermediaries appears to be the driving force behind pathway activation in the response to FPV-NS^{GD}, FPV-NS^{MA}, FPV-NS$^{MA\_D74N}$ and FPV-NS$^{MA\_P3S+R41K+D74N}$. However, a role for differential phosphorylation of signaling intermediaries and other regulatory mechanisms, such as post-transcriptional regulation by microRNAs, cannot be excluded as a contributing mechanism for the activation of host responses. Integration of data from complementary approaches will be required in the future to further understand the molecular events that lead to viral pathogenesis.

The FPV-NS^{MA} induced hyper-activation of IFN-β, IFN-γ and TNF-α pathways synergize to generate a highly pro-inflammatory cytokine/chemokine response that is markedly elevated compared to FPV-NS$^{MA\_D74N}$ and FPV-NS$^{MA\_P3S+R41K+D74N}$ infection which harbour amino acids changes in the NS1-MA segment which are likely to balance the innate immune system to prevent inflammation, contributing to tissue damage. I also observed an increase in inhibitors of certain pathways (e.g. OASL1), which may reflect the cell's attempt to shut off IFN and IFN-related pathways that have been over-activated in response to FPV-NS^{MA}, but this attempt may themselves result in a skew of the innate immune response to one of an increased pro-inflammatory nature.

It may eventually be possible to exploit these quantitative differences in host pathways activated by FPV-NS^{MA} for therapeutic purposes through the use of the appropriate inhibitors. Further investigation into the nature of these inhibitors and their specific targeting mechanisms is a challenging but critical task, and may ultimately result in novel therapeutic strategies that are capable of restoring the equilibrium of the host response and minimizing the impact of highly pathogenic influenza virus infection on the host.

Chapter 6

References

1. Taubenberger, J.K., *The origin and virulence of the 1918 "Spanish" influenza virus.* Proc Am Philos Soc, 2006. 150(1): p. 86-112.
2. Subbarao, K., B.R. Murphy, and A.S. Fauci, *Development of effective vaccines against pandemic influenza.* Immunity, 2006. 24(1): p. 5-9.
3. Chase, G.P., et al., *Influenza virus ribonucleoprotein complexes gain preferential access to cellular export machinery through chromatin targeting.* PLoS Pathog, 2011. 7(9): p. e1002187.
4. Palese, P. and J.F. Young, *Variation of influenza A, B, and C viruses.* Science, 1982. 215(4539): p. 1468-74.
5. Webster, R.G., et al., *Evolution and ecology of influenza A viruses.* Microbiol Rev, 1992. 56(1): p. 152-79.
6. Medina, R.A. and A. Garcia-Sastre, *Influenza A viruses: new research developments.* Nat Rev Microbiol, 2011. 9(8): p. 590-603.
7. Ozawa, M. and Y. Kawaoka, *Taming influenza viruses.* Virus Res, 2011. 162(1-2): p. 8-11.
8. Sims, L.D., et al., *Origin and evolution of highly pathogenic H5N1 avian influenza in Asia.* Vet Rec, 2005. 157(6): p. 159-64.
9. Peiris, J.S., M.D. de Jong, and Y. Guan, *Avian influenza virus (H5N1): a threat to human health.* Clin Microbiol Rev, 2007. 20(2): p. 243-67.
10. Manz, B., M. Schwemmle, and L. Brunotte, *Adaptation of avian influenza A virus polymerase in mammals to overcome the host species barrier.* J Virol, 2010. 87(13): p. 7200-9.
11. Chen, W., et al., *A novel influenza A virus mitochondrial protein that induces cell death.* Nat Med, 2001. 7(12): p. 1306-12.
12. Wise, H.M., et al., *Overlapping signals for translational regulation and packaging of influenza A virus segment 2.* Nucleic Acids Res, 2011. 39(17): p. 7775-90.
13. Jagger, B.W., et al., *An overlapping protein-coding region in influenza A virus segment 3 modulates the host response.* Science, 2012. 337(6091): p. 199-204.
14. Muramoto, Y., et al., *Identification of novel influenza A virus proteins translated from PA mRNA.* J Virol, 2012. 87(5): p. 2455-62.
15. Wise, H.M., et al., *Identification of a novel splice variant form of the influenza A virus M2 ion channel with an antigenically distinct ectodomain.* PLoS Pathog, 2012. 8(11): p. e1002998.
16. Forbes, N.E., et al., *Multifunctional adaptive NS1 mutations are selected upon human influenza virus evolution in the mouse.* PLoS One, 2012. 7(2): p. e31839.
17. Matrosovich, M., J. Stech, and H.D. Klenk, *Influenza receptors, polymerase and host range.* Rev Sci Tech, 2009. 28(1): p. 203-17.
18. Basler, C.F. and P.V. Aguilar, *Progress in identifying virulence determinants of the 1918 H1N1 and the Southeast Asian H5N1 influenza A viruses.* Antiviral Res, 2008. 79(3): p. 166-78.
19. Hale, B.G., et al., *The multifunctional NS1 protein of influenza A viruses.* J Gen Virol, 2008. 89(Pt 10): p. 2359-76.

20. Ludwig, S., et al., *Influenza-virus-induced signaling cascades: targets for antiviral therapy?* Trends Mol Med, 2003. 9(2): p. 46-52.

21. Portela, A. and P. Digard, *The influenza virus nucleoprotein: a multifunctional RNA-binding protein pivotal to virus replication.* J Gen Virol, 2002. 83(Pt 4): p. 723-34.

22. Pleschka, S., et al., *A plasmid-based reverse genetics system for influenza A virus.* J Virol, 1996. 70(6): p. 4188-92.

23. Edinger, T.O., M.O. Pohl, and S. Stertz, *Entry of influenza A virus: host factors and antiviral targets.* J Gen Virol, 2014. 95(Pt 2): p. 263-77.

24. Tong, S., et al., *New world bats harbor diverse influenza A viruses.* PLoS Pathog, 2013. 9(10): p. e1003657.

25. Tong, S., et al., *A distinct lineage of influenza A virus from bats.* Proc Natl Acad Sci U S A, 2012. 109(11): p. 4269-74.

26. Sun, X., et al., *Bat-derived influenza hemagglutinin H17 does not bind canonical avian or human receptors and most likely uses a unique entry mechanism.* Cell Rep, 2013. 3(3): p. 769-78.

27. Zhu, L., H. Ly, and Y. Liang, *PLC-gamma1 signaling plays a subtype-specific role in postbinding cell entry of influenza A virus.* J Virol, 2014. 88(1): p. 417-24.

28. Skehel, J.J. and D.C. Wiley, *Receptor binding and membrane fusion in virus entry: the influenza hemagglutinin.* Annu Rev Biochem, 2000. 69: p. 531-69.

29. Roberts, P.C., W. Garten, and H.D. Klenk, *Role of conserved glycosylation sites in maturation and transport of influenza A virus hemagglutinin.* J Virol, 1993. 67(6): p. 3048-60.

30. Liu, J., et al., *Structures of receptor complexes formed by hemagglutinins from the Asian Influenza pandemic of 1957.* Proc Natl Acad Sci U S A, 2009. 106(40): p. 17175-80.

31. Xu, R., et al., *Structure, receptor binding, and antigenicity of influenza virus hemagglutinins from the 1957 H2N2 pandemic.* J Virol, 2010. 84(4): p. 1715-21.

32. Weis, W., et al., *Structure of the influenza virus haemagglutinin complexed with its receptor, sialic acid.* Nature, 1988. 333(6172): p. 426-31.

33. Sauter, N.K., et al., *Hemagglutinins from two influenza virus variants bind to sialic acid derivatives with millimolar dissociation constants: a 500-MHz proton nuclear magnetic resonance study.* Biochemistry, 1989. 28(21): p. 8388-96.

34. Gamblin, S.J., et al., *The structure and receptor binding properties of the 1918 influenza hemagglutinin.* Science, 2004. 303(5665): p. 1838-42.

35. Bullough, P.A., et al., *Structure of influenza haemagglutinin at the pH of membrane fusion.* Nature, 1994. 371(6492): p. 37-43.

36. Huang, T.S., P. Palese, and M. Krystal, *Determination of influenza virus proteins required for genome replication.* J Virol, 1990. 64(11): p. 5669-73.

37. Desselberger, U., et al., *The 3' and 5'-terminal sequences of influenza A, B and C virus RNA segments are highly conserved and show partial inverted complementarity.* Gene, 1980. 8(3): p. 315-28.

38. Flick, R., et al., *Promoter elements in the influenza vRNA terminal structure.* RNA, 1996. 2(10): p. 1046-57.

39. Beloso, A., et al., *Degradation of cellular mRNA during influenza virus infection: its possible role in protein synthesis shutoff.* J Gen Virol, 1992. 73 (Pt 3): p. 575-81.

40. Fodor, E., D.C. Pritlove, and G.G. Brownlee, *The influenza virus panhandle is involved in the initiation of transcription.* J Virol, 1994. 68(6): p. 4092-6.

41. Vreede, F.T. and E. Fodor, *The role of the influenza virus RNA polymerase in host shut-off.* Virulence, 2010. 1(5): p. 436-9.

42. Fodor, E., *The RNA polymerase of influenza a virus: mechanisms of viral transcription and replication.* Acta Virol, 2013. 57(2): p. 113-22.

43. Lamb, R.A. and M. Takeda, *Death by influenza virus protein.* Nat Med, 2001. 7(12): p. 1286-8.

44. Fodor, E. and M. Smith, *The PA subunit is required for efficient nuclear accumulation of the PB1 subunit of the influenza A virus RNA polymerase complex.* J Virol, 2004. 78(17): p. 9144-53.

45. Shih, S.R. and R.M. Krug, *Novel exploitation of a nuclear function by influenza virus: the cellular SF2/ASF splicing factor controls the amount of the essential viral M2 ion channel protein in infected cells.* EMBO J, 1996. 15(19): p. 5415-27.

46. Garaigorta, U. and J. Ortin, *Mutation analysis of a recombinant NS replicon shows that influenza virus NS1 protein blocks the splicing and nucleo-cytoplasmic transport of its own viral mRNA.* Nucleic Acids Res, 2007. 35(14): p. 4573-82.

47. Satterly, N., et al., *Influenza virus targets the mRNA export machinery and the nuclear pore complex.* Proc Natl Acad Sci U S A, 2007. 104(6): p. 1853-8.

48. Takizawa, N., et al., *Association of functional influenza viral proteins and RNAs with nuclear chromatin and sub-chromatin structure.* Microbes Infect, 2006. 8(3): p. 823-33.

49. Poole, E., et al., *Functional domains of the influenza A virus PB2 protein: identification of NP- and PB1-binding sites.* Virology, 2004. 321(1): p. 120-33.

50. Perales, B., et al., *The replication activity of influenza virus polymerase is linked to the capacity of the PA subunit to induce proteolysis.* J Virol, 2000. 74(3): p. 1307-12.

51. Naffakh, N., P. Massin, and S. van der Werf, *The transcription/replication activity of the polymerase of influenza A viruses is not correlated with the level of proteolysis induced by the PA subunit.* Virology, 2001. 285(2): p. 244-52.

52. Mayer, D., et al., *Identification of cellular interaction partners of the influenza virus ribonucleoprotein complex and polymerase complex using proteomic-based approaches.* J Proteome Res, 2007. 6(2): p. 672-82.

53. Hutchinson, E.C., et al., *Characterisation of influenza A viruses with mutations in segment 5 packaging signals.* Vaccine, 2009. 27(45): p. 6270-5.

54. Bancroft, C.T. and T.G. Parslow, *Evidence for segment-nonspecific packaging of the influenza a virus genome.* J Virol, 2002. 76(14): p. 7133-9.

55. Naito, T., et al., *An influenza virus replicon system in yeast identified Tat-SF1 as a stimulatory host factor for viral RNA synthesis.* Proc Natl Acad Sci U S A, 2007. 104(46): p. 18235-40.

56. Falcon, A.M., et al., *Defective RNA replication and late gene expression in temperature-sensitive influenza viruses expressing deleted forms of the NS1 protein.* J Virol, 2004. 78(8): p. 3880-8.

57. Marion, R.M., et al., *The N-terminal half of the influenza virus NS1 protein is sufficient for nuclear retention of mRNA and enhancement of viral mRNA translation.* Nucleic Acids Res, 1997. 25(21): p. 4271-7.

58. Burgui, I., et al., *PABP1 and eIF4GI associate with influenza virus NS1 protein in viral mRNA translation initiation complexes.* J Gen Virol, 2003. 84(Pt 12): p. 3263-74.

59. Park, Y.W. and M.G. Katze, *Translational control by influenza virus. Identification of cis-acting sequences and trans-acting factors which may regulate selective viral mRNA translation.* J Biol Chem, 1995. 270(47): p. 28433-9.

60. Bier, K., A. York, and E. Fodor, *Cellular cap-binding proteins associate with influenza virus mRNAs.* J Gen Virol, 2011. 92(Pt 7): p. 1627-34.

61. Chen, Z. and R.M. Krug, *Selective nuclear export of viral mRNAs in influenza-virus-infected cells.* Trends Microbiol, 2000. 8(8): p. 376-83.

62. Engelhardt, O.G. and E. Fodor, *Functional association between viral and cellular transcription during influenza virus infection.* Rev Med Virol, 2006. 16(5): p. 329-45.

63. Hutchinson, E.C. and E. Fodor, *Nuclear import of the influenza A virus transcriptional machinery.* Vaccine, 2012. 30(51): p. 7353-8.

64. Resa-Infante, P. and G. Gabriel, *The nuclear import machinery is a determinant of influenza virus host adaptation.* Bioessays, 2013. 35(1): p. 23-7.

65. Martin, K. and A. Helenius, *Transport of incoming influenza virus nucleocapsids into the nucleus.* J Virol, 1991. 65(1): p. 232-44.

66. Greenspan, D., et al., *Expression of influenza virus NS2 nonstructural protein in bacteria and localization of NS2 in infected eucaryotic cells.* J Virol, 1985. 54(3): p. 833-43.

67. Hutchinson, E.C., et al., *Genome packaging in influenza A virus.* J Gen Virol, 2010. 91(Pt 2): p. 313-28.

68. Luque, D., et al., *Infectious bursal disease virus is an icosahedral polyploid dsRNA virus.* Proc Natl Acad Sci U S A, 2009. 106(7): p. 2148-52.

69. Kingsbury, D.W., *Replication and functions of myxovirus ribonucleic acids.* Prog Med Virol, 1970. 12: p. 49-77.

70. Mindich, L., *Packaging, replication and recombination of the segmented genome of bacteriophage Phi6 and its relatives.* Virus Res, 2004. 101(1): p. 83-92.

71. Matrosovich, M.N., et al., *Human and avian influenza viruses target different cell types in cultures of human airway epithelium.* Proc Natl Acad Sci U S A, 2004. 101(13): p. 4620-4.

72. Gambaryan, A., R. Webster, and M. Matrosovich, *Differences between influenza virus receptors on target cells of duck and chicken.* Arch Virol, 2002. 147(6): p. 1197-208.

73. Costa, T., et al., *Distribution patterns of influenza virus receptors and viral attachment patterns in the respiratory and intestinal tracts of seven avian species.* Vet Res, 2012. 43: p. 28.

74. Matrosovich, M., et al., *Early alterations of the receptor-binding properties of H1, H2, and H3 avian influenza virus hemagglutinins after their introduction into mammals.* J Virol, 2000. 74(18): p. 8502-12.

75. Glaser, L., et al., *A single amino acid substitution in 1918 influenza virus hemagglutinin changes receptor binding specificity.* J Virol, 2005. 79(17): p. 11533-6.

76. Chutinimitkul, S., et al., *In vitro assessment of attachment pattern and replication efficiency of H5N1 influenza A viruses with altered receptor specificity.* J Virol, 2010. 84(13): p. 6825-33.

77. Yamada, S., et al., *Haemagglutinin mutations responsible for the binding of H5N1 influenza A viruses to human-type receptors.* Nature, 2006. 444(7117): p. 378-82.

78. Gambaryan, A., et al., *Evolution of the receptor binding phenotype of influenza A (H5) viruses.* Virology, 2006. 344(2): p. 432-8.

79. Stevens, J., et al., *Structure and receptor specificity of the hemagglutinin from an H5N1 influenza virus.* Science, 2006. 312(5772): p. 404-10.

80. Matrosovich, M., et al., *The surface glycoproteins of H5 influenza viruses isolated from humans, chickens, and wild aquatic birds have distinguishable properties.* J Virol, 1999. 73(2): p. 1146-55.

81. Baigent, S.J. and J.W. McCauley, *Glycosylation of haemagglutinin and stalk-length of neuraminidase combine to regulate the growth of avian influenza viruses in tissue culture.* Virus Res, 2001. 79(1-2): p. 177-85.

82. Lowen, A.C., et al., *Blocking interhost transmission of influenza virus by vaccination in the guinea pig model.* J Virol, 2009. 83(7): p. 2803-18.

83. Herfst, S., et al., *Airborne transmission of influenza A/H5N1 virus between ferrets.* Science, 2012. 336(6088): p. 1534-41.

84. Steel, J., et al., *Transmission of influenza virus in a mammalian host is increased by PB2 amino acids 627K or 627E/701N.* PLoS Pathog, 2009. 5(1): p. e1000252.

85. Munster, V.J., et al., *Pathogenesis and transmission of swine-origin 2009 A(H1N1) influenza virus in ferrets.* Science, 2009. 325(5939): p. 481-3.

86. Zhou, B., et al., *Asparagine substitution at PB2 residue 701 enhances the replication, pathogenicity, and transmission of the 2009 pandemic H1N1 influenza A virus.* PLoS One, 2013. 8(6): p. e67616.

87. Naffakh, N., et al., *Genetic analysis of the compatibility between polymerase proteins from human and avian strains of influenza A viruses.* J Gen Virol, 2000. 81(Pt 5): p. 1283-91.

88. Xu, C., et al., *Amino acids 473V and 598P of PB1 from an avian-origin influenza A virus contribute to polymerase activity, especially in mammalian cells.* J Gen Virol, 2012. 93(Pt 3): p. 531-40.

89. Manz, B., M. Schwemmle, and L. Brunotte, *Adaptation of avian influenza A virus polymerase in mammals to overcome the host species barrier.* J Virol, 2013. 87(13): p. 7200-9.

90. Yamada, S., et al., *Biological and structural characterization of a host-adapting amino acid in influenza virus.* PLoS Pathog, 2010. 6(8): p. e1001034.

91. Hatta, M., et al., *Growth of H5N1 influenza A viruses in the upper respiratory tracts of mice.* PLoS Pathog, 2007. 3(10): p. 1374-9.

92. Gabriel, G., et al., *The viral polymerase mediates adaptation of an avian influenza virus to a mammalian host.* Proc Natl Acad Sci U S A, 2005. 102(51): p. 18590-5.

93. Manz, B., et al., *Adaptive mutations in NEP compensate for defective H5N1 RNA replication in cultured human cells.* Nat Commun, 2012. 3: p. 802.

94. Maines, T.R., et al., *Lack of transmission of H5N1 avian-human reassortant influenza viruses in a ferret model.* Proc Natl Acad Sci U S A, 2006. 103(32): p. 12121-6.

95. Zhang, Y., et al., *H5N1 hybrid viruses bearing 2009/H1N1 virus genes transmit in guinea pigs by respiratory droplet.* Science, 2013. 340(6139): p. 1459-63.

96. Imai, M., et al., *Experimental adaptation of an influenza H5 HA confers respiratory droplet transmission to a reassortant H5 HA/H1N1 virus in ferrets.* Nature, 2012. 486(7403): p. 420-8.

97. Lakdawala, S.S., et al., *Eurasian-origin gene segments contribute to the transmissibility, aerosol release, and morphology of the 2009 pandemic H1N1 influenza virus.* PLoS Pathog, 2011. 7(12): p. e1002443.

98. Pascua, P.N., et al., *Virulence and transmissibility of H1N2 influenza virus in ferrets imply the continuing threat of triple-reassortant swine viruses.* Proc Natl Acad Sci U S A, 2012. 109(39): p. 15900-5.

99. Pascua, P.N., et al., *The homologous tripartite viral RNA polymerase of A/swine/Korea/CT1204/2009(H1N2) influenza virus synergistically drives efficient replication and promotes respiratory droplet transmission in ferrets.* J Virol, 2013. 87(19): p. 10552-62.

100. Pearce, M.B., et al., *Pathogenesis and transmission of swine origin A(H3N2)v influenza viruses in ferrets.* Proc Natl Acad Sci U S A, 2012. 109(10): p. 3944-9.

101. Blumenkrantz, D., et al., *The short stalk length of highly pathogenic avian influenza H5N1 virus neuraminidase limits transmission of pandemic H1N1 virus in ferrets.* J Virol, 2013. 87(19): p. 10539-51.

102. Kilbourne, E.D. and J.S. Murphy, *Genetic studies of influenza viruses. I. Viral morphology and growth capacity as exchangeable genetic traits. Rapid in ovo adaptation of early passage Asian strain isolates by combination with PR8.* J Exp Med, 1960. 111: p. 387-406.

103. Garcia-Sastre, A., et al., *Influenza A virus lacking the NS1 gene replicates in interferon-deficient systems.* Virology, 1998. 252(2): p. 324-30.

104. Min, J.Y., et al., *A site on the influenza A virus NS1 protein mediates both inhibition of PKR activation and temporal regulation of viral RNA synthesis.* Virology, 2007. 363(1): p. 236-43.

105. Fortes, P., A.I. Lamond, and J. Ortin, *Influenza virus NS1 protein alters the subnuclear localization of cellular splicing components.* J Gen Virol, 1995. 76 (Pt 4): p. 1001-7.

106. Lamb, R.A. and C.J. Lai, *Sequence of interrupted and uninterrupted mRNAs and cloned DNA coding for the two overlapping nonstructural proteins of influenza virus.* Cell, 1980. 21(2): p. 475-85.

107. Robb, N.C., et al., *Splicing of influenza A virus NS1 mRNA is independent of the viral NS1 protein.* J Gen Virol, 2010. 91(Pt 9): p. 2331-40.

108. Newby, C.M., L. Sabin, and A. Pekosz, *The RNA binding domain of influenza A virus NS1 protein affects secretion of tumor necrosis factor alpha, interleukin-6, and interferon in primary murine tracheal epithelial cells.* J Virol, 2007. 81(17): p. 9469-80.

109. Li, Y., Y. YamaKita, and R.M. Krug, *Regulation of a nuclear export signal by an adjacent inhibitory sequence: the effector domain of the influenza virus NS1 protein.* Proc Natl Acad Sci U S A, 1998. 95(9): p. 4864-9.

110. Melen, K., et al., *Nuclear and nucleolar targeting of influenza A virus NS1 protein: striking differences between different virus subtypes.* J Virol, 2007. 81(11): p. 5995-6006.

111. Hale, B.G., *Conformational plasticity of the influenza A virus NS1 protein.* J Gen Virol, 2014.

112. Wang, W., et al., *RNA binding by the novel helical domain of the influenza virus NS1 protein requires its dimer structure and a small number of specific basic amino acids.* RNA, 1999. 5(2): p. 195-205.

113. Hatada, E., et al., *Binding of the influenza virus NS1 protein to model genome RNAs.* J Gen Virol, 1997. 78 (Pt 5): p. 1059-63.

114. Qiu, Y. and R.M. Krug, *The influenza virus NS1 protein is a poly(A)-binding protein that inhibits nuclear export of mRNAs containing poly(A).* J Virol, 1994. 68(4): p. 2425-32.

115. Qiu, Y., M. Nemeroff, and R.M. Krug, *The influenza virus NS1 protein binds to a specific region in human U6 snRNA and inhibits U6-U2 and U6-U4 snRNA interactions during splicing.* RNA, 1995. 1(3): p. 304-16.

116. Pichlmair, A., et al., *RIG-I-mediated antiviral responses to single-stranded RNA bearing 5'-phosphates.* Science, 2006. 314(5801): p. 997-1001.

117. Marion, R.M., et al., *Influenza virus NS1 protein interacts with viral transcription-replication complexes in vivo.* J Gen Virol, 1997. 78 (Pt 10): p. 2447-51.

118. Aragon, T., et al., *Eukaryotic translation initiation factor 4GI is a cellular target for NS1 protein, a translational activator of influenza virus.* Mol Cell Biol, 2000. 20(17): p. 6259-68.

119. Falcon, A.M., et al., *Interaction of influenza virus NS1 protein and the human homologue of Staufen in vivo and in vitro.* Nucleic Acids Res, 1999. 27(11): p. 2241-7.

120. Goodbourn, S., L. Didcock, and R.E. Randall, *Interferons: cell signaling, immune modulation, antiviral response and virus countermeasures.* J Gen Virol, 2000. 81(Pt 10): p. 2341-64.

121. Hayman, A., et al., *Variation in the ability of human influenza A viruses to induce and inhibit the IFN-beta pathway.* Virology, 2006. 347(1): p. 52-64.

122. Kochs, G., A. Garcia-Sastre, and L. Martinez-Sobrido, *Multiple anti-interferon actions of the influenza A virus NS1 protein.* J Virol, 2007. 81(13): p. 7011-21.

123. Ludwig, S., et al., *The influenza A virus NS1 protein inhibits activation of Jun N-terminal kinase and AP-1 transcription factors.* J Virol, 2002. 76(21): p. 11166-71.

124. Wang, X., et al., *Functional replacement of the carboxy-terminal two-thirds of the influenza A virus NS1 protein with short heterologous dimerization domains.* J Virol, 2002. 76(24): p. 12951-62.

125. Lu, Y., X.Y. Qian, and R.M. Krug, *The influenza virus NS1 protein: a novel inhibitor of pre-mRNA splicing.* Genes Dev, 1994. 8(15): p. 1817-28.

126. Chen, Z., Y. Li, and R.M. Krug, *Influenza A virus NS1 protein targets poly(A)-binding protein II of the cellular 3'-end processing machinery.* EMBO J, 1999. 18(8): p. 2273-83.

127. Nemeroff, M.E., et al., *Influenza virus NS1 protein interacts with the cellular 30 kDa subunit of CPSF and inhibits 3'end formation of cellular pre-mRNAs.* Mol Cell, 1998. 1(7): p. 991-1000.

128. Chen, J., J.J. Skehel, and D.C. Wiley, *N- and C-terminal residues combine in the fusion-pH influenza hemagglutinin HA(2) subunit to form an N cap that terminates the triple-stranded coiled coil.* Proc Natl Acad Sci U S A, 1999. 96(16): p. 8967-72.

129. Wolff, T., R.E. O'Neill, and P. Palese, *NS1-Binding protein (NS1-BP): a novel human protein that interacts with the influenza A virus nonstructural NS1 protein is relocalized in the nuclei of infected cells.* J Virol, 1998. 72(9): p. 7170-80.

130. Thomis, D.C. and C.E. Samuel, *Mechanism of interferon action: evidence for intermolecular autophosphorylation and autoactivation of the interferon-induced, RNA-dependent protein kinase PKR.* J Virol, 1993. 67(12): p. 7695-700.

131. Fernandez-Sesma, A., *The influenza virus NS1 protein: inhibitor of innate and adaptive immunity.* Infect Disord Drug Targets, 2007. 7(4): p. 336-43.

132. Wolff, T., R.E. O'Neill, and P. Palese, *Interaction cloning of NS1-I, a human protein that binds to the nonstructural NS1 proteins of influenza A and B viruses.* J Virol, 1996. 70(8): p. 5363-72.

133. Finkelstein, D.B., et al., *Persistent host markers in pandemic and H5N1 influenza viruses.* J Virol, 2007. 81(19): p. 10292-9.

134. Obenauer, J.C., et al., *Large-scale sequence analysis of avian influenza isolates.* Science, 2006. 311(5767): p. 1576-80.

135. Lowy, R.J., *Influenza virus induction of apoptosis by intrinsic and extrinsic mechanisms.* Int Rev Immunol, 2003. 22(5-6): p. 425-49.

136.	Seo, S.H., E. Hoffmann, and R.G. Webster, *The NS1 gene of H5N1 influenza viruses circumvents the host anti-viral cytokine responses.* Virus Res, 2004. 103(1-2): p. 107-13.

137.	Zhirnov, O.P., et al., *Segment NS of influenza A virus contains an additional gene NSP in positive-sense orientation.* Dokl Biochem Biophys, 2007. 414: p. 127-33.

138.	Schultz-Cherry, S., et al., *Influenza virus ns1 protein induces apoptosis in cultured cells.* J Virol, 2001. 75(17): p. 7875-81.

139.	Noah, D.L., K.Y. Twu, and R.M. Krug, *Cellular antiviral responses against influenza A virus are countered at the posttranscriptional level by the viral NS1A protein via its binding to a cellular protein required for the 3' end processing of cellular pre-mRNAS.* Virology, 2003. 307(2): p. 386-95.

140.	Zhirnov, O.P., et al., *NS1 protein of influenza A virus down-regulates apoptosis.* J Virol, 2002. 76(4): p. 1617-25.

141.	Takizawa, T., *[Mechanism of the induction of apoptosis by influenza virus infection].* Nihon Rinsho, 1996. 54(7): p. 1836-41.

142.	Li, S., et al., *Binding of the influenza A virus NS1 protein to PKR mediates the inhibition of its activation by either PACT or double-stranded RNA.* Virology, 2006. 349(1): p. 13-21.

143.	Min, J.Y. and R.M. Krug, *The primary function of RNA binding by the influenza A virus NS1 protein in infected cells: Inhibiting the 2'-5' oligo (A) synthetase/RNase L pathway.* Proc Natl Acad Sci U S A, 2006. 103(18): p. 7100-5.

144.	Zhirnov, O.P. and H.D. Klenk, *Control of apoptosis in influenza virus-infected cells by up-regulation of Akt and p53 signaling.* Apoptosis, 2007. 12(8): p. 1419-32.

145.	Kelley, L.A. and M.J. Sternberg, *Protein structure prediction on the Web: a case study using the Phyre server.* Nat Protoc, 2009. 4(3): p. 363-71.

146.	Bornholdt, Z.A. and B.V. Prasad, *X-ray structure of NS1 from a highly pathogenic H5N1 influenza virus.* Nature, 2008. 456(7224): p. 985-8.

147.	Chew, T.H., et al., *birgHPC: creating instant computing clusters for bioinformatics and molecular dynamics.* Bioinformatics, 2011. 27(9): p. 1320-1.

148.	Jiang, W., et al., *High-performance scalable molecular dynamics simulations of a polarizable force field based on classical Drude oscillators in NAMD.* J Phys Chem Lett, 2011. 2(2): p. 87-92.

149.	Jiang, W., et al., *Generalized Scalable Multiple Copy Algorithms for Molecular Dynamics Simulations in NAMD.* Comput Phys Commun, 2014. 185(3): p. 908-916.

150.	Phillips, J.C., et al., *Scalable molecular dynamics with NAMD.* J Comput Chem, 2005. 26(16): p. 1781-802.

151.	Humphrey, W., A. Dalke, and K. Schulten, *VMD: visual molecular dynamics.* J Mol Graph, 1996. 14(1): p. 33-8, 27-8.

152.	Mackerell, A.D., Jr., M. Feig, and C.L. Brooks, 3rd, *Extending the treatment of backbone energetics in protein force fields: limitations of gas-phase quantum mechanics in reproducing protein conformational distributions in molecular dynamics simulations.* J Comput Chem, 2004. 25(11): p. 1400-15.

153.	Hulse, D.J., et al., *Molecular determinants within the surface proteins involved in the pathogenicity of H5N1 influenza viruses in chickens.* J Virol, 2004. 78(18): p. 9954-64.

154.	Rogers, G.N., et al., *Single amino acid substitutions in influenza haemagglutinin change receptor binding specificity.* Nature, 1983. 304(5921): p. 76-8.

155.	Imai, H., et al., *The HA and NS genes of human H5N1 influenza A virus contribute to high virulence in ferrets.* PLoS Pathog, 2010. 6(9): p. e1001106.

156.	Hatta, M., et al., *Molecular basis for high virulence of Hong Kong H5N1 influenza A viruses.* Science, 2001. 293(5536): p. 1840-2.

157.	Seo, S.H., E. Hoffmann, and R.G. Webster, *Lethal H5N1 influenza viruses escape host anti-viral cytokine responses.* Nat Med, 2002. 8(9): p. 950-4.

158.	Labadie, K., et al., *Host-range determinants on the PB2 protein of influenza A viruses control the interaction between the viral polymerase and nucleoprotein in human cells.* Virology, 2007. 362(2): p. 271-82.

159.	Robb, N.C., et al., *The influenza A virus NS1 protein interacts with the nucleoprotein of viral ribonucleoprotein complexes.* J Virol, 2011. 85(10): p. 5228-31.

160.	Wang, Z., et al., *NS reassortment of an H7-type highly pathogenic avian influenza virus affects its propagation by altering the regulation of viral RNA production and antiviral host response.* J Virol, 2010. 84(21): p. 11323-35.

161.	Kuo, R.L. and R.M. Krug, *Influenza a virus polymerase is an integral component of the CPSF30-NS1A protein complex in infected cells.* J Virol, 2009. 83(4): p. 1611-6.

162.	Li, Z., et al., *Molecular basis of replication of duck H5N1 influenza viruses in a mammalian mouse model.* J Virol, 2005. 79(18): p. 12058-64.

163.	Scheiblauer, H., A.P. Kendal, and R. Rott, *Pathogenicity of influenza A/Seal/Mass/1/80 virus mutants for mammalian species.* Arch Virol, 1995. 140(2): p. 341-8.

164.	Paterson, D. and E. Fodor, *Emerging roles for the influenza A virus nuclear export protein (NEP).* PLoS Pathog, 2012. 8(12): p. e1003019.

165.	Hutchinson, E.C. and E. Fodor, *Transport of the influenza virus genome from nucleus to nucleus.* Viruses, 2013. 5(10): p. 2424-46.

166.	Greenspan, D., P. Palese, and M. Krystal, *Two nuclear location signals in the influenza virus NS1 nonstructural protein.* J Virol, 1988. 62(8): p. 3020-6.

167.	Volmer, R., et al., *Nucleolar localization of influenza A NS1: striking differences between mammalian and avian cells.* Virol J, 2010. 7: p. 63.

168.	Shimizu, K., et al., *Regulation of influenza virus RNA polymerase activity by cellular and viral factors.* Nucleic Acids Res, 1994. 22(23): p. 5047-53.

169.	Salvatore, M., et al., *Effects of influenza A virus NS1 protein on protein expression: the NS1 protein enhances translation and is not required for shutoff of host protein synthesis.* J Virol, 2002. 76(3): p. 1206-12.

170.	Hay, A.J., et al., *Transcription of the influenza virus genome.* Virology, 1977. 83(2): p. 337-55.

171.	Vreede, F.T., T.E. Jung, and G.G. Brownlee, *Model suggesting that replication of influenza virus is regulated by stabilization of replicative intermediates.* J Virol, 2004. 78(17): p. 9568-72.

172.	Kawaguchi, A., T. Naito, and K. Nagata, *Involvement of influenza virus PA subunit in assembly of functional RNA polymerase complexes.* J Virol, 2005. 79(2): p. 732-44.

173.	McCauley, J.W. and C.R. Penn, *The critical cut-off temperature of avian influenza viruses.* Virus Res, 1990. 17(3): p. 191-8.

174.	Massin, P., S. van der Werf, and N. Naffakh, *Residue 627 of PB2 is a determinant of cold sensitivity in RNA replication of avian influenza viruses.* J Virol, 2001. 75(11): p. 5398-404.

175. Baigent, S.J. and J.W. McCauley, *Influenza type A in humans, mammals and birds: determinants of virus virulence, host-range and interspecies transmission.* Bioessays, 2003. 25(7): p. 657-71.

176. Subbarao, E.K., W. London, and B.R. Murphy, *A single amino acid in the PB2 gene of influenza A virus is a determinant of host range.* J Virol, 1993. 67(4): p. 1761-4.

177. Tumpey, T.M., et al., *Characterization of the reconstructed 1918 Spanish influenza pandemic virus.* Science, 2005. 310(5745): p. 77-80.

178. Carrillo, B., et al., *The influenza A virus protein NS1 displays structural polymorphism.* J Virol, 2014. 88(8): p. 4113-22.

179. Ma, W., et al., *The NS segment of an H5N1 highly pathogenic avian influenza virus (HPAIV) is sufficient to alter replication efficiency, cell tropism, and host range of an H7N1 HPAIV.* J Virol, 2010. 84(4): p. 2122-33.

180. Bao, Y., et al., *The influenza virus resource at the National Center for Biotechnology Information.* J Virol, 2008. 82(2): p. 596-601.

181. Li, S.Q., M. Orlich, and R. Rott, *Generation of seal influenza virus variants pathogenic for chickens, because of hemagglutinin cleavage site changes.* J Virol, 1990. 64(7): p. 3297-303.

182. Randall, R.E. and S. Goodbourn, *Interferons and viruses: an interplay between induction, signaling, antiviral responses and virus countermeasures.* J Gen Virol, 2008. 89(Pt 1): p. 1-47.

183. Fukuyama, S. and Y. Kawaoka, *The pathogenesis of influenza virus infections: the contributions of virus and host factors.* Curr Opin Immunol, 2011. 23(4): p. 481-6.

184. Ehrhardt, C., et al., *Interplay between influenza A virus and the innate immune signaling.* Microbes Infect, 2010. 12(1): p. 81-7.

185. Garaigorta, U., A.M. Falcon, and J. Ortin, *Genetic analysis of influenza virus NS1 gene: a temperature-sensitive mutant shows defective formation of virus particles.* J Virol, 2005. 79(24): p. 15246-57.

186. Krug, R.M., et al., *Intracellular warfare between human influenza viruses and human cells: the roles of the viral NS1 protein.* Virology, 2003. 309(2): p. 181-9.

187. Marazzi, I., et al., *Suppression of the antiviral response by an influenza histone mimic.* Nature, 2012. 483(7390): p. 428-33.

188. Guo, Z., et al., *NS1 protein of influenza A virus inhibits the function of intracytoplasmic pathogen sensor, RIG-I.* Am J Respir Cell Mol Biol, 2007. 36(3): p. 263-9.

189. Mibayashi, M., et al., *Inhibition of retinoic acid-inducible gene I-mediated induction of beta interferon by the NS1 protein of influenza A virus.* J Virol, 2007. 81(2): p. 514-24.

190. Opitz, B., et al., *IFNbeta induction by influenza A virus is mediated by RIG-I which is regulated by the viral NS1 protein.* Cell Microbiol, 2007. 9(4): p. 930-8.

191. Pauli, E.K., et al., *Influenza A virus inhibits type I IFN signaling via NF-kappaB-dependent induction of SOCS-3 expression.* PLoS Pathog, 2008. 4(11): p. e1000196.

192. Pothlichet, J., M. Chignard, and M. Si-Tahar, *Cutting edge: innate immune response triggered by influenza A virus is negatively regulated by SOCS1 and SOCS3 through a RIG-I/IFNAR1-dependent pathway.* J Immunol, 2008. 180(4): p. 2034-8.

193. Hatada, E., S. Saito, and R. Fukuda, *Mutant influenza viruses with a defective NS1 protein cannot block the activation of PKR in infected cells.* J Virol, 1999. 73(3): p. 2425-33.

194. Kurokawa, M., et al., *Influenza virus overcomes apoptosis by rapid multiplication.* Int J Mol Med, 1999. 3(5): p. 527-30.

195.   Ehrhardt, C., et al., *Influenza A virus NS1 protein activates the PI3K/Akt pathway to mediate antiapoptotic signaling responses.* J Virol, 2007. 81(7): p. 3058-67.

196.   Lam, W.Y., et al., *Avian influenza virus A/HK/483/97(H5N1) NS1 protein induces apoptosis in human airway epithelial cells.* J Virol, 2008. 82(6): p. 2741-51.

197.   Ehrhardt, C., T. Wolff, and S. Ludwig, *Activation of phosphatidylinositol 3-kinase signaling by the nonstructural NS1 protein is not conserved among type A and B influenza viruses.* J Virol, 2007. 81(21): p. 12097-100.

198.   Zhang, C., et al., *Highly pathogenic avian influenza A virus H5N1 NS1 protein induces caspase-dependent apoptosis in human alveolar basal epithelial cells.* Virol J, 2010. 7: p. 51.

199.   Basler, C.F., et al., *Sequence of the 1918 pandemic influenza virus nonstructural gene (NS) segment and characterization of recombinant viruses bearing the 1918 NS genes.* Proc Natl Acad Sci U S A, 2001. 98(5): p. 2746-51.

200.   Fortes, P., A. Beloso, and J. Ortin, *Influenza virus NS1 protein inhibits pre-mRNA splicing and blocks mRNA nucleocytoplasmic transport.* EMBO J, 1994. 13(3): p. 704-12.

201.   Qian, X.Y., F. Alonso-Caplen, and R.M. Krug, *Two functional domains of the influenza virus NS1 protein are required for regulation of nuclear export of mRNA.* J Virol, 1994. 68(4): p. 2433-41.

202.   Briedis, D.J., et al., *Migration of influenza virus-specific polypeptides from cytoplasm to nucleus of infected cells.* Virology, 1981. 111(1): p. 154-64.

203.   Talon, J., et al., *Activation of interferon regulatory factor 3 is inhibited by the influenza A virus NS1 protein.* J Virol, 2000. 74(17): p. 7989-96.

204.   Ozaki, H. and H. Kida, *Extensive accumulation of influenza virus NS1 protein in the nuclei causes effective viral growth in vero cells.* Microbiol Immunol, 2007. 51(5): p. 577-80.

205.   Cros, J.F. and P. Palese, *Trafficking of viral genomic RNA into and out of the nucleus: influenza, Thogoto and Borna disease viruses.* Virus Res, 2003. 95(1-2): p. 3-12.

206.   Elton, D., et al., *Interaction of the influenza virus nucleoprotein with the cellular CRM1-mediated nuclear export pathway.* J Virol, 2001. 75(1): p. 408-19.

207.   Ma, K., A.M. Roy, and G.R. Whittaker, *Nuclear export of influenza virus ribonucleoproteins: identification of an export intermediate at the nuclear periphery.* Virology, 2001. 282(2): p. 215-20.

208.   Pleschka, S., et al., *Influenza virus propagation is impaired by inhibition of the Raf/MEK/ERK signaling cascade.* Nat Cell Biol, 2001. 3(3): p. 301-5.

209.   O'Neill, R.E., J. Talon, and P. Palese, *The influenza virus NEP (NS2 protein) mediates the nuclear export of viral ribonucleoproteins.* EMBO J, 1998. 17(1): p. 288-96.

210.   Yasuda, J., et al., *Molecular assembly of influenza virus: association of the NS2 protein with virion matrix.* Virology, 1993. 196(1): p. 249-55.

211.   Wolstenholme, A.J., et al., *Influenza virus-specific RNA and protein syntheses in cells infected with temperature-sensitive mutants defective in the genome segment encoding nonstructural proteins.* J Virol, 1980. 35(1): p. 1-7.

212.   Li, O.T., et al., *Full factorial analysis of mammalian and avian influenza polymerase subunits suggests a role of an efficient polymerase for virus adaptation.* PLoS One, 2009. 4(5): p. e5658.

213. Donelan, N.R., C.F. Basler, and A. Garcia-Sastre, *A recombinant influenza A virus expressing an RNA-binding-defective NS1 protein induces high levels of beta interferon and is attenuated in mice.* J Virol, 2003. 77(24): p. 13257-66.

214. Zhao, C., et al., *ISG15 conjugation system targets the viral NS1 protein in influenza A virus-infected cells.* Proc Natl Acad Sci U S A, 2010. 107(5): p. 2253-8.

215. Chen, G., et al., *Cellular DDX21 RNA helicase inhibits influenza A virus replication but is counteracted by the viral NS1 protein.* Cell Host Microbe, 2014. 15(4): p. 484-93.

216. Dundon, W.G. and I. Capua, *A Closer Look at the NS1 of Influenza Virus.* Viruses, 2009. 1(3): p. 1057-72.

217. Long, J.X., et al., *Virulence of H5N1 avian influenza virus enhanced by a 15-nucleotide deletion in the viral nonstructural gene.* Virus Genes, 2008. 36(3): p. 471-8.

218. Li, W., J.W. Noah, and D.L. Noah, *Alanine substitutions within a linker region of the influenza A virus non-structural protein 1 alter its subcellular localization and attenuate virus replication.* J Gen Virol, 2011. 92(Pt 8): p. 1832-42.

219. Jia, D., et al., *Influenza virus non-structural protein 1 (NS1) disrupts interferon signaling.* PLoS One, 2010. 5(11): p. e13927.

220. Uze, G. and D. Monneron, *IL-28 and IL-29: newcomers to the interferon family.* Biochimie, 2007. 89(6-7): p. 729-34.

221. Silverman, R.H., *Viral encounters with 2',5'-oligoadenylate synthetase and RNase L during the interferon antiviral response.* J Virol, 2007. 81(23): p. 12720-9.

222. Atasheva, S., E.I. Frolova, and I. Frolov, *Interferon-stimulated poly(ADP-Ribose) polymerases are potent inhibitors of cellular translation and virus replication.* J Virol, 2014. 88(4): p. 2116-30.

223. Gale, M., Jr. and M.G. Katze, *Molecular mechanisms of interferon resistance mediated by viral-directed inhibition of PKR, the interferon-induced protein kinase.* Pharmacol Ther, 1998. 78(1): p. 29-46.

224. Lee, S.M., et al., *Systems-level comparison of host-responses elicited by avian H5N1 and seasonal H1N1 influenza viruses in primary human macrophages.* PLoS One, 2009. 4(12): p. e8072.

225. Kalai, M., et al., *Tipping the balance between necrosis and apoptosis in human and murine cells treated with interferon and dsRNA.* Cell Death Differ, 2002. 9(9): p. 981-94.

Der Lebenslauf wurde aus der elektronischen Version der Arbeit entfernt.

The curriculum vitae was removed from the electronic version of the paper.

Chapter 8

Acknowledgements

Now for the less serious stuff… or not.

I want to start off by acknowledging firstly my SELF and YOU. But not forgetting, ever, those who deserve to be mentioned by name.

I am grateful to Stephan Pleschka for his endless support and advice. Likewise, past and present members of the group have been invaluable for practical help, discussions, and constructive criticism. My knowledge has greatly increased thanks to him, and I am really, truly grateful.

I am sincerely grateful to Prof. Dr. Peter Friedhoff and Dr. Anja Drescher for giving me the opportunity to join the IRTG 1384 (Enzymes and Multienzyme Complexes acting on Nucleic Acids) PhD program. I must add that it was a tough yet very educational program, from which I benefited a great deal, and I'm not joking. I want to thank at this point too, all Professors for accompanying us in the "education", and for putting up with so many of my "probably" stubborn doubts, patiently. They were very helpful all along. Of course not wanting to forget all my colleagues of the IRTG 1384, the good times we all had as well, in our never-ending Wednesday nights after IRTG seminar. All the nice colleagues I had and good friends I made. Thanks to all for being there and supporting me throughout this "kind of difficult and stressful" yet fun time. Still regarding the IRTG 1384 program, I would like to thank all the supporting members, who helped make it work, for all of us, and who took part in our yearly retreat which was generally very good.

I would also like to thank the director of our institute, Prof. Dr. John Zebuhr for providing me the chance to work in an outstanding institute and accompanying with me in discussion and suggestions about my experimental results and for putting up with so many situations of me.

My great appreciation to former and current colleagues in my research group; Dr. Zhongfang Wang, Eva Lenz, Mattias Riedl, Ebru Erogan, Julia Dzieciolowski, Ahmed

Elsayed, Christin Müller, Sharmistha Dam for their support during my study in Gießen. Thanks to those of you who were always willing to help me in many situations and those who helped create such a nice working environment.

I would also like to thank my "huge" family and friends back home, for moral support throughout this time.

In this paragraph I would like to acknowledge those who are nearest to my heart. Those who permit that I breathe. Those who have supported me silently throughout another one of my "adventures", who believe in me no matter what, to whom I owe more than words can say; my family, I especially thank my mom, dad, and brother. My hard-working parents have sacrificed their lives for my brother and me and provided unconditional love and care. I love them so much, and I would not have made it this far without them. My brother has been my best friend all my life and I love him dearly and thank him for all his support. I would like thank my boyfriend. I met the best person out there for me. Marco is the only person who can appreciate my quirkiness and sense of humour. Marco has been a true and great supporter and has unconditionally loved me during my good and bad times. He has been non-judgmental of me and instrumental of instilling confidence. These past three years have not been an easy ride, both academically and personally. I truly thank Marco for sticking by my side, even when I was irritable and depressed. I feel that we both learned a lot about life and strengthened our commitment and determination to each other and to live life to the fullest.